

2  
AD-A276 737

# NAVAL POSTGRADUATE SCHOOL

## Monterey, California



DTIC  
ELECTED  
MAR 14 1994

### THESIS

AN ANALOG PREPROCESSING ARCHITECTURE  
FOR HIGH-SPEED  
ANALOG-TO-DIGITAL CONVERSION  
by

Jorge A. Esparza

December, 1993

Thesis Advisor:

Thesis Co-Advisor:

Phillip E. Pace

Douglas J. Fouts

Approved for public release; distribution is unlimited.

94 3 11 160

94-08207



## UNCLASSIFIED

SECURITY CLASSIFICATION OF THIS PAGE

## REPORT DOCUMENTATION PAGE

1a. REPORT SECURITY CLASSIFICATION UNCLASSIFIED		1b. RESTRICTIVE MARKINGS	
2a. SECURITY CLASSIFICATION AUTHORITY		3. DISTRIBUTION/AVAILABILITY OF REPORT  Approved for public release; distribution is unlimited.	
2b. DECLASSIFICATION/DOWNGRADING SCHEDULE			
4. PERFORMING ORGANIZATION REPORT NUMBER(S)		5. MONITORING ORGANIZATION REPORT NUMBER(S)	
6a. NAME OF PERFORMING ORGANIZATION  Naval Postgraduate School	6b. OFFICE SYMBOL <i>(If applicable)</i>  EC	7a. NAME OF MONITORING ORGANIZATION  Naval Postgraduate School	
8c. ADDRESS (City, State, and ZIP Code)  Monterey, CA 93943-5000	7b. ADDRESS (City, State, and ZIP Code)  Monterey, CA 93943-5000		
8a. NAME OF FUNDING/SPONSORING ORGANIZATION	8b. OFFICE SYMBOL <i>(If applicable)</i>	9. PROCUREMENT INSTRUMENT IDENTIFICATION NUMBER	
8c. ADDRESS (City, State, and ZIP Code)		10. SOURCE OF FUNDING NUMBERS	
		Program Element No.	Project No.
		Task No.	Work Unit Accession Number
11. TITLE <i>(Include Security Classification)</i> AN ANALOG PREPROCESSING ARCHITECTURE FOR HIGH-SPEED ANALOG-TO-DIGITAL CONVERSION			
12. PERSONAL AUTHOR(S) Esperza, Jorge A.			
13a. TYPE OF REPORT Master's Thesis	13b. TIME COVERED From                          To	14. DATE OF REPORT <i>(year, month, day)</i> December 1993	15. PAGE COUNT 168
16. SUPPLEMENTARY NOTATION The views expressed in this thesis are those of the author and do not reflect the official policy or position of the Department of Defense or the U. S. Government.			
17. COSATI CODES		18. SUBJECT TERMS <i>(Continue on reverse if necessary and identify by block number)</i>  Analog-to-Digital Converter;Symmetrical number system :Analog preprocessing for analog-to-digital conversion	
19. ABSTRACT <i>(Continue on reverse if necessary and identify by block number)</i>  This thesis investigates the feasibility of implementing an analog-to-digital converter (ADC) based on a new symmetrical number system (SNS). This preprocessing architecture decomposes the analog amplitude analyzing function of an ADC into a number of sub-operations (moduli). Each sub-operation tells the analog signal with a folding period proportional to the value of the modulus. Through the use of the SNS encoding and recombining the results of the sub-operations, a definitive performance enhancement is achieved. The number of comparators required is reduced considerably, allowing more bandwidth to be used in the folding circuits. The overall design effort demonstrates a 8-bit design with a total of 23 comparators. SPICE simulations are developed and the performance demonstrated. Also identified are the areas in which further research is required.			
20. DISTRIBUTION/AVAILABILITY OF ABSTRACT <input checked="" type="checkbox"/> UNCLASSIFIED/UNLIMITED <input type="checkbox"/> SAME AS REPORT <input type="checkbox"/> DTIC USERS		21. ABSTRACT SECURITY CLASSIFICATION Unclassified	
22a. NAME OF RESPONSIBLE INDIVIDUAL Philip E. Pace		22b. TELEPHONE <i>(Include Area Code)</i> (408) 658-3286	22c. OFFICE SYMBOL EC/PC

Approved for public release; distribution is unlimited.

AN ANALOG PREPROCESSING ARCHITECTURE  
FOR HIGH-SPEED ANALOG-TO-DIGITAL CONVERSION

by

Jorge A. Esparza  
Captain, United States Marine Corps  
B.S., United States Naval Academy, 1987

Submitted in partial fulfillment  
of the requirements for the degree of

MASTER OF SCIENCE IN ELECTRICAL ENGINEERING

from the

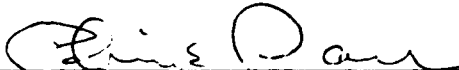
NAVAL POSTGRADUATE SCHOOL

December 1993

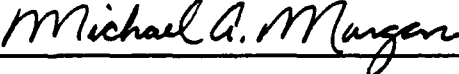
Author:

  
Jorge A. Esparza

Approved by:

  
Phillip E. Pace, Thesis Advisor

  
Douglas J. Fouts, Co-Advisor

  
Michael A. Morgan

Michael A. Morgan, Chairman  
Department of Electrical and Computer Engineering

## **ABSTRACT**

This thesis investigates the feasibility of implementing an analog-to-digital converter (ADC) based on a new symmetrical number system (SNS). This preprocessing architecture decomposes the analog amplitude analyzing function of an ADC into a number of sub-operations (moduli). Each sub-operation folds the analog signal with a folding period proportional to the value of the modulus. Through the use of the SNS encoding and recombining the results of the sub-operations, a definitive performance enhancement is achieved. The number of comparators required is reduced considerably, allowing more bandwidth to be used in the folding circuits. The overall design effort demonstrates a 9-bit design with a total of 23 comparators. SPICE simulations are developed and the performance demonstrated. Also identified are the areas in which further research is required.

Accesion For	
NTIS CRA&I	<input checked="" type="checkbox"/>
DTIC TAB	<input type="checkbox"/>
Unannounced	<input type="checkbox"/>
Justification .....	
By .....	
Distribution /	
Availability Codes	
Dist	Avail and / or Special
A-1	

## TABLE OF CONTENTS

I.	INTRODUCTION . . . . .	1
II.	BACKGROUND . . . . .	3
	A. TYPES OF ANALOG-TO-DIGITAL CONVERTERS . . . . .	3
	B. RESEARCH TRENDS . . . . .	8
III.	ANALOG PREPROCESSING ARCHITECTURE . . . . .	15
	A. GENERAL OVERVIEW . . . . .	15
	B. SYMMETRICAL NUMBER SYSTEM I . . . . .	15
	C. SYMMETRICAL NUMBER SYSTEM II . . . . .	17
	D. SYMMETRICAL NUMBER SYSTEM AND ANALOG PREPROCESSING . . . . .	19
	1. Initial Design Concepts . . . . .	19
	2. Design Modifications . . . . .	21
IV.	DESIGN AND SIMULATION RESULTS . . . . .	25
	A. ANALOG CIRCUIT DESIGN . . . . .	25
	1. Folding Circuit Design and Simulation . . .	25
	2. Comparator Design and Simulation . . . . .	69
	B. DIGITAL CIRCUIT DESIGN . . . . .	76
V.	STRENGTHS, LIMITATIONS, AND FUTURE DEVELOPMENTS . .	100

APPENDIX A SPICE INPUT FILE . . . . .	102
APPENDIX B INPUT FILE FOR PLA GENERATION . . . . .	136
APPENDIX C MATLAB PROGRAM TO GENERATE PLA TRUTH TABLE .	147
APPENDIX D DIGITAL SIMULATION OF PLA . . . . .	151
LIST OF REFERENCES . . . . .	152
BIBLIOGRAPHY . . . . .	154
INITIAL DISTRIBUTION LIST . . . . .	155

## LIST OF FIGURES

<b>Figure 2.1:</b> Dual slope ADC. . . . .	4
<b>Figure 2.2:</b> Output of integrator during the signal and reference integrate phases.	
. . . . .	6
<b>Figure 2.3:</b> Successive Approximation ADC. . . . .	7
<b>Figure 2.4:</b> 3-bit flash (parallel) ADC. . . . .	9
<b>Figure 2.5:</b> Two-stage ADC with coarse and fine quantization. . . . .	11
<b>Figure 2.6:</b> Folding ADC block diagram utilizing coarse and fine quantization. . . . .	12
<b>Figure 2.7:</b> Ideal and distorted folded output. . . . .	14
<b>Figure 3.1:</b> Block diagram of an analog-to-digital converter with analog preprocessing. . . . .	23
<b>Figure 3.2:</b> PLA block diagram. . . . .	24
<b>Figure 4.1:</b> A folding circuit. . . . .	26
<b>Figure 4.2:</b> Folding circuit DC transfer curve . . . .	27
<b>Figure 4.3:</b> Folding circuit's output as the input approaches the value of the power supplies. . . . .	28
<b>Figure 4.4:</b> Periodicity in the folding circuit's output. . . . .	30
<b>Figure 4.5:</b> Modulus 23 folding circuit block diagram.	31
<b>Figure 4.6:</b> Modulus 23 folding circuit schematic. . . .	32

<b>Figure 4.7:</b> Comparator outputs of simulated mod 23 folding circuit . . . . .	35
<b>Figure 4.8:</b> Mod 23 folding circuit output from a transient analysis at 10 Hz. . . . .	36
<b>Figure 4.9:</b> Mod 23 folding circuit output from a transient analysis at 1 KHz. . . . .	37
<b>Figure 4.10:</b> Mod 23 folding circuit transient analysis at 10 Khz. . . . .	38
<b>Figure 4.11:</b> DC transfer curve of one fold with a 0.05 mA current source. . . . .	39
<b>Figure 4.12:</b> DC transfer curve of one fold with a current source of 0.2 mA. . . . .	40
<b>Figure 4.13:</b> Narrow fold width due to small current source. . . . .	42
<b>Figure 4.14:</b> Wide fold width due to larger current source. . . . .	43
<b>Figure 4.15:</b> Loading problem in folding circuits. . . .	44
<b>Figure 4.16:</b> Voltage shifter circuit. . . . .	45
<b>Figure 4.17:</b> Revised modulus folding circuit. . . . .	46
<b>Figure 4.18:</b> Fold height inconsistency in modulus folding circuit. . . . .	48
<b>Figure 4.19:</b> Fold height inconsistency variations. . .	51
<b>Figure 4.20:</b> Bottom of folds from Figure 4.19. . . . .	52
<b>Figure 4.21:</b> Fold height inconsistency test part 1. . .	53
<b>Figure 4.22:</b> Fold height inconsistency test part 2. . .	54
<b>Figure 4.23:</b> Modulus 20 folding circuit output. . . . .	59

<b>Figure 4.24:</b> Modulus 7 folding circuit output. . . . .	61
<b>Figure 4.25:</b> Modulus 8 folding circuit output. . . . .	62
<b>Figure 4.26:</b> Modulus 11 folding circuits output. . . . .	63
<b>Figure 4.27:</b> Modulus 7 comparator levels. . . . . . .	64
<b>Figure 4.28:</b> Modulus 8 comparator levels. . . . . . .	65
<b>Figure 4.29:</b> Modulus 11 comparator levels. . . . . . .	66
<b>Figure 4.30:</b> Clocked comparator circuit diagram. . . . .	70
<b>Figure 4.31:</b> Clocked comparator's output when threshold voltage is greater than the input voltage. . . . .	71
<b>Figure 4.32:</b> Clocked comparator's output when the threshold voltage is less than the input voltage. . . . .	73
<b>Figure 4.33:</b> Clocked comparator output with oscillations. . . . . . . . . . . . . . . . .	74
<b>Figure 4.34:</b> Static comparator with transmission gate. . . . .	75
<b>Figure 4.35:</b> Operation of a transmission gate. . . . .	77
<b>Figure 4.36:</b> Mod 7 comparator outputs. . . . . . . . .	78
<b>Figure 4.37:</b> Mod 7 comparator and 1st decoder outputs. . . . .	79
<b>Figure 4.38:</b> Mod 7 1st and 2nd decoder outputs. . . . .	80
<b>Figure 4.39:</b> Mod 8 comparator outputs. . . . . . . . .	81
<b>Figure 4.40:</b> Mod 8 comparator and 1st decoder outputs. . . . .	82
<b>Figure 4.41:</b> Mod 8 1st decoder outputs. . . . . . . . .	83
<b>Figure 4.42:</b> Mod 8 2nd decoder output. . . . . . . . .	84
<b>Figure 4.43:</b> Mod 11 comparator outputs. . . . . . . . .	85
<b>Figure 4.44:</b> Mod 11 comparator outputs continued. . . . .	86
<b>Figure 4.45:</b> Mod 11 1st decoder output. . . . . . . . .	87
<b>Figure 4.46:</b> Mod 11 1st decoder output continued. . . . .	88

<b>Figure 4.47:</b> Mod 11 2nd decoder output. . . . .	89
<b>Figure 4.48:</b> First half of the mod 7 decoder. . . . .	91
<b>Figure 4.49:</b> CMOS gates used in decoder design. . . . .	92
<b>Figure 4.50:</b> 1st decoder simulation showing the input comparator levels. . . . . . . . . . . . . . . . .	93
<b>Figure 4.51:</b> 1st decoder simulation showing decoder output. .	94
<b>Figure 4.52:</b> Second half of the mod 7 decoder. . . . .	96
<b>Figure 4.53:</b> 2nd decoder simulation showing the decoder output. .	97
<b>Figure 4.54:</b> Partial layout of a PLA. . . . . . . . . . .	98

#### **ACKNOWLEDGEMENT**

I would like to thank the Marine Corps for giving me the opportunity to be intellectually challenged at the Naval Postgraduate School.

I would like to express my sincere appreciation to Professor P.E. Pace, my thesis advisor, for his encouragement and guidance, and to Professor D.J. Fouts, my thesis co-advisor, for his assistance through many hours of computer simulations.

Last but not least, I want to thank my wife, Tracy, my son, Antonio, and my daughter, GiGi, for their support, patience, and moral support.

## I. INTRODUCTION

This thesis begins with a discussion on the theory of analog-to-digital converters. The discussion progresses from the slowest type of ADC's, like the dual slope, to the fastest type which is the flash or parallel converter. Advantages and disadvantages are discussed for each type of converter, but current research trends have been to improve on the flash type converter. One of these improvements is the basis of this thesis.

This thesis proposes a new analog preprocessing architecture for analog-to-digital converters (ADC) which is based on a symmetrical number system (SNS). The number system lends itself favorably to the folding circuit methodology which is used in the design that is presented here and in other designs which have been presented by other researchers. Utilizing both the symmetrical number system and folding circuits, this thesis will demonstrate a considerable decrease in the number of comparators that are used in the quantization process. The number of comparators is one of the major factors driving flash analog-to-digital converter in terms of speed, size, and power consumption.

After the background discussion on the theory of analog-to-digital converters, the mathematical basis for the symmetrical number system is reviewed. Additionally, a

discussion on how this number system can be incorporated into an analog preprocessing architecture to improve flash type ADC's ensues. The bulk of this thesis documents the research conducted in the design and simulation of the analog folding circuits utilizing a 2 micron CMOS process. There were many challenges and obstacles which presented itself in this research effort such as frequency response and loading problems, but most of these were resolved.

After the analog portion of the ADC design is accomplished, the digital design of the ADC is presented. The design and simulation of the decoder and the PLA which are used in the design are quite straight forward with no major problem encountered. This thesis discusses the digital logic involved in the operation of the decoder in terms of truth tables and simulations, and the purpose and functionality of the programmable logic array (PLA) is reviewed with simulation used as validation.

Finally, this thesis ends with a recapitulation of strengths and problems of the design presented in this thesis. Also, this thesis proposes possible solutions to the pending problems and improvements for further design work. Future research areas based on this thesis are also examined.

## **II. BACKGROUND**

### **A. TYPES OF ANALOG-TO-DIGITAL CONVERTERS**

Analog-to Digital converters accept an analog signal as an input and convert it into a digital form as an output. Computers use these devices to sample information from its external environment and manipulate the data as may be necessary to perform a useful function. Depending on the conversion rates of the ADC, the device can be used to process a variety of analog signals from slow moving voltage signals to faster video signals. There are generally three different types of ADC's: dual slope, successive approximation, and flash (or parallel). Dual slope ADC's have the slowest conversion rates, approximately 300 ms. The conversion process is divided into two phases. The first phase is the signal integrate phase where an input signal,  $V_{in}$ , is applied to an integrator (see Figure 2.1). The output voltage of the integrator,  $V_{out}$ , ramps with a slope proportional to  $V_{in}$  and ceases after a predetermined time has transpired. The next phase is the reference integrate phase, which where the analog-to-digital conversion takes place. At this point, the integrator is disconnected from  $V_{in}$  and connected to the reference voltage,  $V_{ref}$ . Concurrently, a counter begins

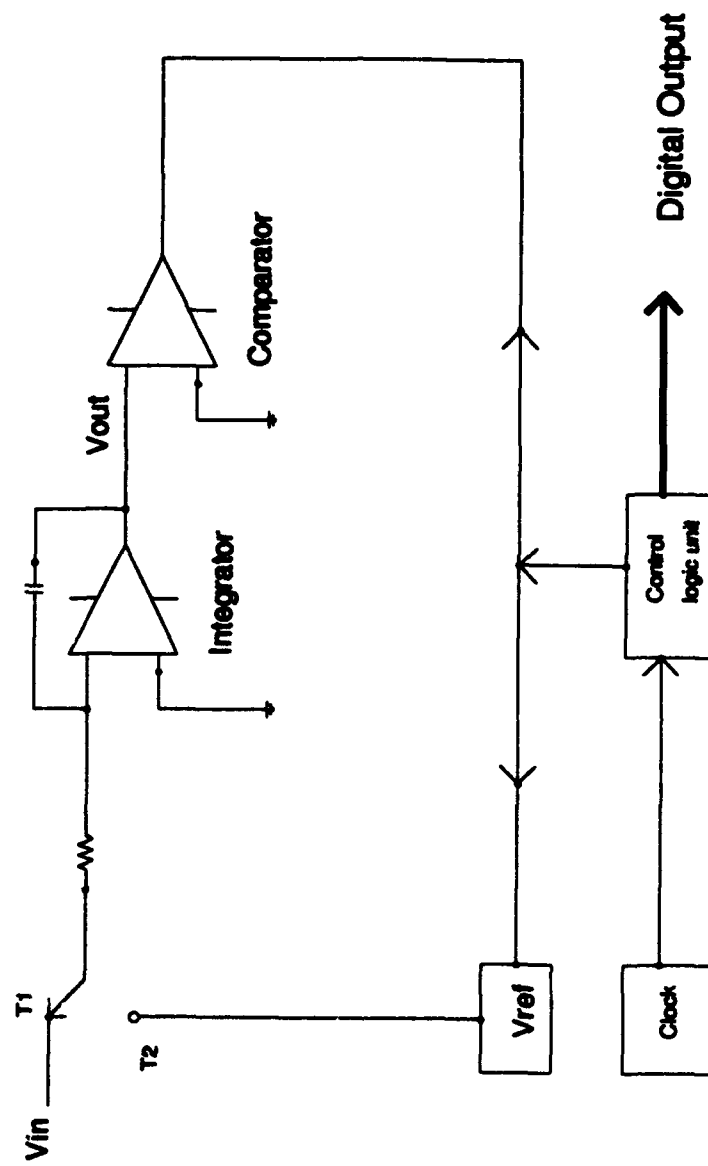


**Figure 2.1:** Dual slope ADC.

to count at a specified rate,  $f_c$ .  $V_{out}$  ramps at a constant rate in the opposite direction of  $V_{out}$  from the signal integrate phase. Once  $V_{out}$  reaches 0.0V, the comparator tells the control logic to terminate this phase and stop the counter. As can be seen in Figure 2.2,  $T_2$  is proportional to  $V_{out}$  which in turn is proportional to  $V_{in}$ :

$$T_2 = T_1 \frac{V_{in}}{V_{ref}}. \quad (2.1)$$

The digital output is contained in the contents of the counter and may be derived using the following equation:

$$D_{out} = f_c T_1 \frac{V_{in}}{V_{ref}} \quad (2.2)$$

where  $D_{out}$  is the digital output,  $f_c$  is the frequency of the clock driving the counter [Refs. 1-4].

A faster type of analog-to-digital converter is the successive approximation ADC. These ADC's have conversion times of several microseconds and are used primarily to digitize audio signals. The conversion begins when a start conversion signal is applied (See Figure 2.3). The successive approximation register, SAR, applies a digital signal to a digital-to-analog converter (DAC) with the most significant bit (MSB) set and the other bits cleared. The DAC produces an analog output,  $V_o$ , which is applied to a comparator. The

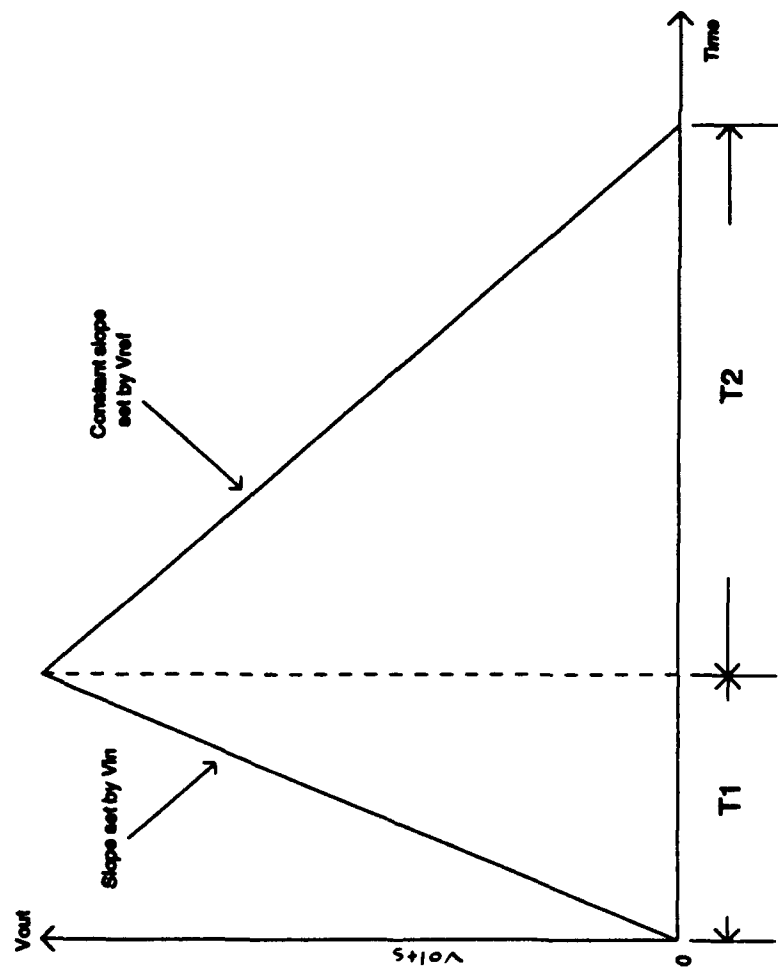


**Figure 2.2:** Output of integrator during the signal and reference integrate phases.

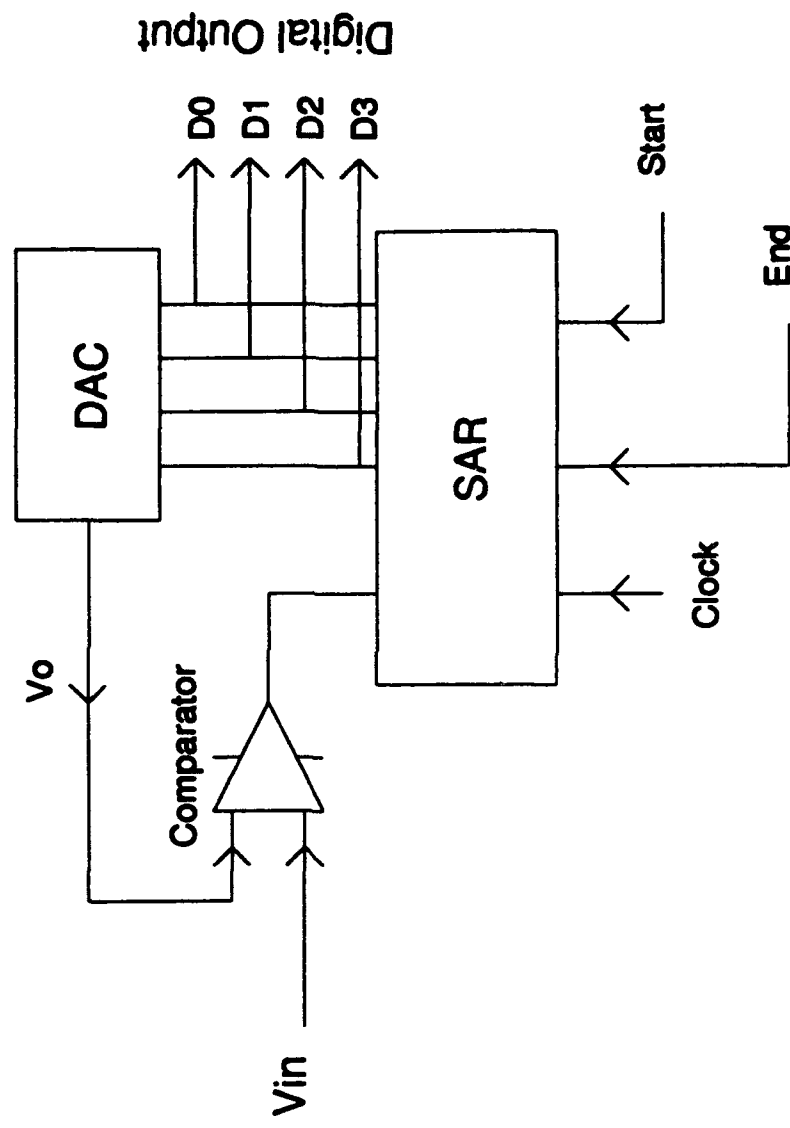


**Figure 2.3:** Successive Approximation ADC.

comparator compares  $V_o$  and the analog input signal,  $V_a$ . If  $V_a > V_o$ , the bit being resolved remains set. If  $V_a < V_o$ , then the bit being resolved is cleared. Once the bit is resolved, the conversion cycle is considered complete. The SAR will then set the next lower significant bit which begins a new conversion cycle. When the last bit has been converted, an end of conversion signal is produced, indicating that the digital output is valid [Refs. 1-4].

The fastest type of analog-to-digital converter is the Flash or Parallel ADC. These ADC's are generally used for video signals because conversion rates are in the hundreds of microseconds. With this type of ADC, an input voltage signal is applied to a parallel bank of  $2^n - 1$  comparators which compares the input signal to  $2^n - 1$  reference voltages, where n is the number of bits in the resolution (See Figure 2.4). To realize a digital representation of the input signal, combinational logic is utilized to convert the output of the comparators to a standard binary format [Refs. 1-4].

## B. RESEARCH TRENDS

Current research has endeavored to retain aspects of the Flash ADC architecture due to its high-speed characteristic. Also, there exists a need to reduce chip area and power consumption. Current trends have suggested reducing the number of comparators to address the chip area and power problem. One area of research is in optimizing the coarse-

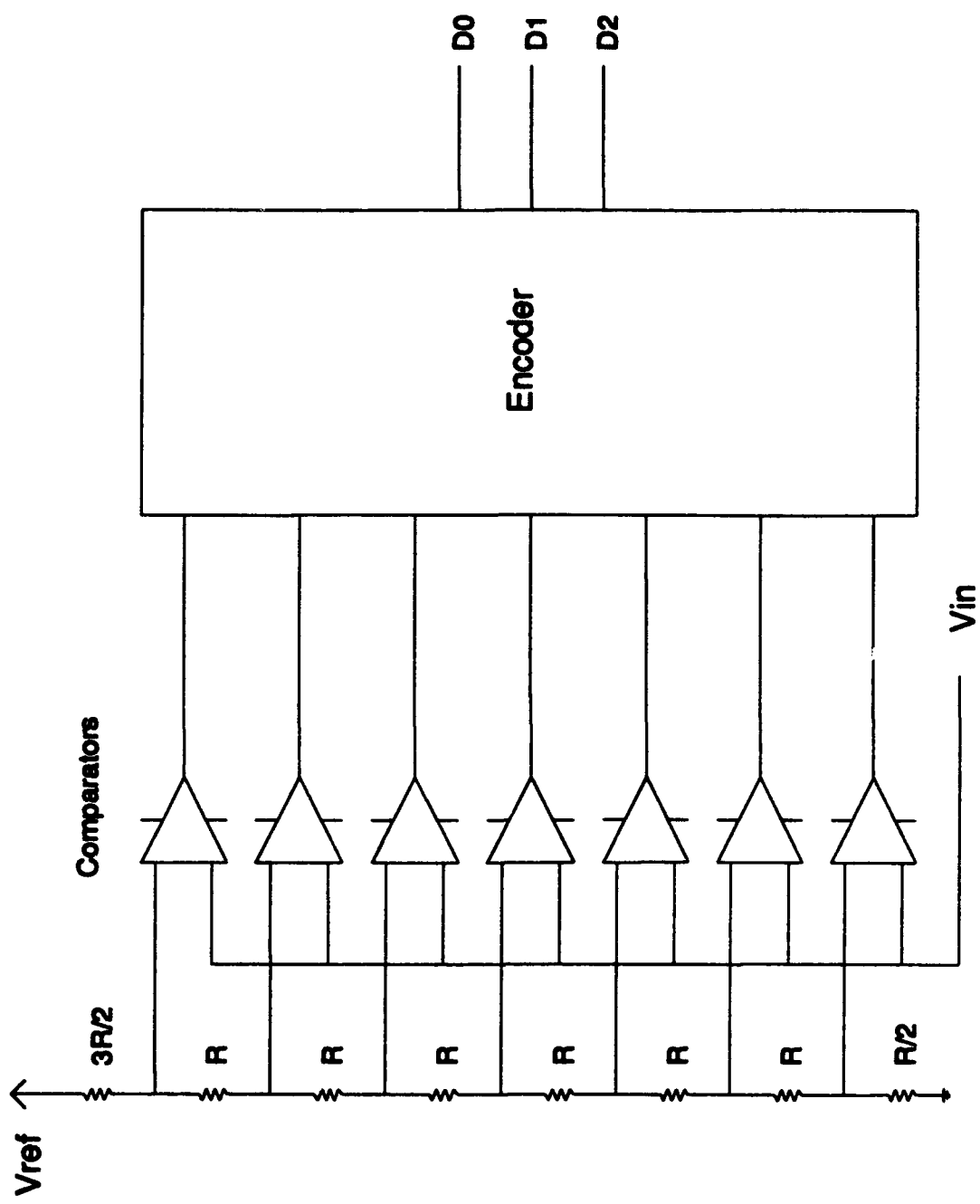


**Figure 2.4:** 3-bit flash (parallel) ADC.

fine quantization approach. In this approach, the input signal is applied to a coarse analog-to-digital converter to resolve the most significant bits (MSB's). These MSB's are then converted into an analog form utilizing a digital-to-analog converter. This analog value is then subtracted from the input signal and the result is applied to a second analog-to-digital converter to resolve the remaining least significant bits (LSB's). This approach dramatically reduces the number of comparators used in the quantization process. For example, in a pure flash ADC, 255 comparators would be needed to resolved 8-bits. However, in the course-fine quantization using a 3-bit flash comparator for the course and a 5-bit flash comparator for the fine quantization only 40 would comparators would be needed (see Figure 2.5). The drawback to this approach is the need to incorporate a digital-to-analog converter which introduces a timing problem [Refs. 5-6].

Another method in reducing the number of comparators in a flash comparator configuration is the use of folding analog preprocessing [Refs. 7,8]. In this process shown in Figure 2.6, the input signal goes through a course quantization using flash ADC to resolve the MSB's. Simultaneously, the input signal is transformed into an approximately triangular waveform. This waveform is then quantized using a flash ADC to obtain the LSB's. The number of comparators used in this

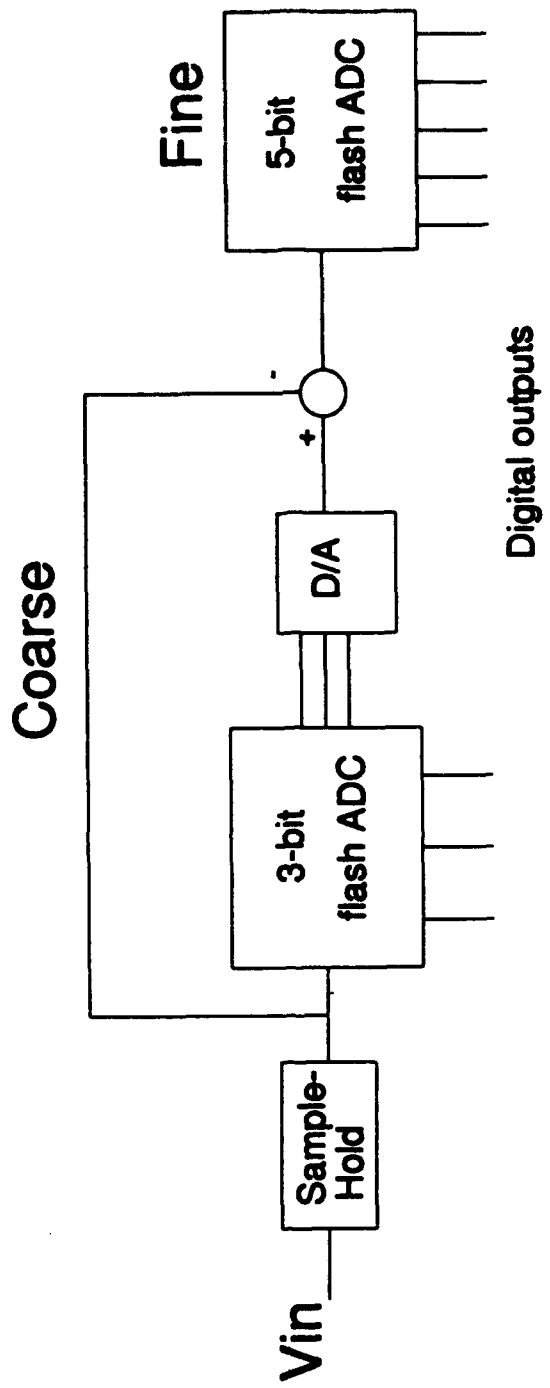


**Figure 2.5:** Two-stage ADC with coarse and fine quantization.

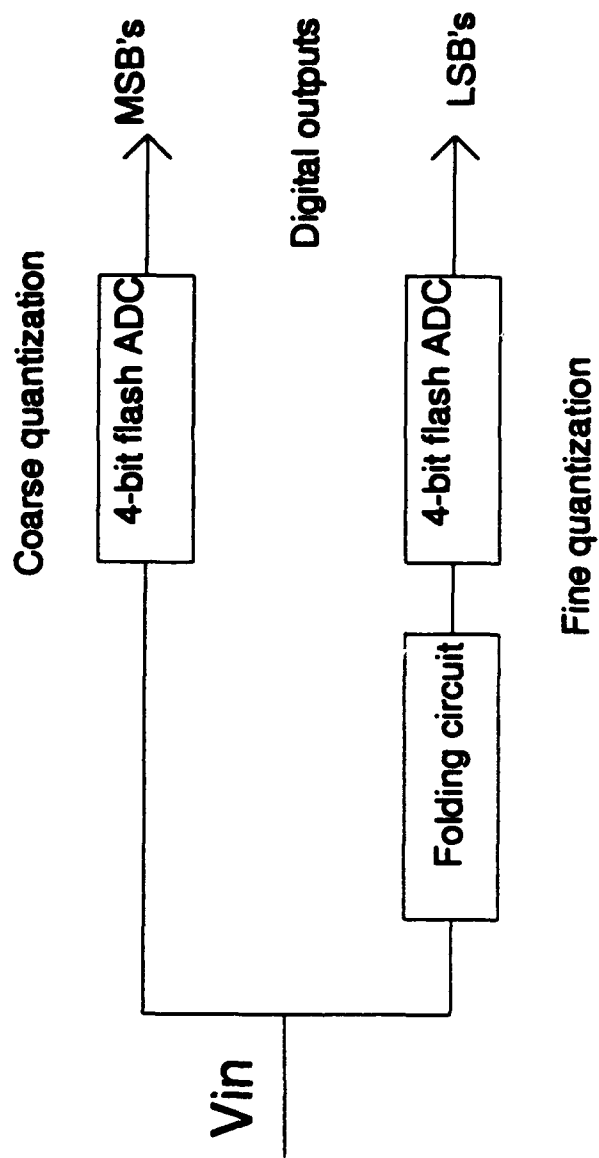


**Figure 2.6:** Folding ADC block diagram utilizing coarse and fine quantization.

folding technique is less than that of the course-fine quantization technique. This is very desirable but the drawback is the reduction of resolution of input signals at high frequencies because the tips of the triangular waveform tend to round off [Ref. 6] (see Figure 2.7). These round off regions in the waveform introduce errors in the conversion process. One method to resolve this problem is to use a double folding circuit. In this method, when one of the outputs of the double folding circuit moves into a rounded region, the other output will take over as it comes into its linear region [Ref. 9].

Incorporating folding and interpolation techniques to ADC design is another research trend which seeks to reduce the required number of comparators [Refs. 5,10,11]. In this technique, a certain number of folding-amplifier blocks are omitted. The output signals of the omitted folding-amplifier blocks are reconstructed from the remaining folding-amplifier blocks. The omission of these folding blocks directly translates into the reduction of the number of comparators. In one 8-bit implementation the number of required comparators was 64 [Ref. 10].

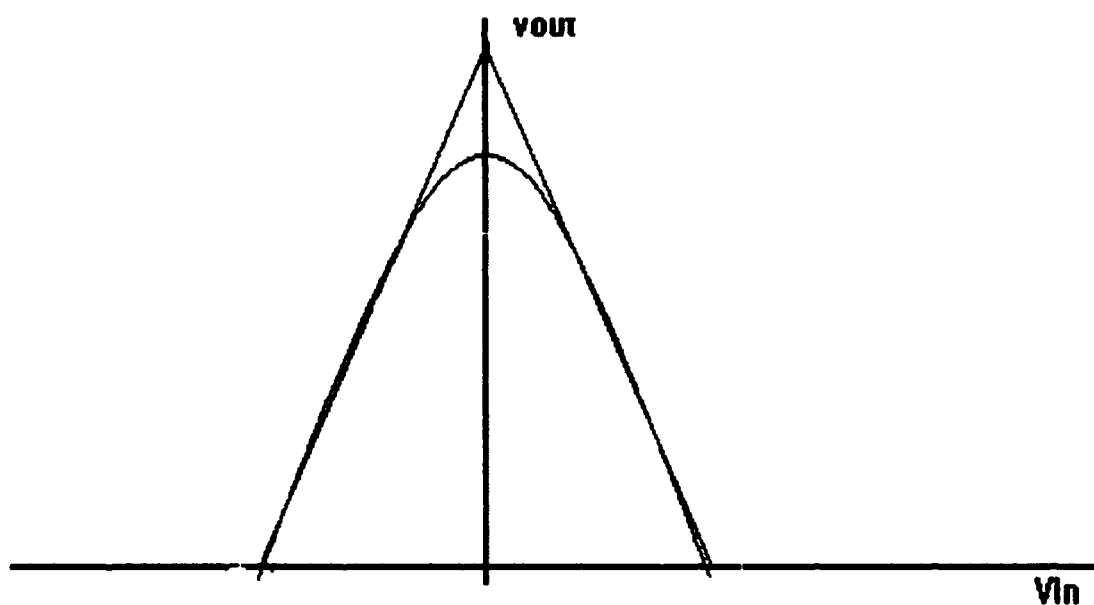


**Figure 2.7:** Ideal and distorted folded output.

### **III. ANALOG PREPROCESSING ARCHITECTURE**

#### **A. GENERAL OVERVIEW**

This thesis seeks to modify the basic flash ADC configuration by incorporating a folding analog preprocessing architecture before the signal is quantized by a parallel set of comparators. Through the use of the symmetrical number system (SNS) as discussed below, the preprocessing architecture decomposes the analog input signal into sub-operations or moduli. Within each modulus circuit, the analog input signal folds with a period corresponding to the value corresponding to the modulus. In effect, this system reduces the preprocessing problem to a set of simpler, parallel operations. The result of these compartmentalized operations are combined and later digitally converted. This digital conversion produces an output which represents the input signal in the SNS format and later to the standard binary format.

#### **B. SYMMETRICAL NUMBER SYSTEM I**

The first version of the symmetrical number system (SNS I) used in the initial design is composed of a set of pairwise relatively prime moduli  $m$ , [Ref. 12]. Each modulus is formed by a unique set of integer values. This series of integer values repeats itself after the number of elements within a

modulus set equals the value of the modulus. In effect, the modulus generates a symmetrical waveform which fold with a period equal to the value of the modulus. The equation that generates an individual odd modulus set is

$$X_m = [0, 1, \dots, \lfloor \frac{m}{2} \rfloor, \lfloor \frac{m}{2} \rfloor, \dots, 1] \quad (3.1)$$

where the function  $\lfloor x \rfloor$  is the greatest integer less than or equal to  $x$ . For an individual even modulus set the equation is

$$X_m = [0, 1, \dots, \frac{m}{2}, \frac{m}{2}-1, \dots, 1] \quad (3.2)$$

Using these equation, a modulus 5 (mod 5) set would be  $\{0, 1, 2, 2, 1, 0, 1, 2, \dots\}$ .

A combination of these moduli describe a number system which has a one-to-one correspondence with the residue system up to a certain range. The numerical patterns produced by the merging of a set of moduli will not repeat until a dynamic range has been reached. The dynamic range for a set of moduli where one modulus is even is

$$\hat{M} = \min\left\{\frac{m_{\text{even}}}{2}, \prod_{l=2}^j m_{il} + \prod_{l=j+1}^N m_{il}\right\} \quad (3.3)$$

where  $N$  is the number of moduli,  $j$  ranges from 2 to  $N-1$  and the subscripts  $i$ , run over all permutations  $\{2, 3, \dots, N\}$ .

When the set of moduli are all odd, the dynamic range is given by

$$M = \min\left\{\frac{1}{2} \prod_{l=1}^j m_{i_l} + \frac{1}{2} \prod_{l=j+1}^N m_{i_l}\right\} \quad (3.4)$$

where  $j$  ranges from 1 to  $N-1$  and the subscripts  $i_l$  run over all permutations  $\{1, 2, \dots, N\}$ . From the two above equations, the dynamic range would be larger for a set of moduli containing an even modulus than for a set of all odd moduli where the even modulus is increased by one. For example, the dynamic range for the set of moduli,  $m_1=3$ ,  $m_2=5$ ,  $m_3=7$ , is calculated to be  $M=3.5+7.5 = 11$ . When  $m_1=3$  is changed to  $m_1=2$  then the dynamic range increases to 12, and is illustrated in Table 3.1. Thus, a greater efficiency is obtained when an even modulus is used in combination with odd moduli.

### C. SYMMETRICAL NUMBER SYSTEM II

The second version of the symmetrical number system (SNS II) used in the final design is composed of a set of pairwise relatively prime moduli  $m_i$ , as in the SNS I. Each modulus is formed by a unique set of integer values. This series of integer values repeats itself after the number of elements within each modulus set is equal to twice the value of the modulus. As in the SNS I, the modulus generates a symmetrical waveform, but the fold period of the waveform is equal to twice the value of the modulus. The equation that generates an individual modulus set is

**TABLE 3.1 TWO SNS SYSTEMS  
SHOWING THE INCREASED EFFICIENCY  
OF AN EVEN MODULUS**

SNS MODULI							
Dynamic Range	3	5	7		2	5	7
0	0	0	0		0	0	0
1	1	1	1		1	1	1
2	1	2	2		0	2	2
3	0	2	3		1	2	3
4	1	1	3		0	1	3
5	1	0	2		1	0	2
6	0	1	1		0	1	1
7	1	2	0		1	2	0
8	1	2	1		0	2	1
9	0	1	2		1	1	2
10	1	0	3		0	0	3
11	1	1	3		1	1	3
12	0	2	2		0	2	2

$$x_m = [0, 1, \dots, m-1, m-1, \dots, 1, 0]. \quad (3.5)$$

Using this equation, a modulus 4 (mod 4) set would be  $(0, 1, 2, 3, 3, 2, 1, 0, \dots)$ . Similar to the SNS I, the system based on a set of moduli will produce SNS vectors which will not repeat until the dynamic range has been reached. The dynamic range  $M$  for a given set of SNS II moduli is given by:

$$M = \prod_{i=1}^N m_i. \quad (3.6)$$

For example, if the system is defined by the moduli,  $m_1=3$  and  $m_2=4$ , the dynamic range  $M$  would be equal to 12 as is shown in Table 3.2 [Ref. 13].

#### D. SYMMETRICAL NUMBER SYSTEM AND ANALOG PREPROCESSING

##### 1. Initial Design Concepts

This thesis endeavored to incorporate the symmetrical number system as the basis for the design of an analog preprocessing for an analog-to-digital converter. In this design, an input signal is applied in parallel to an appropriate number of modulus folding circuits as shown in Figure 3.1. The folding circuits will fold the input signal with a period based on the value of the respective modulus. The output of each fold is then quantized by a bank of comparators connected in parallel. At this point, the number of comparators that are high represents the value of the input signal in the SNS format.

TABLE 3.2 DYNAMIC RANGE OF AN  
SNS II SYSTEM

Dynamic Range	SNS II Moduli	
	4	3
0	0	0
1	1	1
2	2	2
3	3	2
4	3	1
5	2	0
6	1	0
7	0	1
8	0	2
9	1	2
10	2	1
11	3	0
12	3	0

After the input signal has been preprocessed and quantized, the outputs of the comparators are applied to a decoder. This decoder transforms the comparator output values into a binary thermometer format, and then to a straight binary number. This binary vector represents the highest comparator level reached by the input signal within each modulus. When combined, the output of each of the modulus decoders represents the input value in its SNS binary format. Since the SNS binary format is not easily recognizable, a programmable logic array (PLA) is used to convert a SNS binary number to a standard binary number (see Figures 3.1 and 3.2).

## 2. Design Modifications

Although the initial design of the analog preprocessing architecture was based on the first version of the symmetrical number system, a second version of the symmetrical number system caused slight modifications of the initial design. In this system, the dynamic range,  $M$ , is simply the product of the values of the moduli. For the moduli used in this thesis,  $m_1=7$ ,  $m_2=8$ , and  $m_3=11$ , the dynamic range is calculated to be  $M=7 \times 8 \times 11 = 616$ , which is well above 512 which is needed for a 9-bit resolution. The decision to change number systems was based on the benefits realized from the newer version. First, the new version reduces the number of moduli required to generate a specific dynamic range. In

the old design, four moduli were required to generate a dynamic range large enough to be represented by nine bits. The SNS II only requires three moduli. Second, because of the reduction of the number of moduli, the total number of comparators utilized is also reduced. Also, within each modulus of the new design, the number of comparators is less than the older design. In the first design, the number of comparator per modulus,  $m_i$ , is  $[m_i/2]$ . But, in the second design, the values of each modulus are considerably less than the moduli used in the first design for the same dynamic range. Because of this, the number of comparators for the second design,  $m_i-1$ , will be less than those contained in the first design.

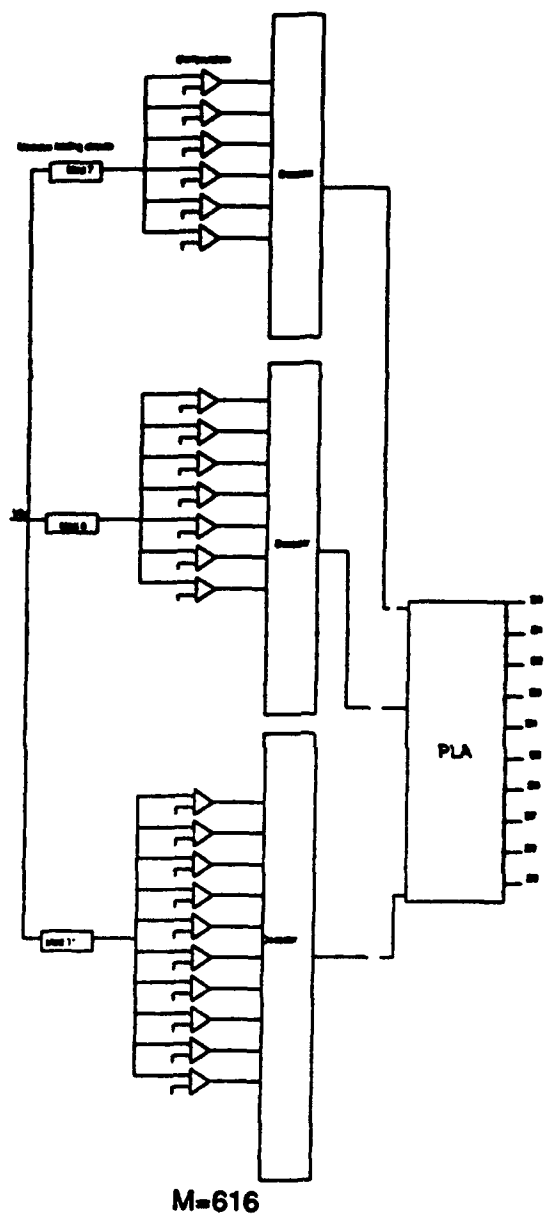
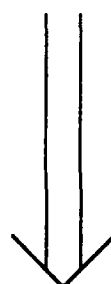
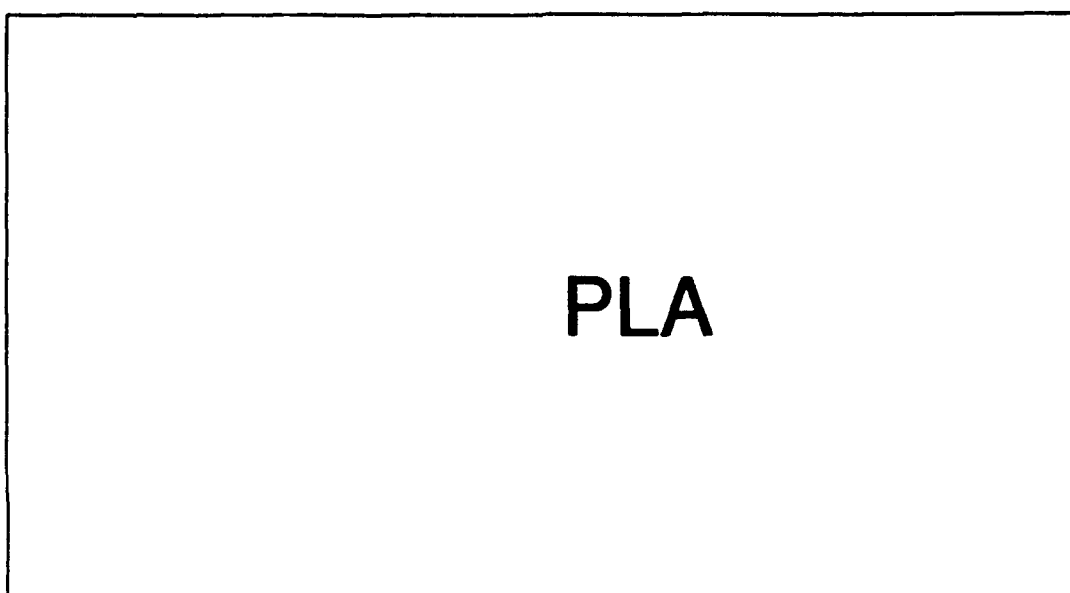
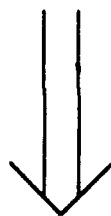


**Figure 3.1:** Block diagram of an analog-to-digital converter with analog preprocessing.

SNS Representation



Binary Representation

**Figure 3.2:** PLA block diagram.

## IV. DESIGN AND SIMULATION RESULTS

### A. ANALOG CIRCUIT DESIGN

#### 1. Folding Circuit Design and Simulation

The first step in the design of the analog preprocessing architecture is the design of the folding circuit. The folding circuit as shown in Figure 4.1 is composed of a pair of MOS differential amplifiers. An input signal ( $V_{in}$ ) is applied to the gate of M3 of the lower differential amplifier, and a reference voltage ( $V_{ref}$ ) is applied to the gate of M4. The output ( $V_{out}$ ) of the folding circuit is taken from the source of M1 and M2. The resulting transfer function is depicted in Figure 4.2. This relationship is achieved because the lower differential amplifier consisting of M3 and M4 provide the straight-line section symmetrical about  $V_{ref}$ , while the upper differential amplifier consisting of M1 and M2 provide an analog OR function. This function transfers the higher of the base voltages of M1 and M2 to the output  $V_{out}$ .

Spice simulations of the folding circuit demonstrated that as the value of  $V_{ref}$  reached the value of the power supplies driving the circuit, the folded output,  $V_{out}$ , became distorted as shown in Figure 4.3. This indicated that the value of the final reference voltage, and thus the dynamic

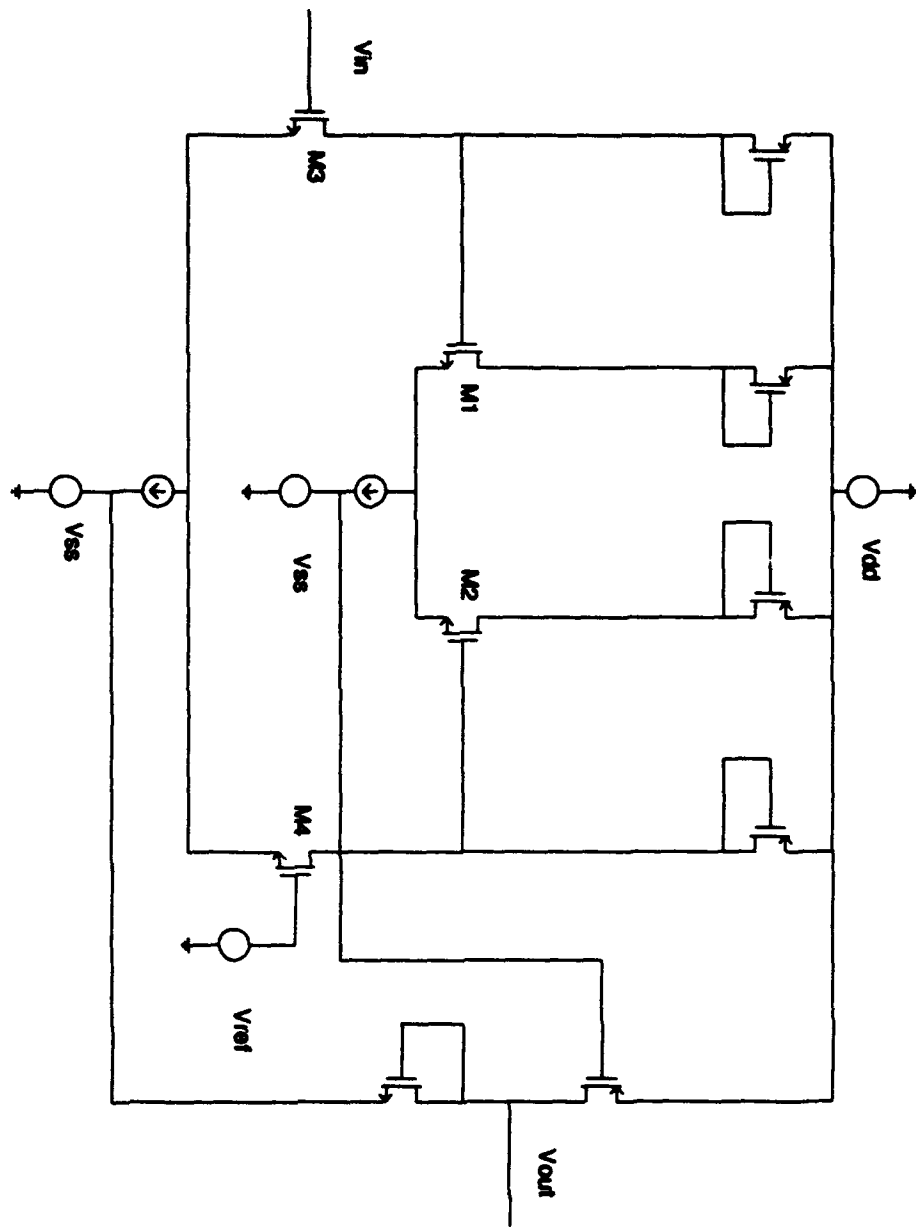


**Figure 4.1:** A folding circuit.

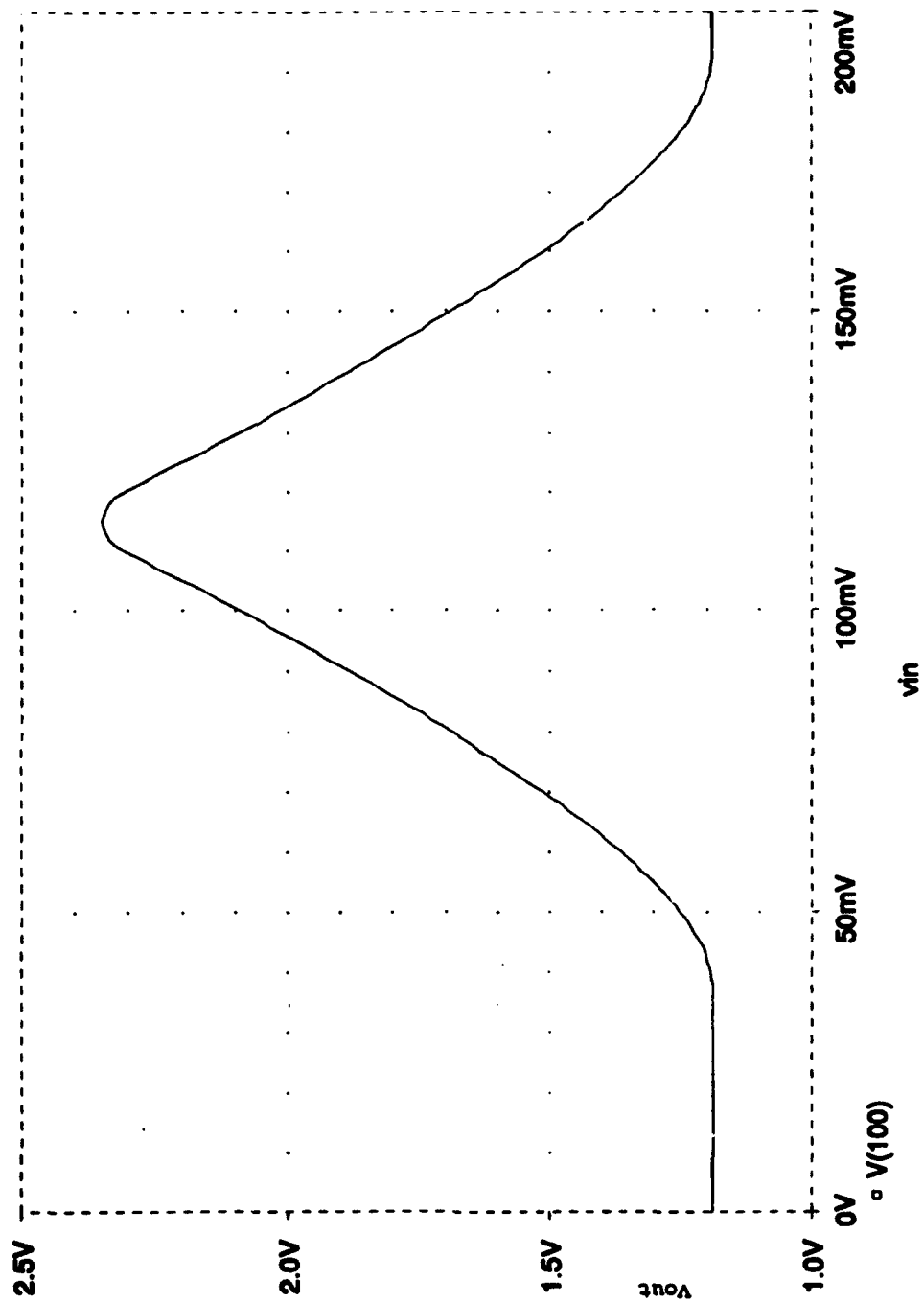


**Figure 4.2:** Folding circuit DC transfer curve.

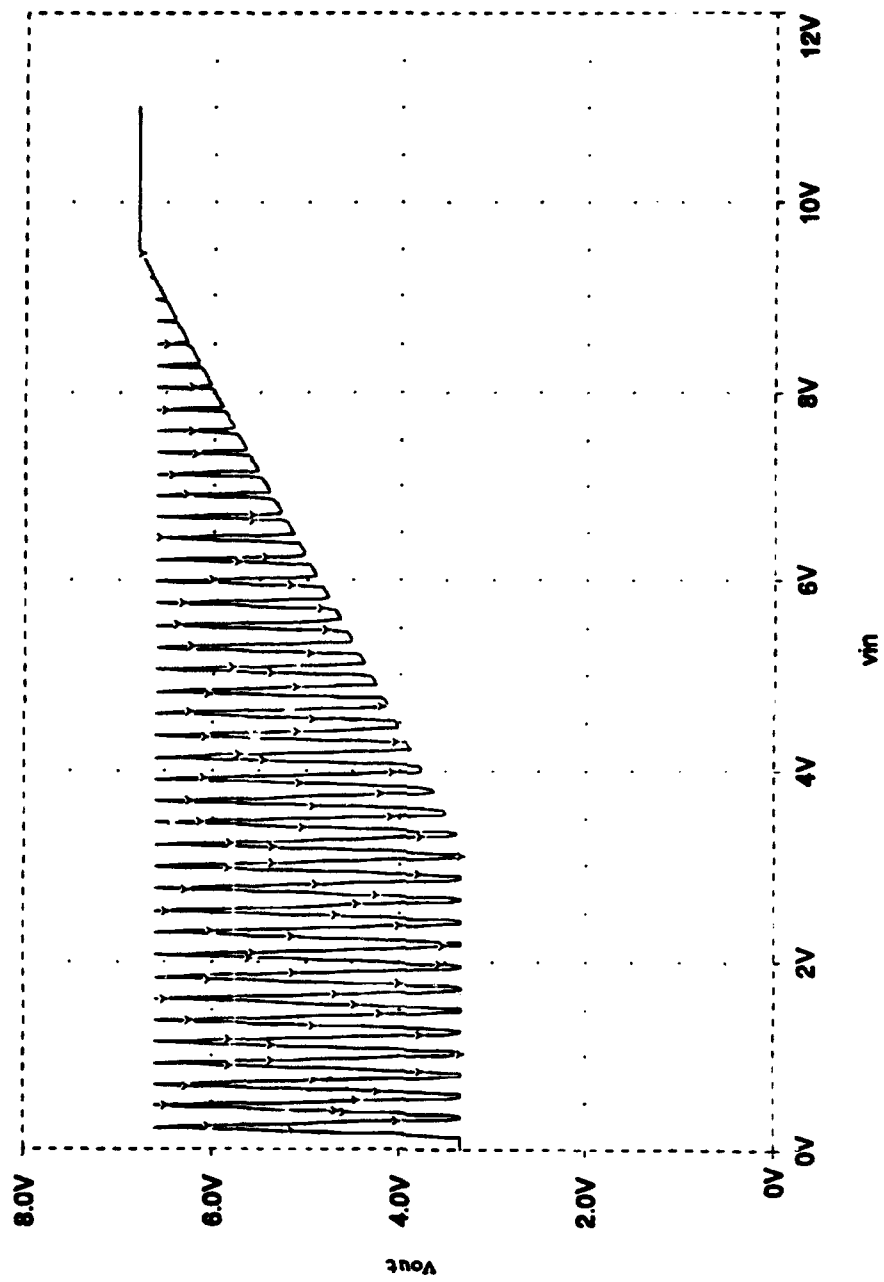


**Figure 4.3:** Folding circuit's output as the input approaches the value of the power supplies.

range for a particular modulus folding circuit must be adequately less than the value of the power supplies in order to avoid distortion. By supplying the proper equidistant reference voltages (separated by the modulus), the output folding waveform results as shown in Figure 4.4.

For the initial design, the folding circuits for a 10-bit SNS ADC were simulated using moduli  $m_1=23$ ,  $m_2=24$ ,  $m_3=29$ , and  $m_4=31$ . Using Equation 3.3 the SNS dynamic range was calculated to be

$$\frac{1}{2}m_2m_4 + m_1m_3 = 12(31) + 23(29) = 1039. \quad (4.1)$$

This SNS dynamic range was converted to an analog dynamic range of 5.2 volts by dividing by 200. Similarly, each modulus was divided by 200 to determine the reference voltages. This was done to enable the folding circuits to operate properly within the power supplies. Specifically, in the case of the modulus 23 folding circuit as shown in Figure 4.5 and 4.6, a linear ramp,  $V_m$ , covering the dynamic range was applied to the input. The folding waveform has a period of 0.115 volts ( $\text{mod}23/200 = 0.115$ ). Each folded output will be quantized by  $\lfloor m/2 \rfloor$  properly biased comparators. Each comparator must be biased to encode the input voltage correctly. In this case, the number of comparators, and

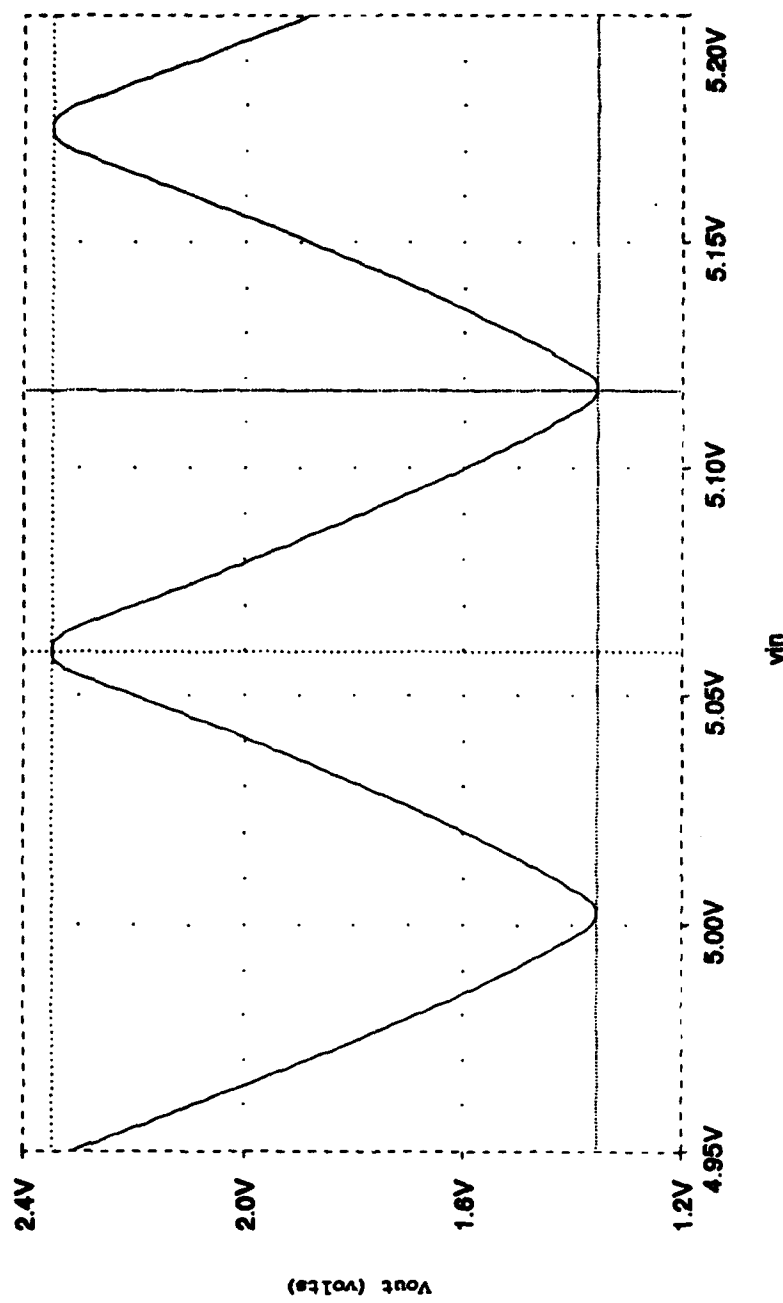


**Figure 4.4:** Periodicity in the folding circuit's output.

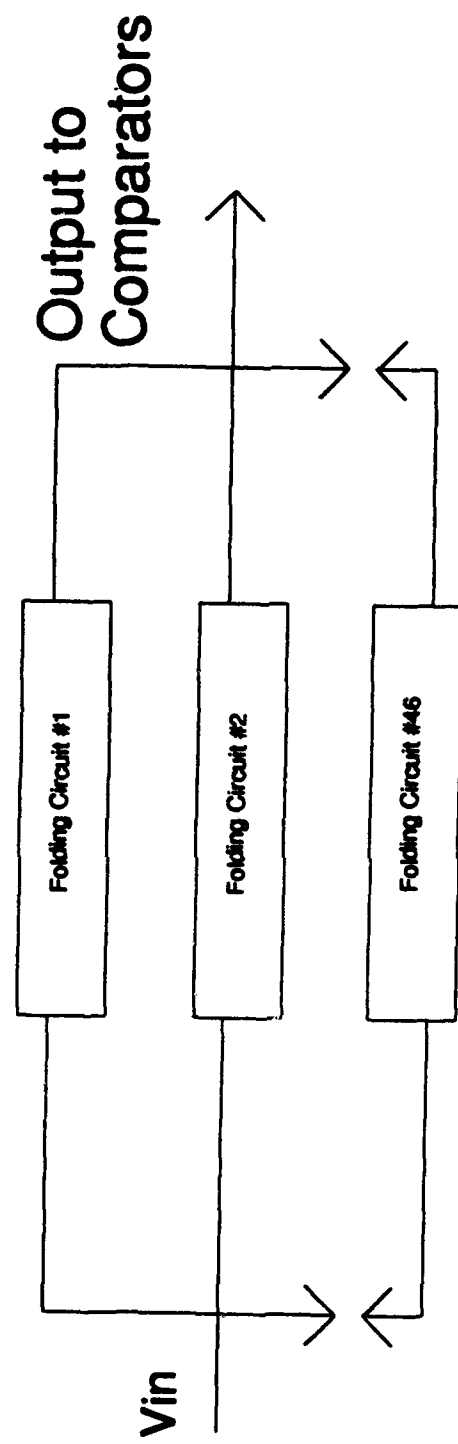


**Figure 4.5:** Modulus 23 folding circuit block diagram.

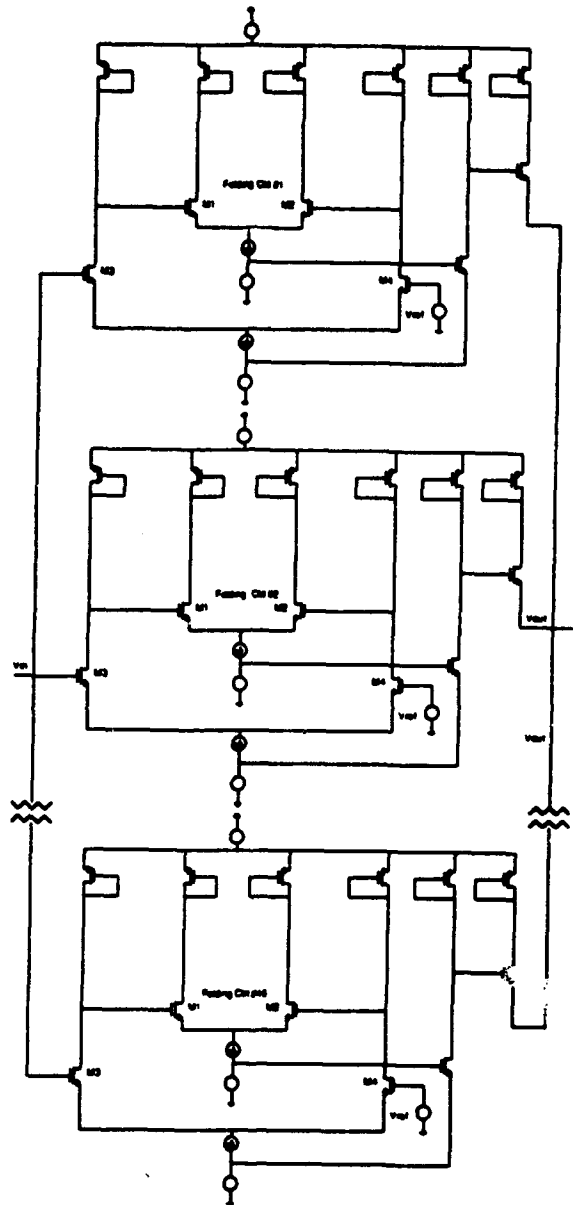


**Figure 4.6:** Modulus 23 folding circuit schematic.

consequently the number of threshold voltages, is equal to 11 ( $\lfloor 23/2 \rfloor = \lfloor 11.5 \rfloor$ ). To arrive at the threshold voltages, the period of the fold is quantized by two times the desired number of threshold voltages. For a mod 23 folding circuit, this would mean that for every 5.23 mV change in  $V_m$ , starting from 0.0V up to the dynamic range, the value of the folded output would correspond to the threshold voltage level. The voltage threshold values for the mod 23 folding circuit are tabulated below in Table 4.1.

TABLE 4.1 VOLTAGE THRESHOLD  
LEVELS FOR A MOD 23 FOLDING CIRCUIT

Voltage Threshold Level	Value (Volts)
1	2.34
2	2.24
3	2.13
4	2.02
5	1.91
6	1.81
7	1.71
8	1.61
9	1.52
10	1.44
11	1.37

The results of the simulation of the mod23 folding circuit and connected comparators are shown in Figure 4.4 and Figure 4.7. As can be seen from the latter, the output of the

comparators are high as the output of the modulus folding circuit passes the determined comparator threshold voltages.

After the DC analysis was conducted, a transient analysis was performed on the mod23 folding circuit and connected comparators. This was done by ramping the input  $V_i$  through the dynamic range over a specific period of time. As can be seen in Figures 4.8-4.10, as the frequency of the ramped input increases, the output of the modulus folding circuit becomes distorted. To correct this problem, two possible solutions were explored. The first remedy was to reduce the width of the transistors comprising the differential amplifiers in the folding circuit. This would decrease the capacitance associated with the transistors and increase the gain. The second idea was to increase the amount of current flowing through current sources of the folding circuit.

Changing the geometries of the transistors had minimal effect on the transient response of the folding circuits. However, the opposite was true when the current of the folding circuits were increased. In Figures 4.11 and 4.12, the current sources of the folding circuits were 0.05 mA and 0.2 mA, respectfully. As can be seen from these simulation results, the increase in the current improved the frequency response from 100Hz to 100KHz. The frequency response can be further improved, but there is a drawback. As the current

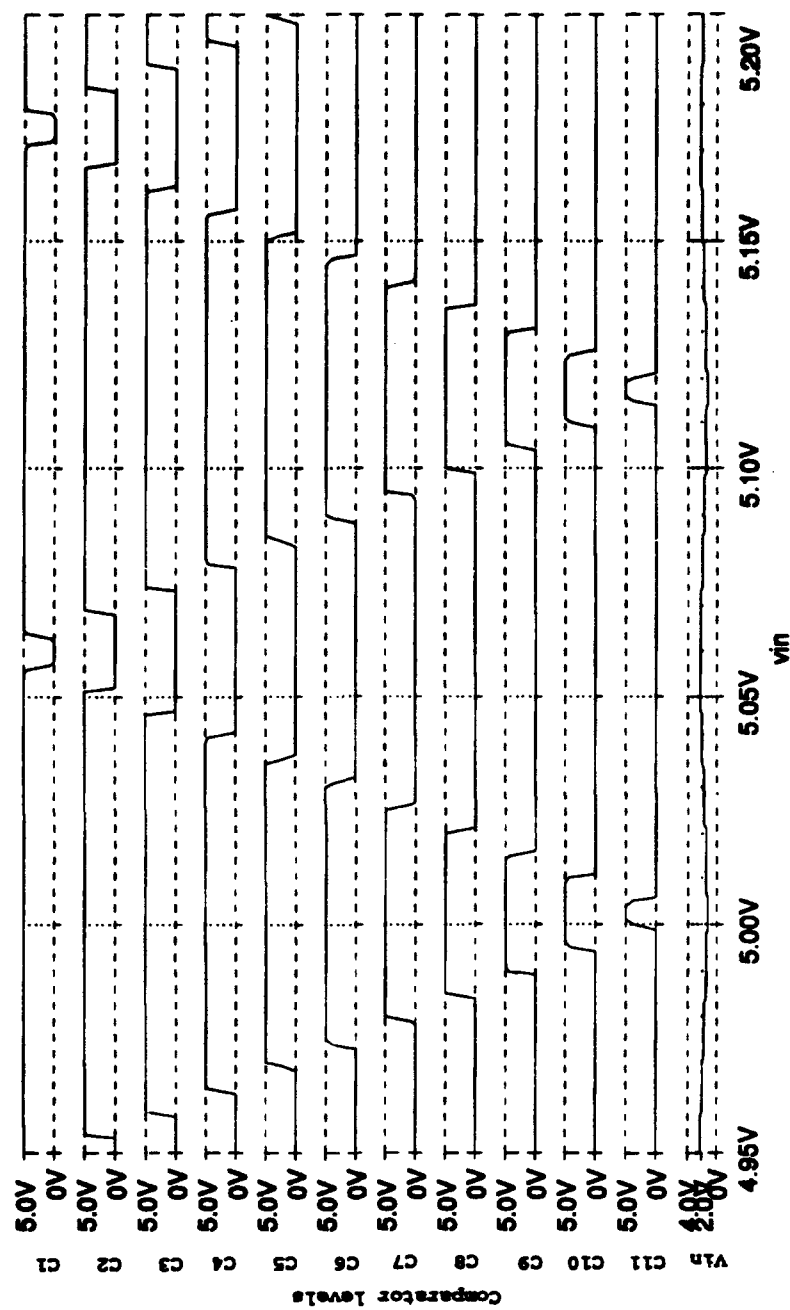


**Figure 4.7:** Comparator outputs of simulated mod 23 folding circuit.

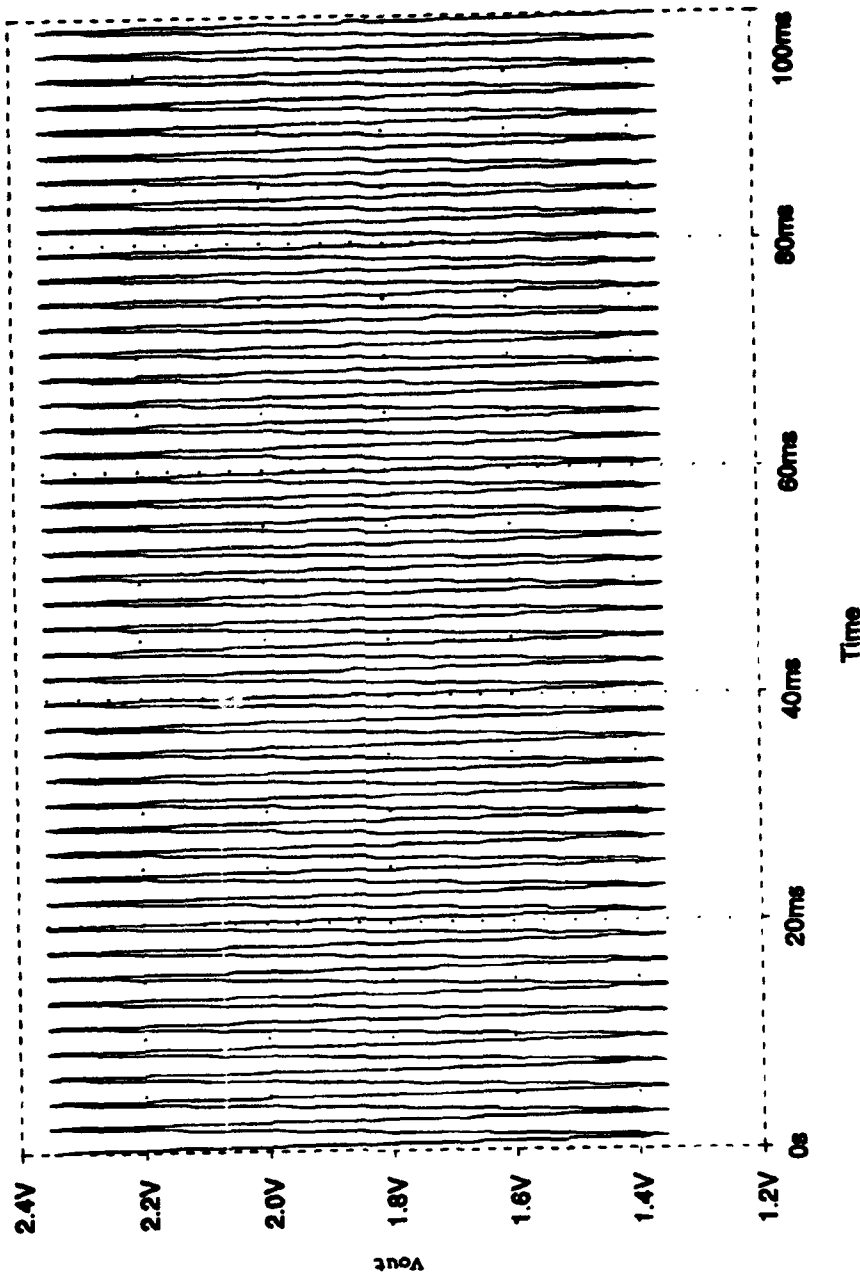


**Figure 4.8:** Mod 23 folding circuit output from a transient analysis at 10 Hz.

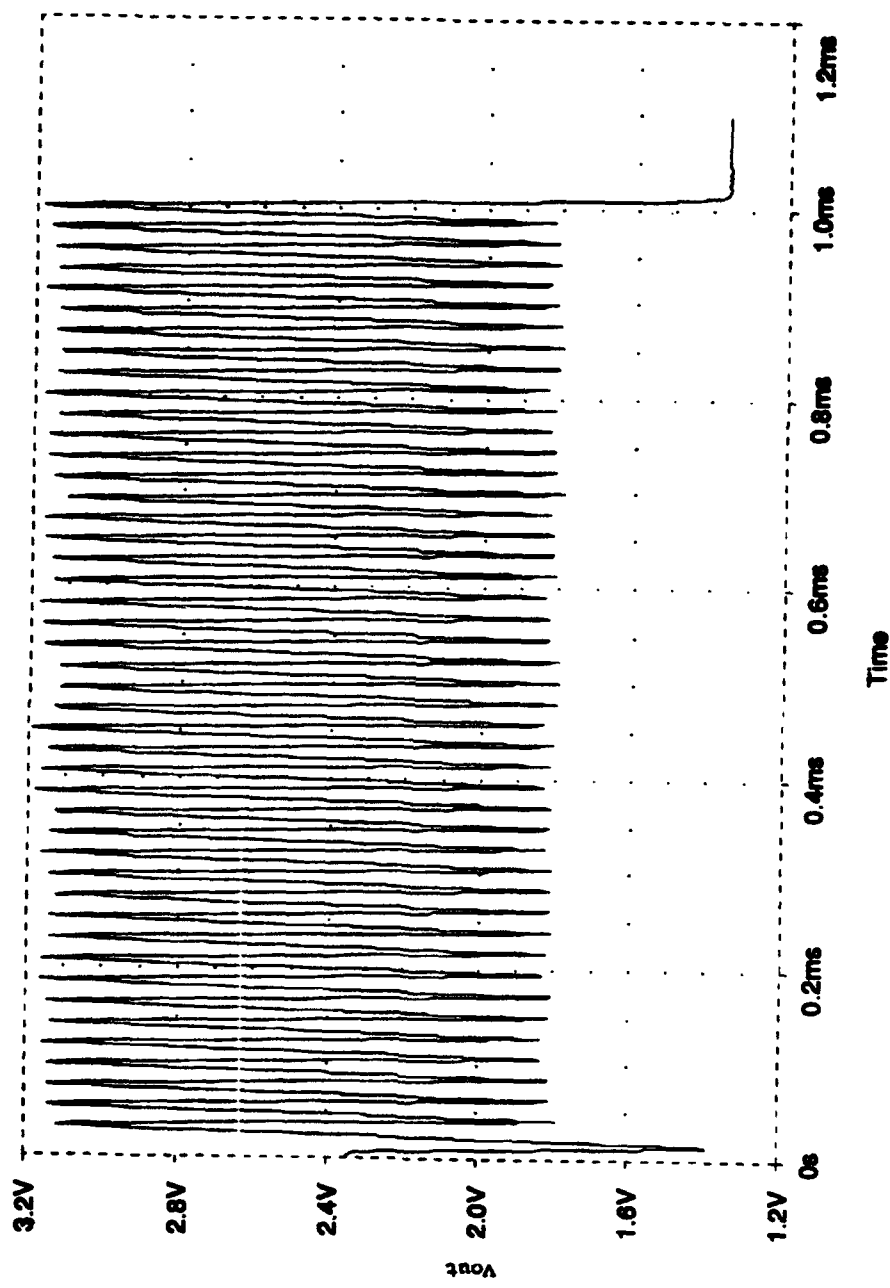


**Figure 4.9:** Mod 23 folding circuit output from a transient analysis at 1 KHz.

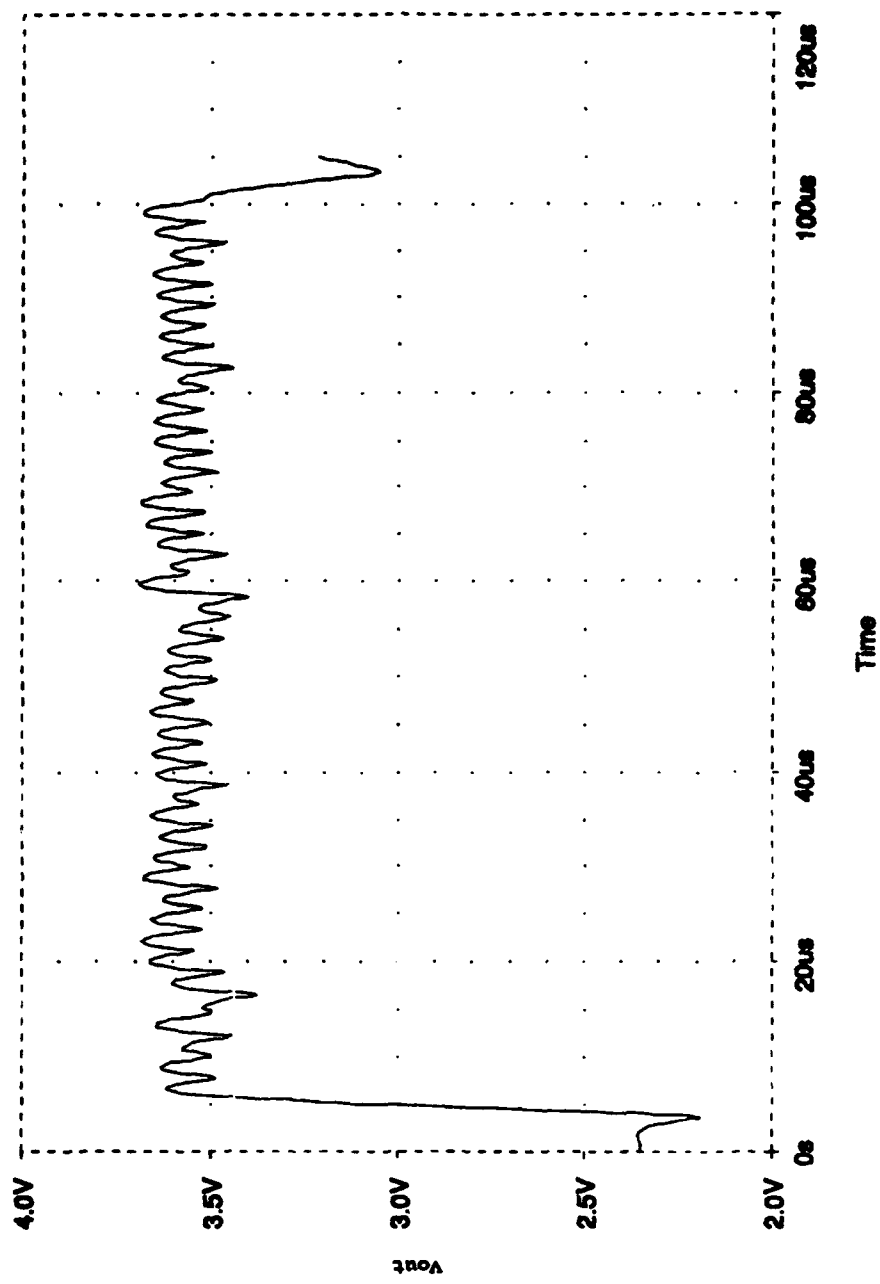


**Figure 4.10:** Mod 23 folding circuit transient analysis  
at 10 Khz.

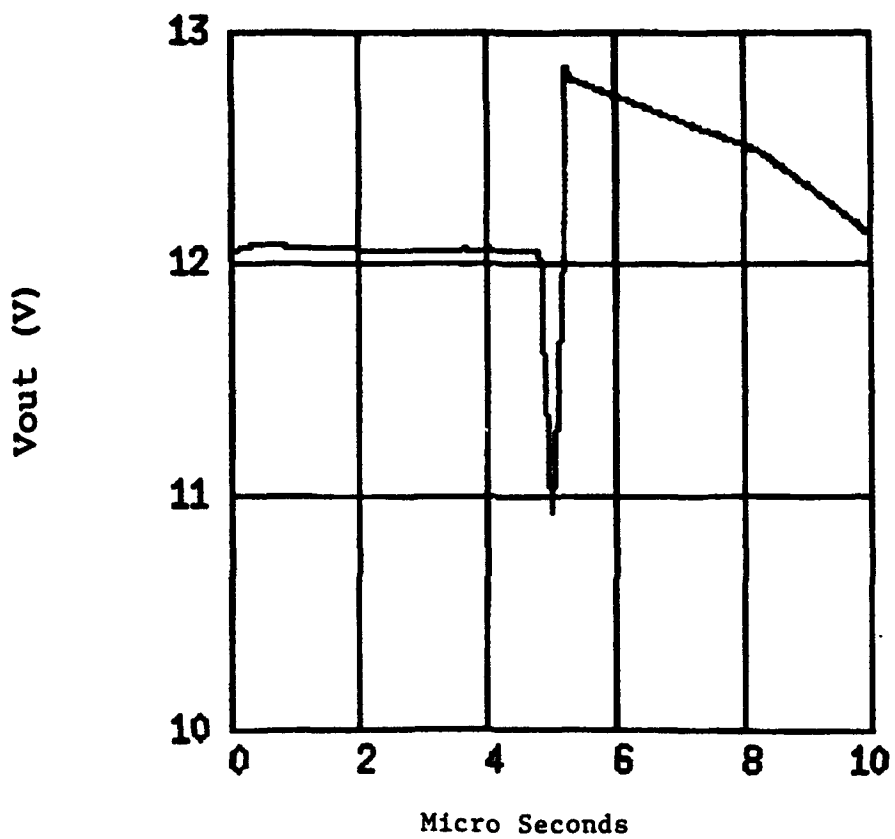


**Figure 4.11:** DC transfer curve of one fold with a 0.05 mA current source.

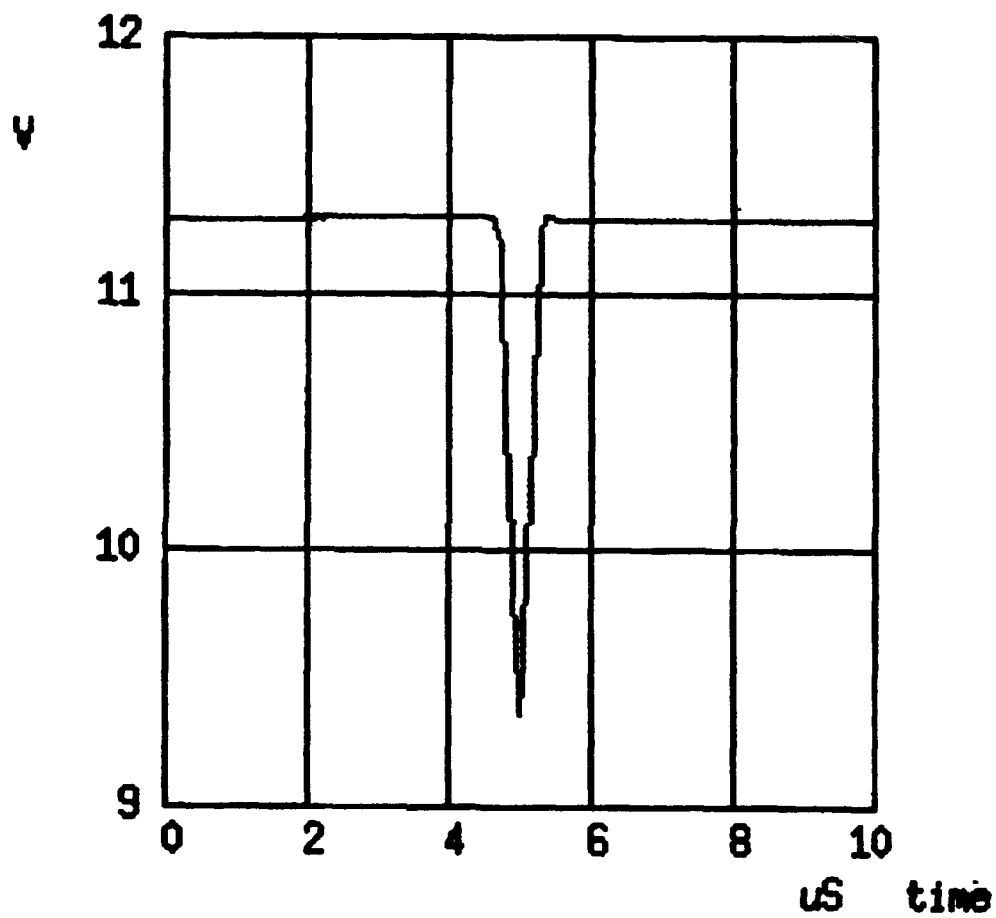


**Figure 4.12:** DC transfer curve of one fold with a current source of 0.2 mA.

flowing through the pair of differential amplifiers comprising the folding circuits was increased, the width of the folded output waveform expanded (see Figures 4.13 and 4.14). If the width of the folds become to large, then the required periodic folded output waveform cannot be achieved. Additionally, the power limitation of the device being fabricated is, in effect, an upper limit on how much the current sources can be increased. Thus, the frequency response that can be achieved in this particular design is dependent on the power limitation and on the semiconductor process that will be used for fabrication.

While investigating the frequency response difficulty, a new problem arose. As each folding circuit's output was connected together in parallel, the height of each of the folded output of the combined circuit decreased, as shown in Figure 4.15. One approach to solve this loading problem was to reduce the output resistance of the folding circuit. Various output amplifiers were connected to the folding circuits to try to reduce this value, but none solved the loading problem. One amplifier, called a voltage shifter and shown in Figure 4.16, was retained in the final design. As shown in Figure 4.17, it provided some flexibility in shifting the folded output waveform. After some adjustments to the current sources in the folding circuits, it was determined not to effect the loading problem. It was also found that by

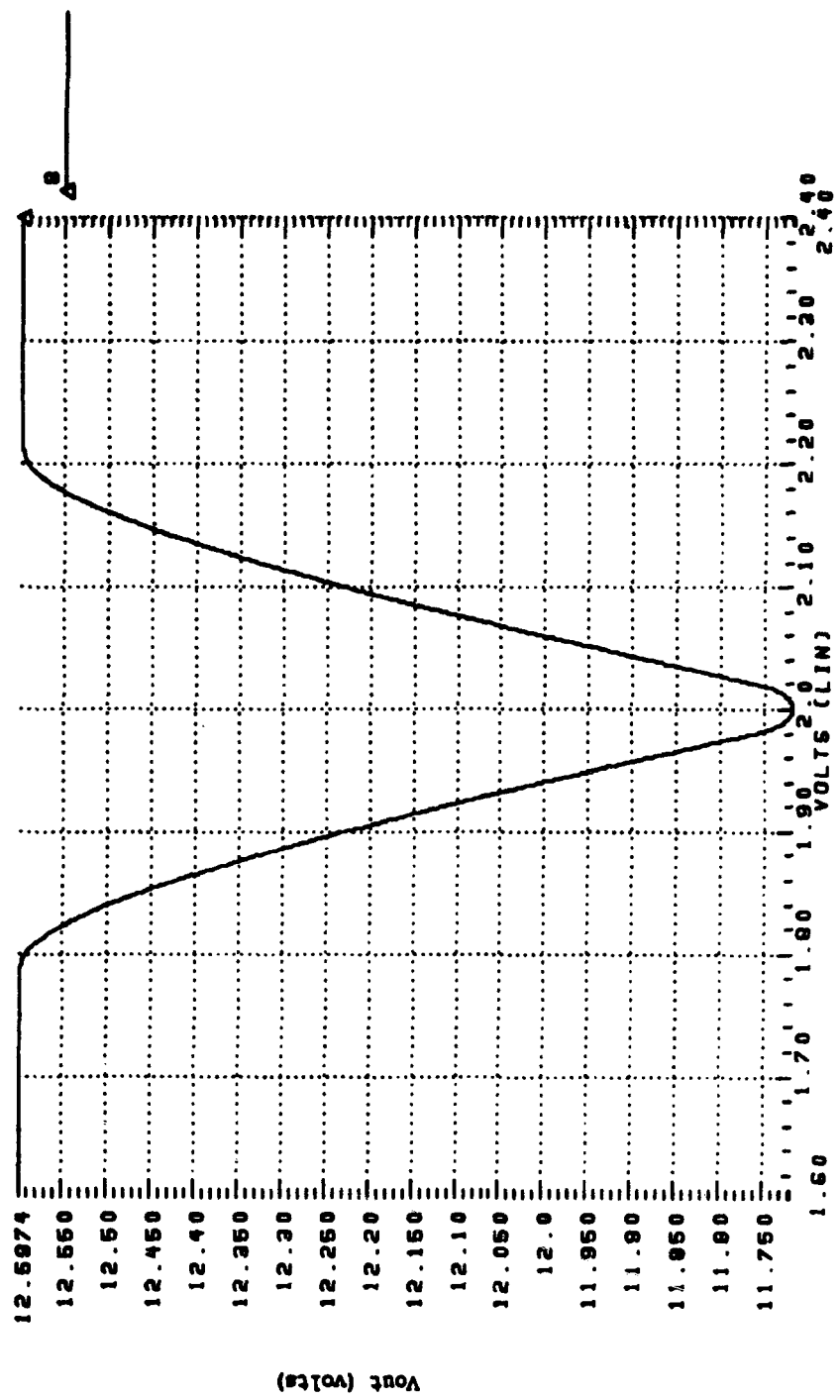


**Figure 4.13:** Narrow fold width due to small current source.

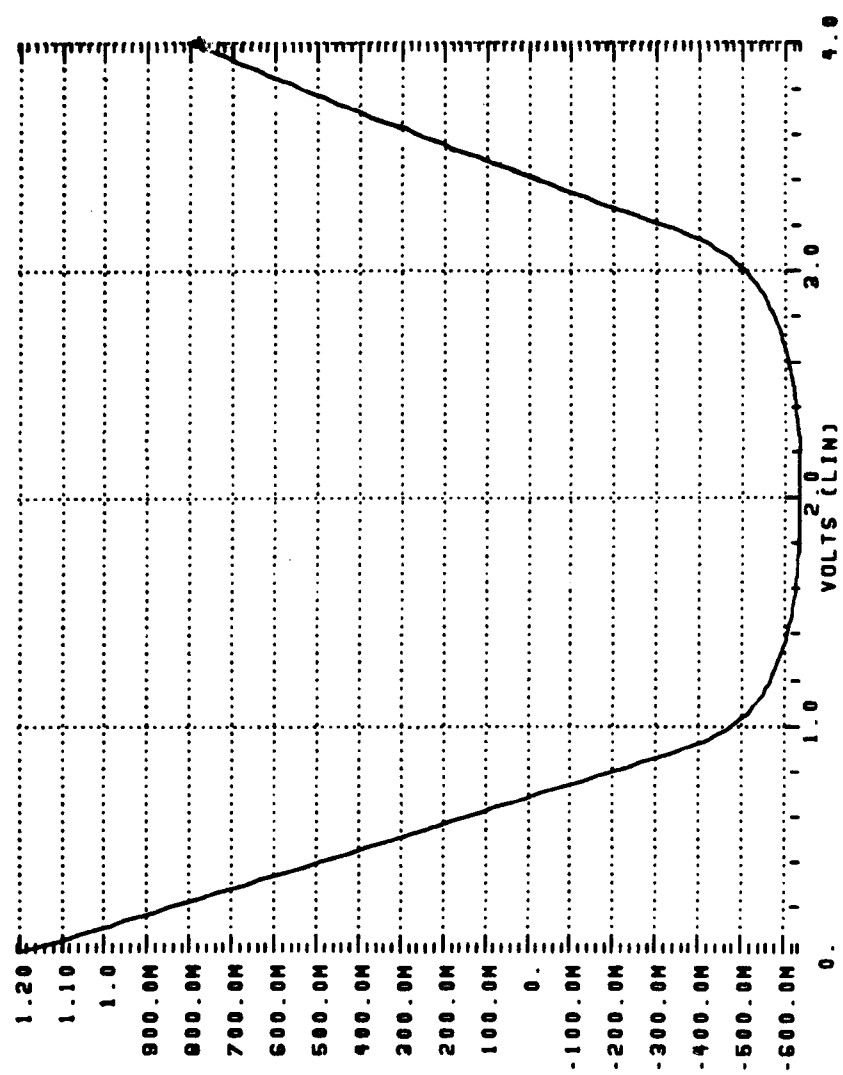


**Figure 4.14:** Wide fold width due to larger current source.

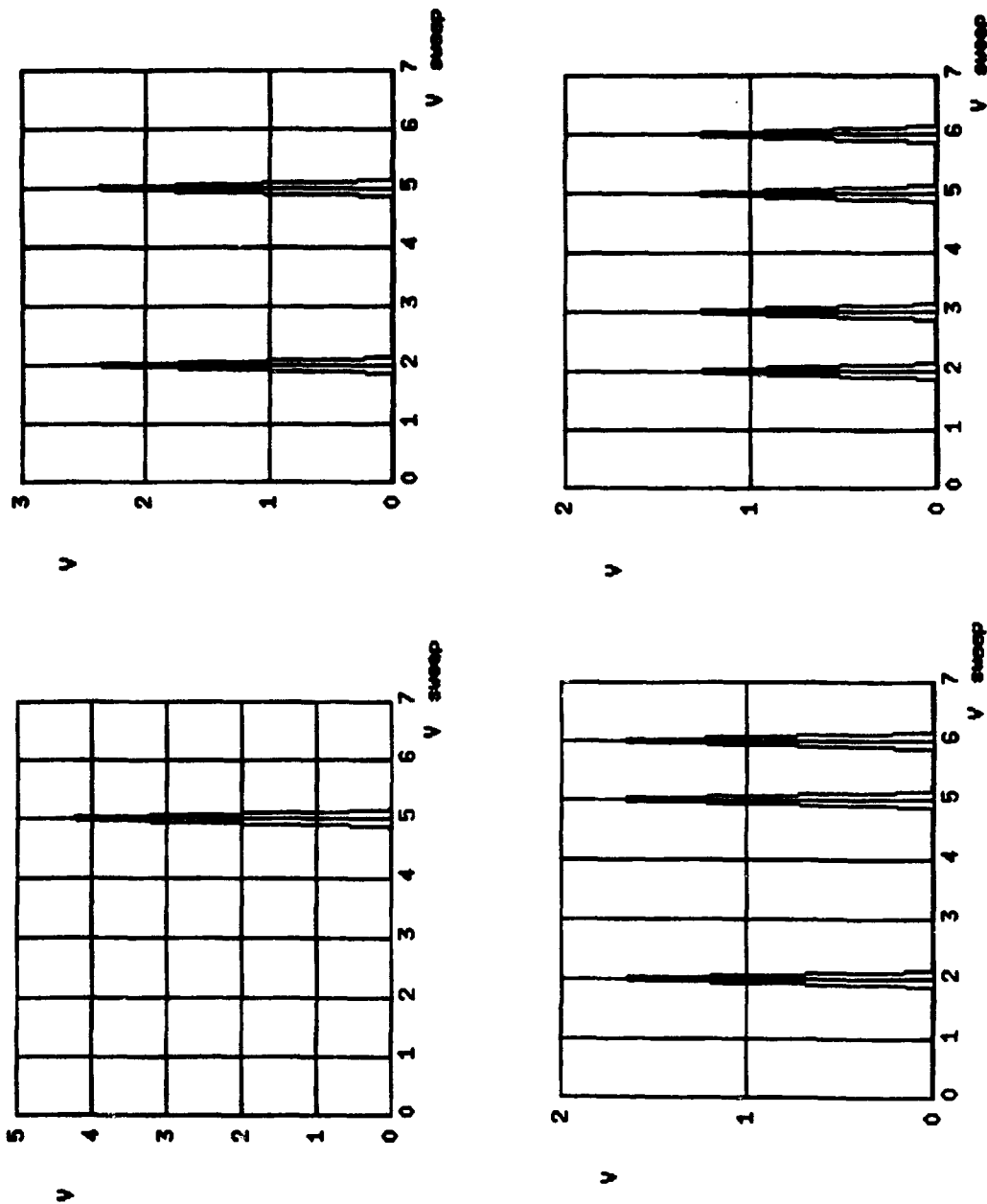


**Figure 4.15:** Loading problem in folding circuits.

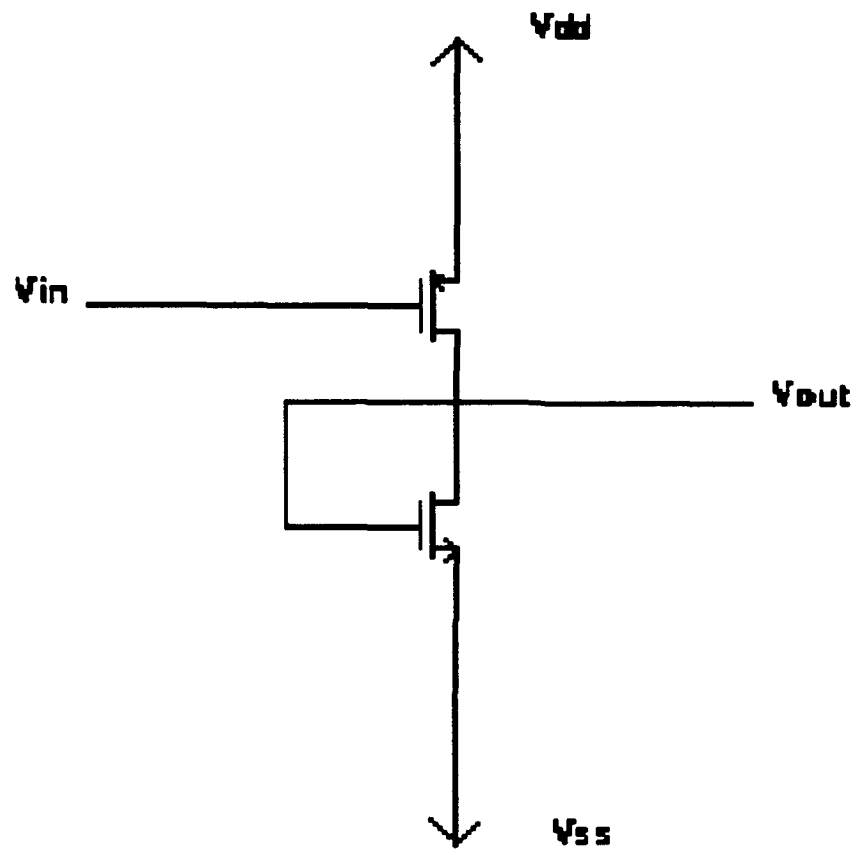


**Figure 4.16:** Voltage shifter circuit.

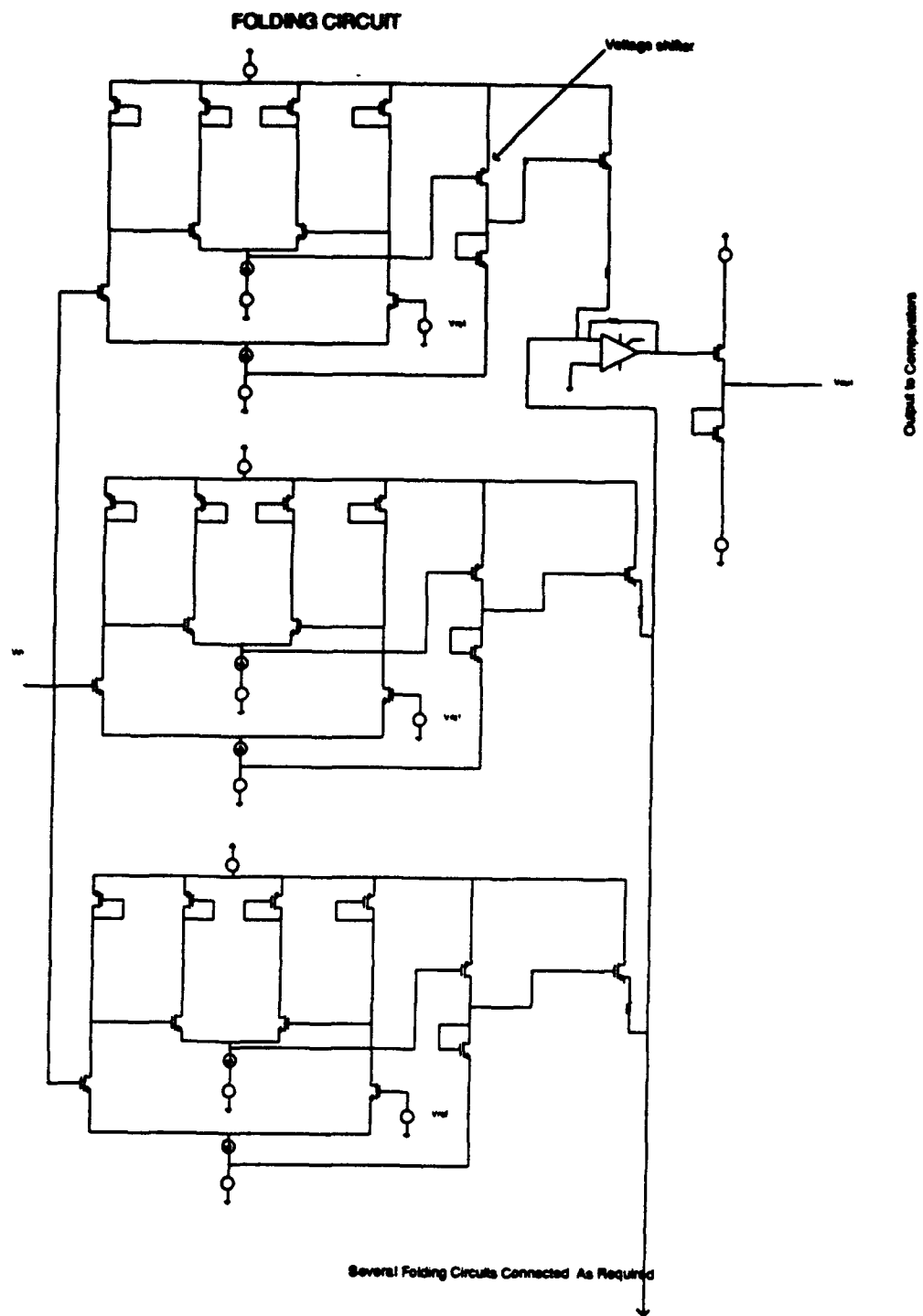


**Figure 4.17:** Revised modulus folding circuit.

removing the inverter portion of the inverter/source-follower amplifier of the folding circuit, the loading problem disappeared. The inverter was introducing some resistance as seen from the output. As a result, the output of the modulus folding circuit sees an increasing equivalent resistance as each folding circuit is connected in parallel.

Once the load problem was resolved, a modulus circuit was simulated by sweeping the input voltage from 0.0V to the dynamic range, which was 15.5V. As the simulation results in Figure 4.18 indicate, the height of the folds in the output are not consistent as the input voltage is swept. At first, it was believed that this fold height inconsistency was another loading problem and some investigation into the output resistance of the folding circuit was again undertaken. Specifically, the length and width of the MOSFET comprising the emitter follower was adjusted to achieve different gain values. However, this prove to be not productive. Another explanation for the fold height inconsistency was postulated to be the inability of the node, where all the folding circuits are connected together, to resolve its final value. Since all the folding circuit's outputs, with different output values at any given instant, are connected to this node, there might be a possibility that this node may not be able to settle to a final value. For this reason, an operational amplifier (op amp) in a summer configuration was introduced

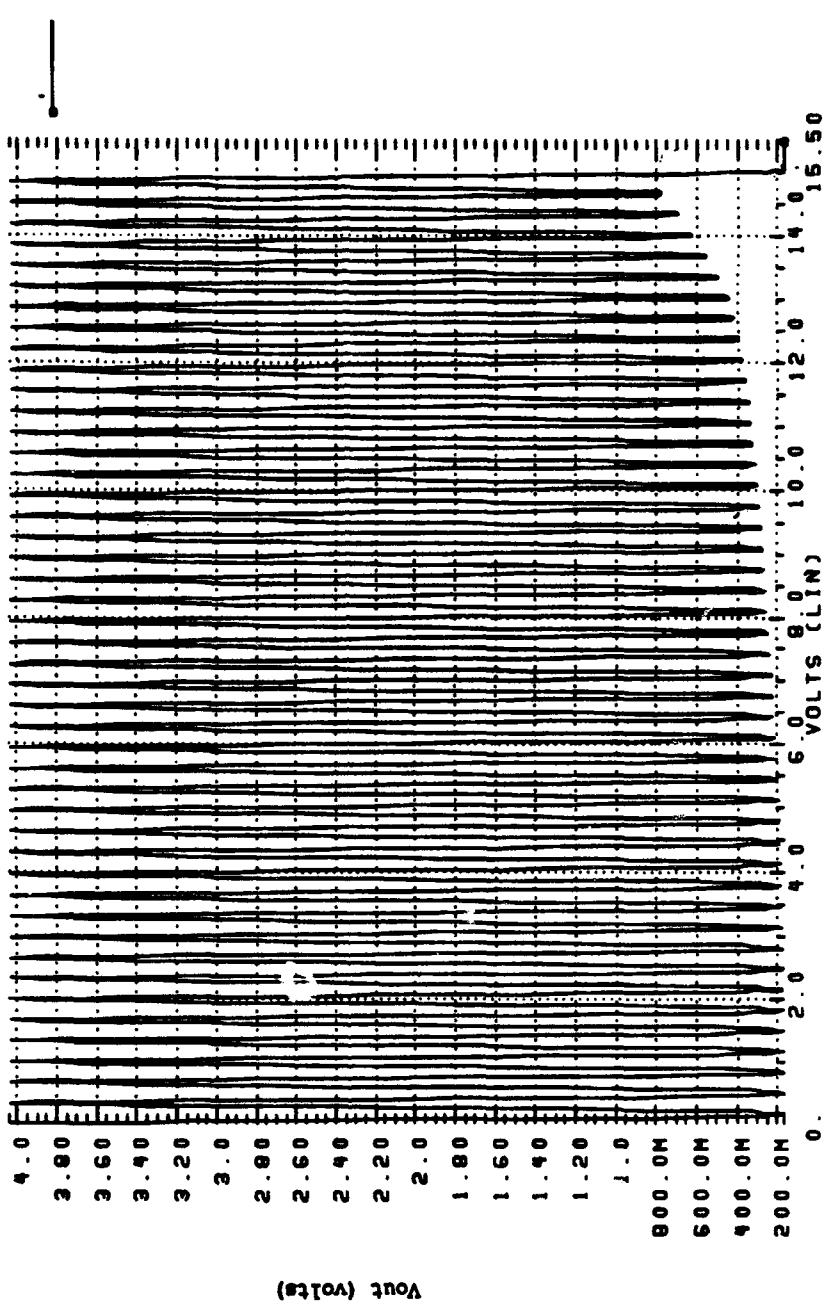


**Figure 4.18:** Fold height inconsistency in modulus folding circuit.

into the circuit, as shown in Figure 4.17. This summer would take the output of each folding circuit and sum it in a uniform manner, providing more stability for the output of the modulus folding circuit than without it. Yet, when this newly configured modulus folding circuit was simulated an unexpected result occurred. In Figures 4.19 and 4.20 the height of the folded output of the modulus folding circuit can be seen to increase and then to decrease as in the previous modulus folding circuits. Even though the opamp did not resolve this problem, it did produce an output that was shaped better than previous attempts and more conducive to the preprocessing operation.

Another test was devised to ascertain the reason for the fold height inconsistency problem. Instead of simulating the modulus folding circuit over the entire dynamic range, the simulation would be conducted in two parts, each part being associated with half the dynamic range. In each simulation only the affected folding circuits would actually be connected. If the beginning of the second simulation resulted in the output of the modulus folding circuit continuing at the point where the first half of the simulation ended, this would indicate that the problem lay somewhere in the individual folding circuit itself. If second-half simulation looked similar to the first-half simulation, then this would indicate that a loading problem exists. Figure 4.21 and 4.22 show the results of this test. As can be seen,

the test indicates that the problem is associated with the folding circuit itself.

To isolate the problem within the folding circuit, an intense investigation was conducted to determine the specific effect each element of the folding circuit had on the overall output. Table 4.2 tabulates the result of this investigation. After conducting this inquiry, it was established that the fold height inconsistency problem was a bias problem. This is because the reference voltages of each folding circuit increases in order to provide a folding process that accommodates the desired dynamic range. To compensate for the difference in the biasing of each folding circuit, the widths of the mosfets comprising the pair of diffamps were changed. Changing the widths of the mosfets kept the height and the width of each fold constant to produce a truly periodic folded output. This process took a considerable amount of time because each fold had to be simulated and adjusted individually.

Once the loading and fold height inconsistency problem was resolved, the design and simulation of the modulus folding circuits could go forward. However, some modification to the original design were made. In the final circuit, the comparator levels associated with each folding circuit were quite close. If the number of bits and numerical values of the moduli were lowered, then the total number of comparators and thus comparator levels would be smaller, as governed by

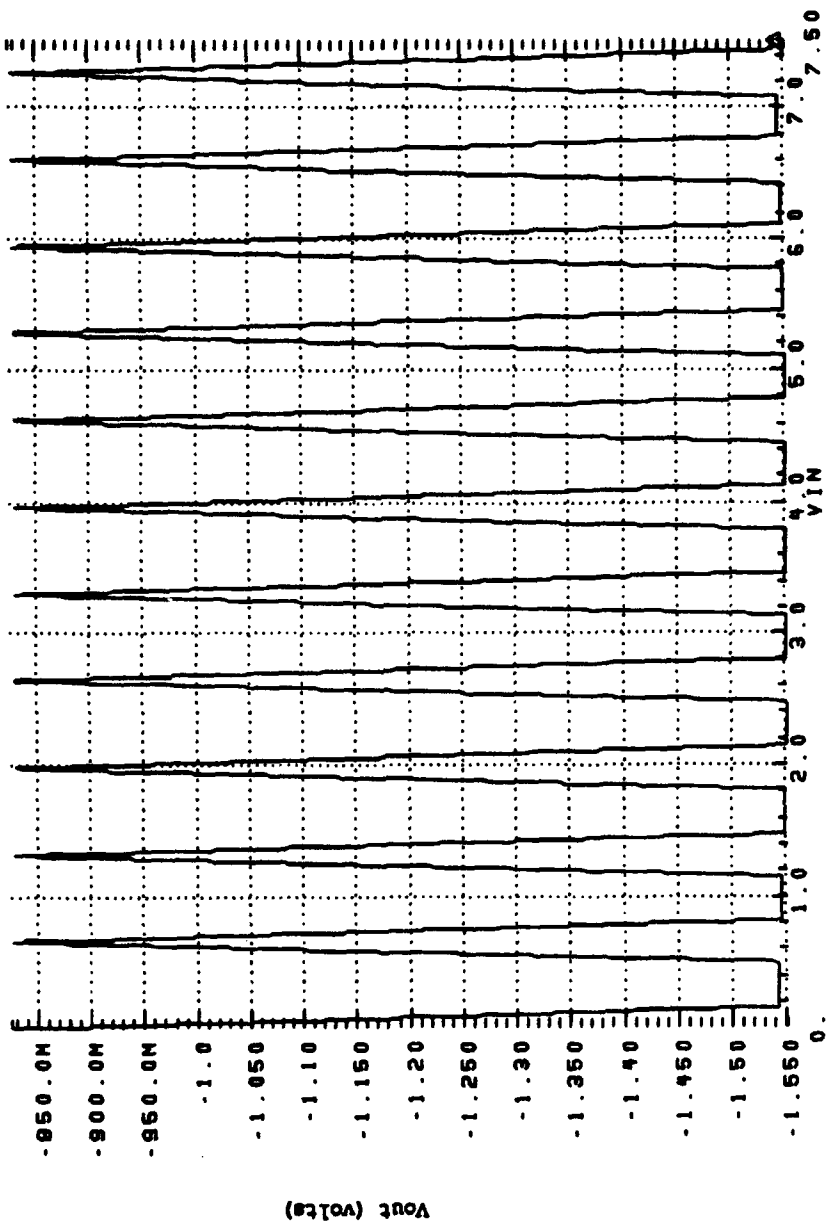


**Figure 4.19:** Fold height inconsistency variations.

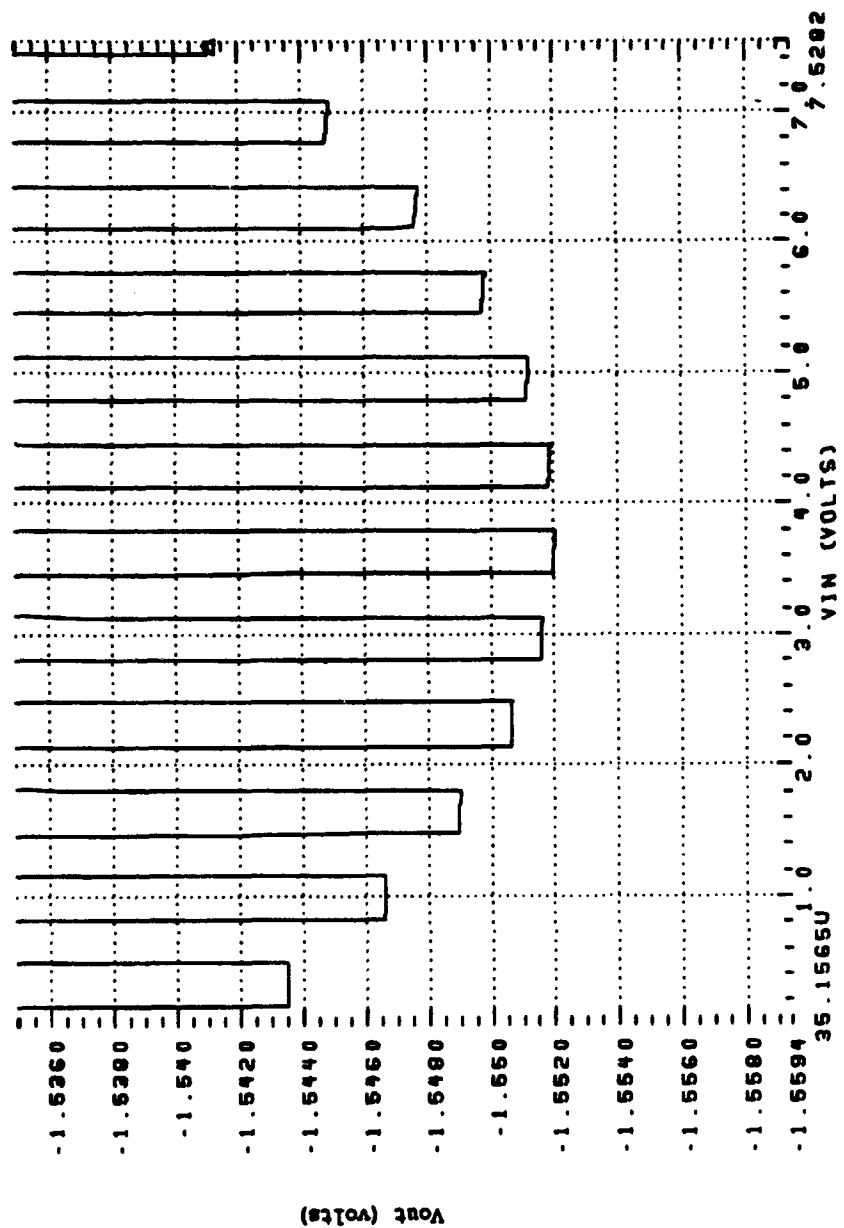


**Figure 4.20:** Bottom of folds from Figure 4.19.

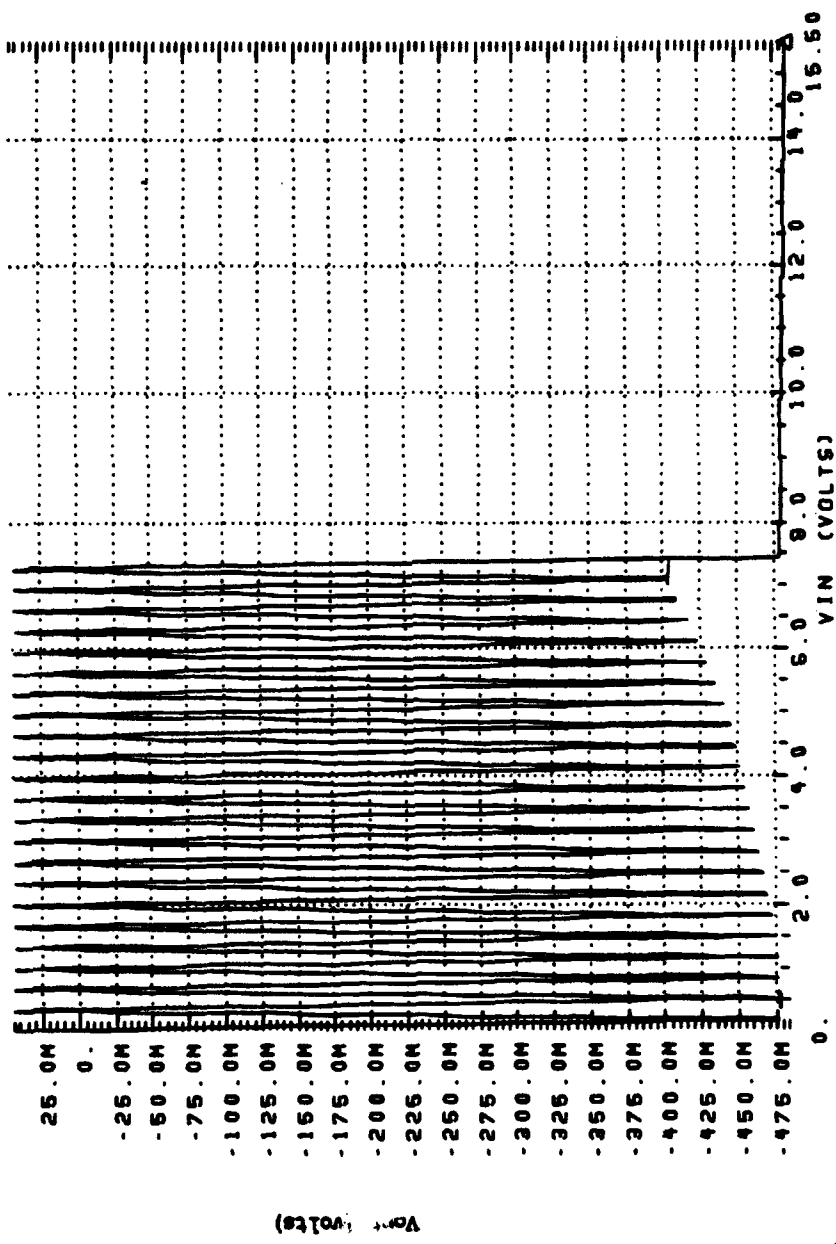
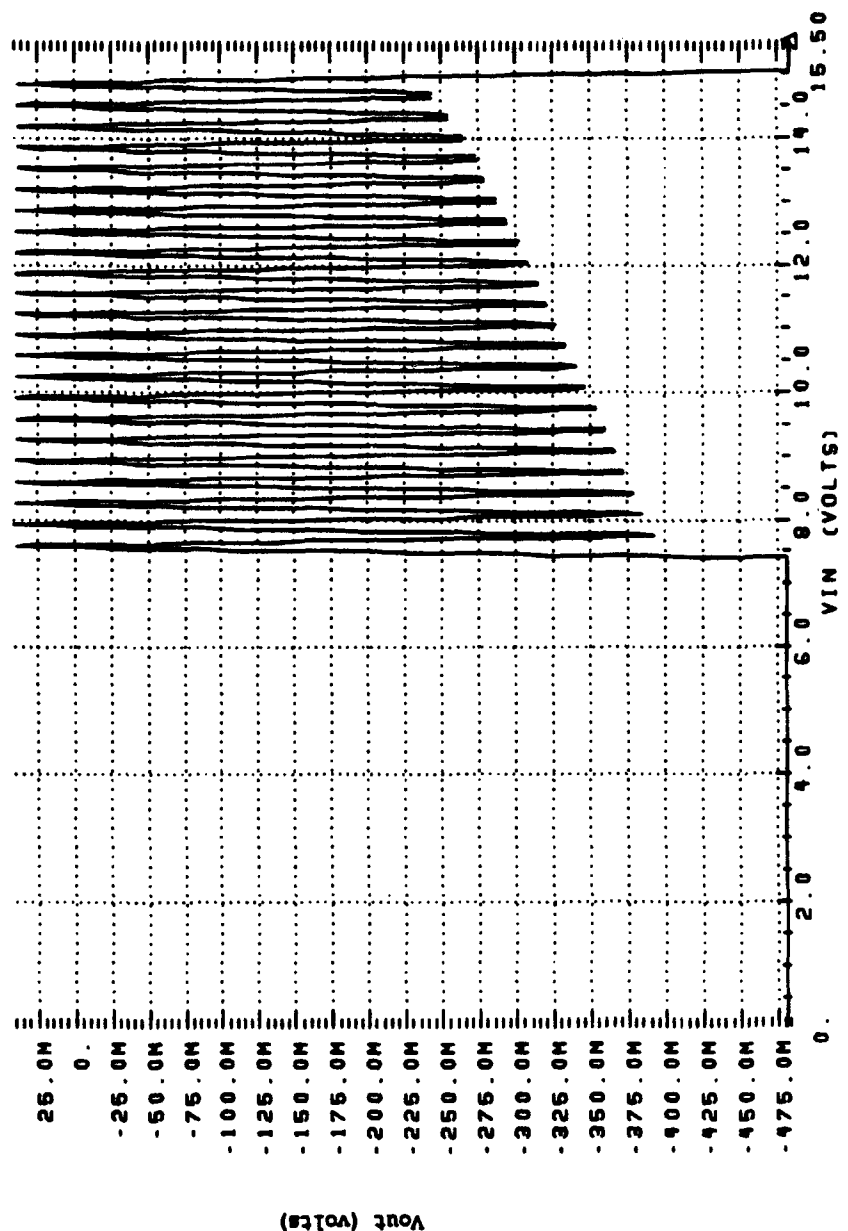


Figure 4.21: Fold height inconsistency test part 1.



**Figure 4.22:** Fold height inconsistency test part 2.

TABLE 4.2 DEVICE PARAMETERS EFFECTS ON FOLDED OUTPUT

Elements	Parameter Changed	Effect on Fold
Internal Active Loads	Increase Width	Decrease Height of Fold
Voltage Shifter Pfet	Increase Width	Fold Shifts Up in Voltage
Emitter Follower	Increase Width	Fold Shifts Up in Voltage
External Active Load	Increase Width	Fold Height Increases
Upper Diffamp	Increase Width	Fold Height Increases
Lower Diffamp	Increase Width	Fold Width Decreases
Current Sources	Increase Current	Fold Height Decreases and Fold Width Increases

the equation  $\lfloor m/2 \rfloor$ . By keeping the same fold height, the distance between each comparator level increases. This aids the comparators to discriminate more effectively. Another modification to the original design was to increase the voltage dynamic range to 15.0V. In the original design, the width of the mosfets M3 and M4 in Figure 4.1 were inordinately large in order to achieve the required fold width,  $V_{width}$ . The fold width can be calculated by using the equation,

$$V_{width} = \frac{Vm_i}{M} \quad (4.2)$$

where V is the dynamic range as expressed in volts and M is the decimal value of the dynamic range. Table 4.3 gives some results of simulation which show the relationship of the widths of the mosfets M3 and M4 and the fold width.

TABLE  
RELATIONSHIP BETWEEN DEVICE WIDTH  
AND FOLD WIDTH

Width of M3 and M4 ( $\mu\text{m}$ )	Fold Width (volts)
400	0.37
300	0.42
200	0.51

For practical purposes, mosfet widths should be below 200  $\mu\text{m}$ . From the above information and Equation 4.2, a determination can be made as to the minimum value of a modulus. For

instance, for a 10-bit resolution using 15.0V as a dynamic range, the minimum value for a set of moduli is

$$m_1 = \frac{V_{width}M}{V} = \frac{(0.51)(1024)}{15} = 34. \quad (4.3)$$

However, for a 9-bit resolution using 15.0V as a dynamic range, the minimum value for a set of moduli is

$$m_1 = \frac{(0.51)(512)}{15} \approx 17. \quad (4.4)$$

As can be seen, the change in using a 9-bit resolution and a 15.0V dynamic range is much more practical both in terms of mosfet size and the number of comparators.

To achieve a 9-bit resolution under the above constraints, the moduli chosen were 20, 23, 25, and 27. Using Equation 3.3, the SNS dynamic range for this set of moduli is

$$\hat{M} = \frac{1}{2}(20)(27) + (23)(25) = 845 \quad (4.5)$$

This is well above the 9-bit resolution of 512. Using Equation 4.2, the fold widths or periods for each of the moduli are

$$V_{width} = \frac{(15V)(20)}{512} = 0.59V \quad (4.6)$$

$$V_{width_{23}} = \frac{(15V)(23)}{512} = 0.67V \quad (4.7)$$

$$V_{width_{25}} = \frac{(15V)(25)}{512} = 0.73V \quad (4.8)$$

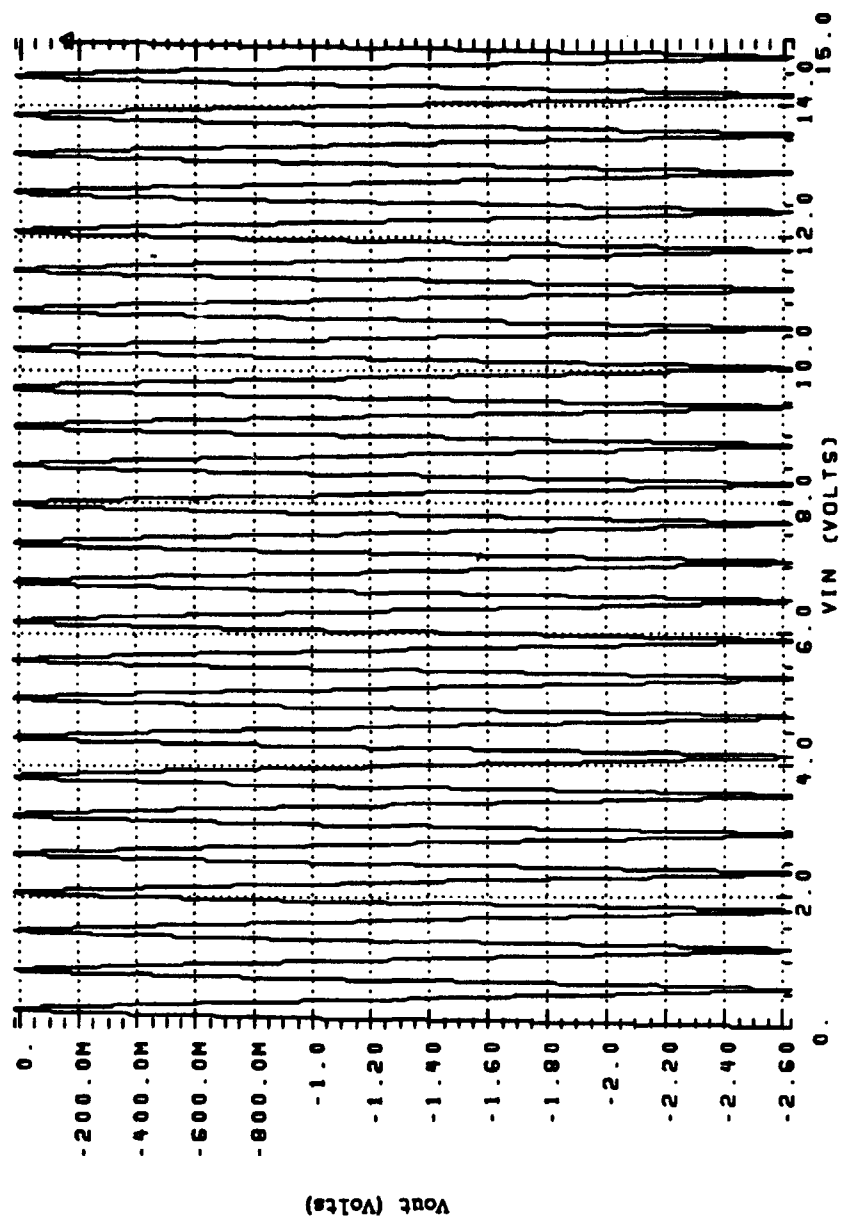
$$V_{width_{27}} = \frac{(15V)(27)}{512} = 0.79V. \quad (4.9)$$

Figure 4.23 shows the output of the mod 20 folding circuit, demonstrating the validity of the derived design parameters.

Before further progress was made with this modified design, a new version of the symmetrical number system was introduced, as was discussed in Chapter III. Because of the benefits discussed in Chapter III, the decision was made to modify the design again in order to incorporate the new symmetrical number system as the basis for the analog preprocessing architecture. To achieve a 9-bit resolution, the set of moduli chosen were  $m_1=7$ ,  $m_2=8$ , and  $m_3=11$ . Using Equation 3.6, the new SNS dynamic range for this set of moduli is

$$\hat{M} = \prod_{i=1}^n m_i = (7)(8)(11). \quad (4.10)$$

This is well above the 9-bit resolution of 512. Under this new symmetrical number system, the fold width of period can be calculated to be



**Figure 4.23:** Modulus 20 folding circuit output.

$$V_{width} = \frac{2m_i V}{M}. \quad (4.11)$$

Using Equation 4.11, the fold width or period for each of the moduli is

$$V_{width_1} = \frac{(15V)(14)}{512} = 0.41V \quad (4.12)$$

$$V_{width_2} = \frac{(15V)(16)}{512} = 0.47V \quad (4.13)$$

$$V_{width_{11}} = \frac{(15V)(22)}{512} = 0.67V. \quad (4.14)$$

From these parameters and the generic modulus folding circuit in Figure 4.1, each modulus folding circuit as was designed and simulated by applying an input which ramped from 0.0V to 15.0V. Figures 4.24-26 show the results of these simulations which validate the strength of the design. Figures 4.27-29 were used to determine the comparator levels for each modulus folding circuit. In the new SNS, the number of comparator levels required is  $m_i - 1$ . As was discussed before in the beginning of this chapter, the comparator threshold levels are determined by quantizing the period of a particular fold by two times the desired number of threshold voltages. As the input voltage,  $V_{in}$ , arrives at one of these quantization points as it sweeps from 0.0V to 15.0V, the value of the folded output at that point would correspond to a threshold voltage level. The threshold voltages for each of the moduli used in this final design are tabulated in Tables 4.4-4.6.

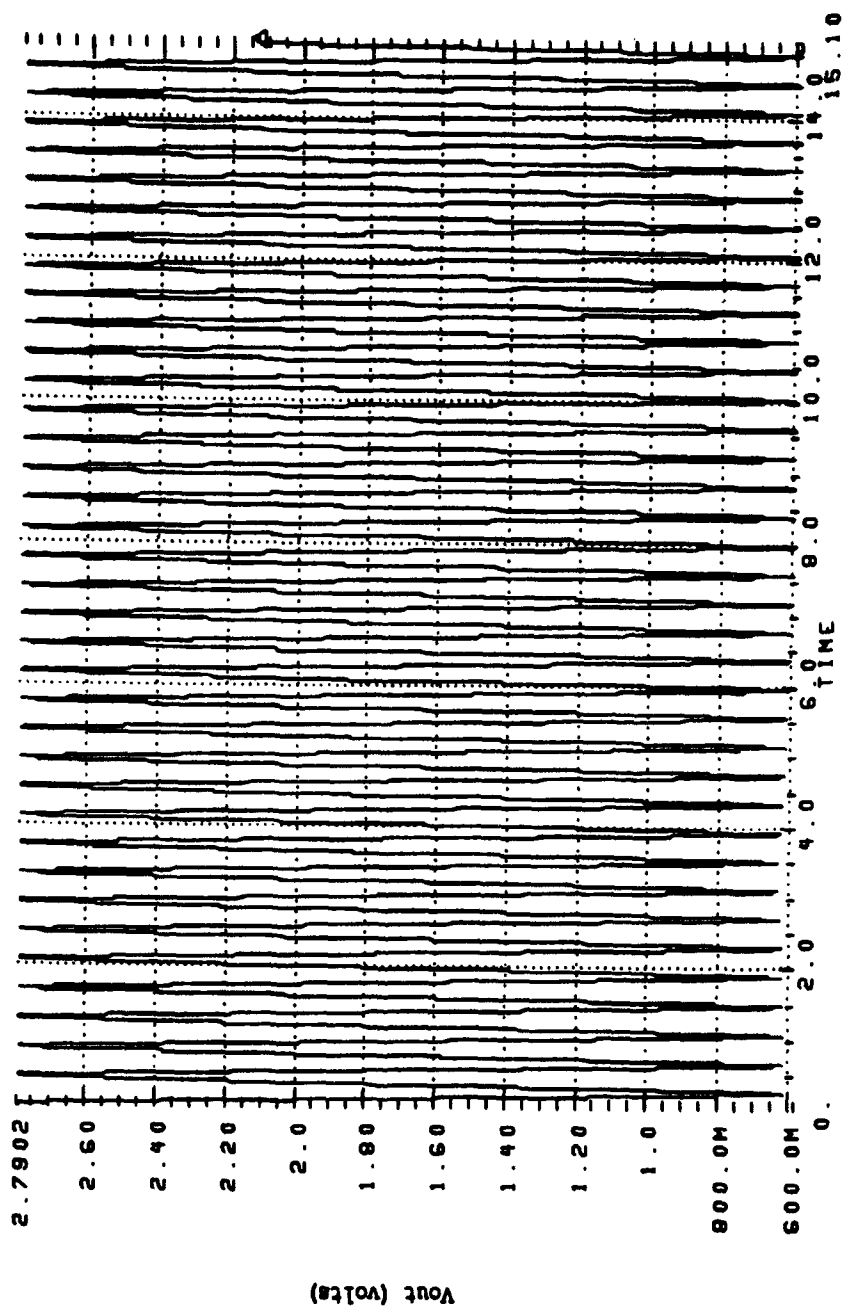


**Figure 4.24:** Modulus 7 folding circuit output.

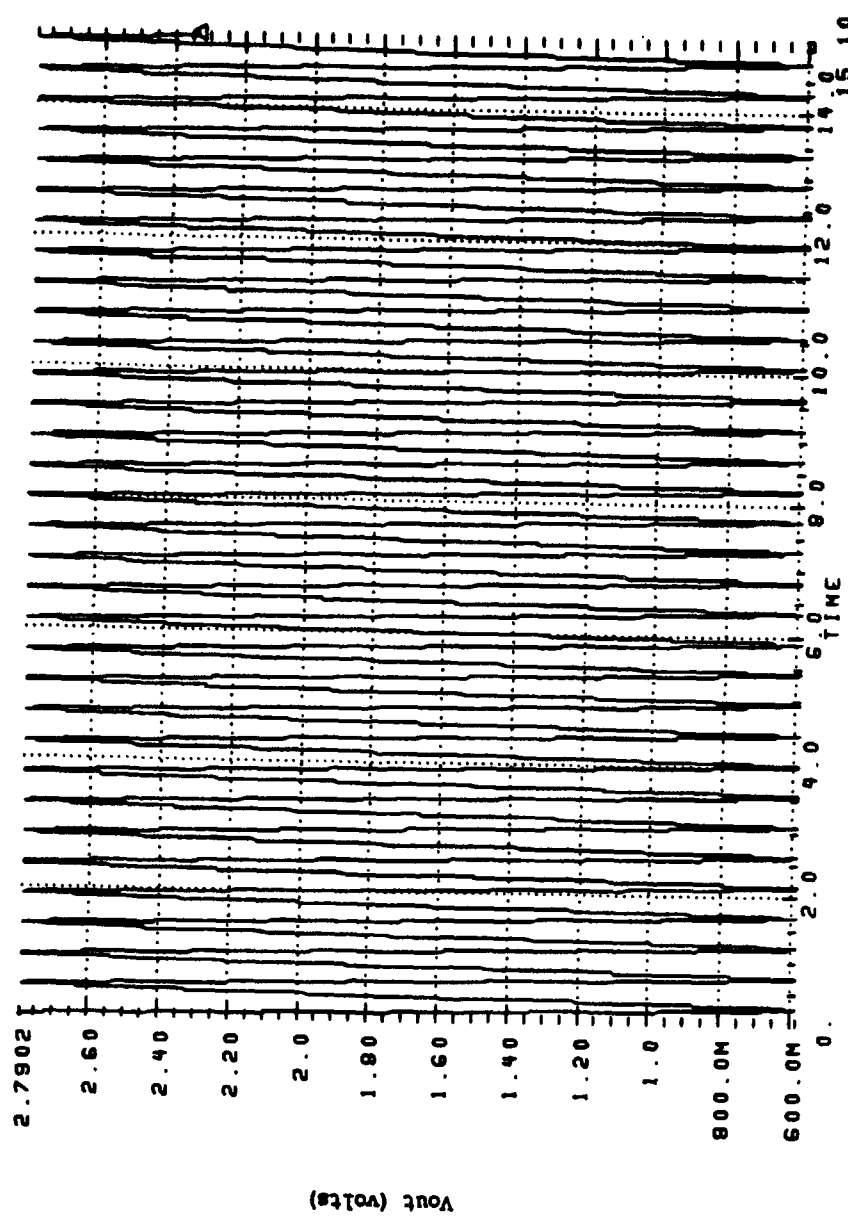


**Figure 4.25:** Modulus 8 folding circuit output.

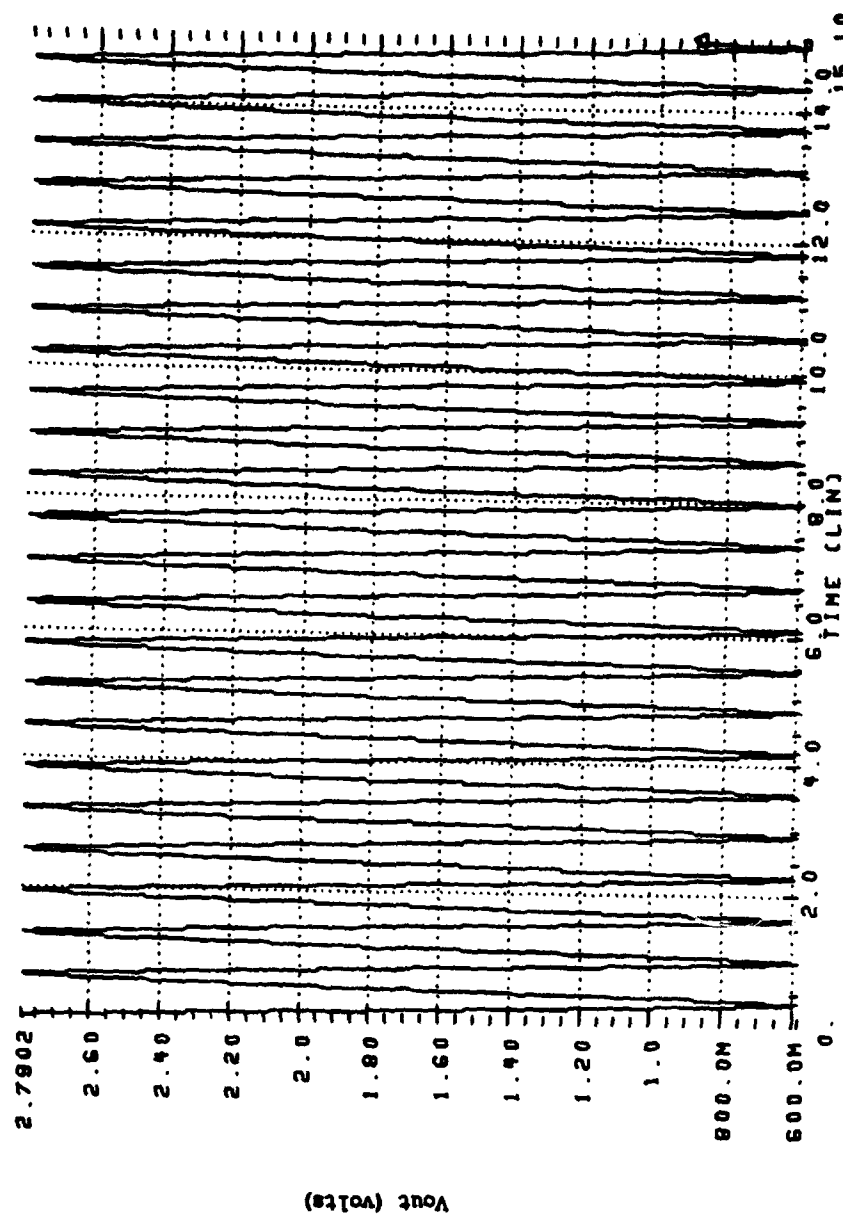


**Figure 4.26:** Modulus 11 folding circuits output.

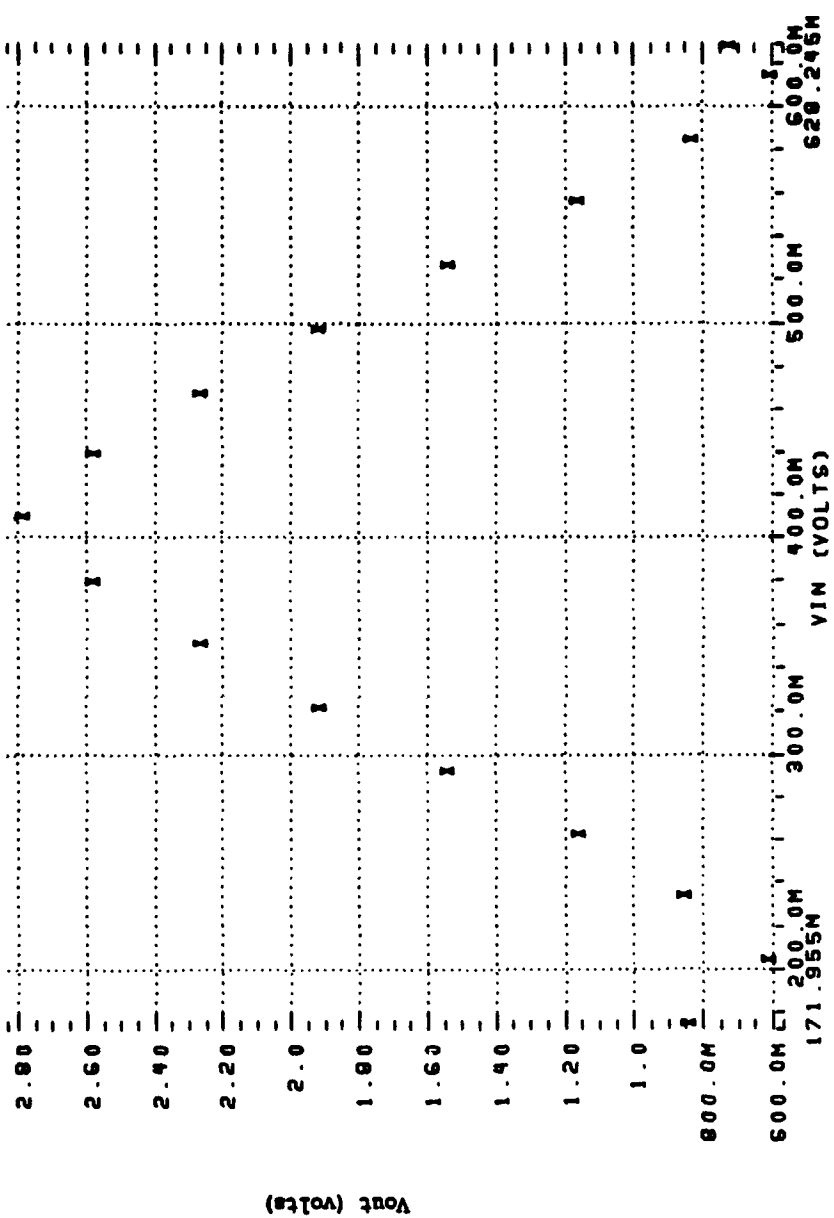


**Figure 4.27:** Modulus 7 comparator levels.

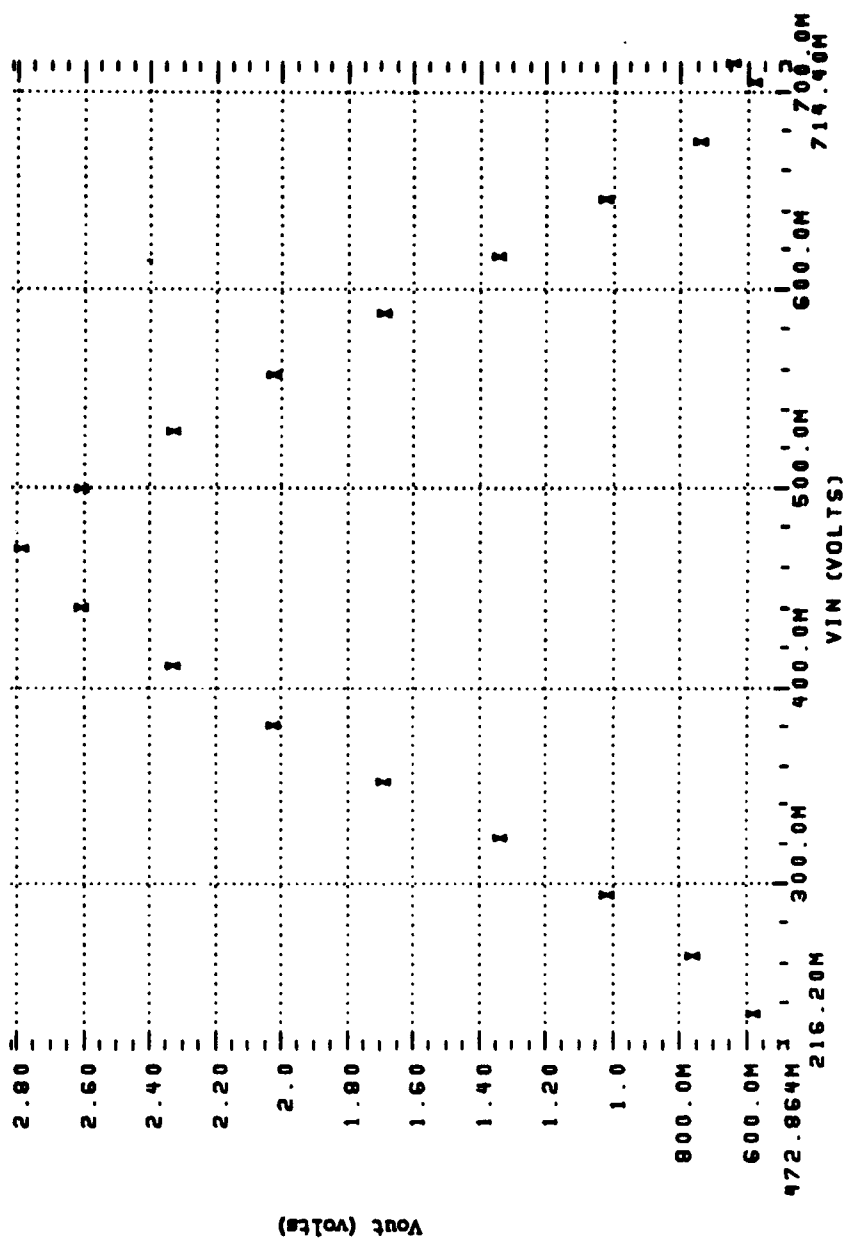


**Figure 4.28:** Modulus 8 comparator levels.

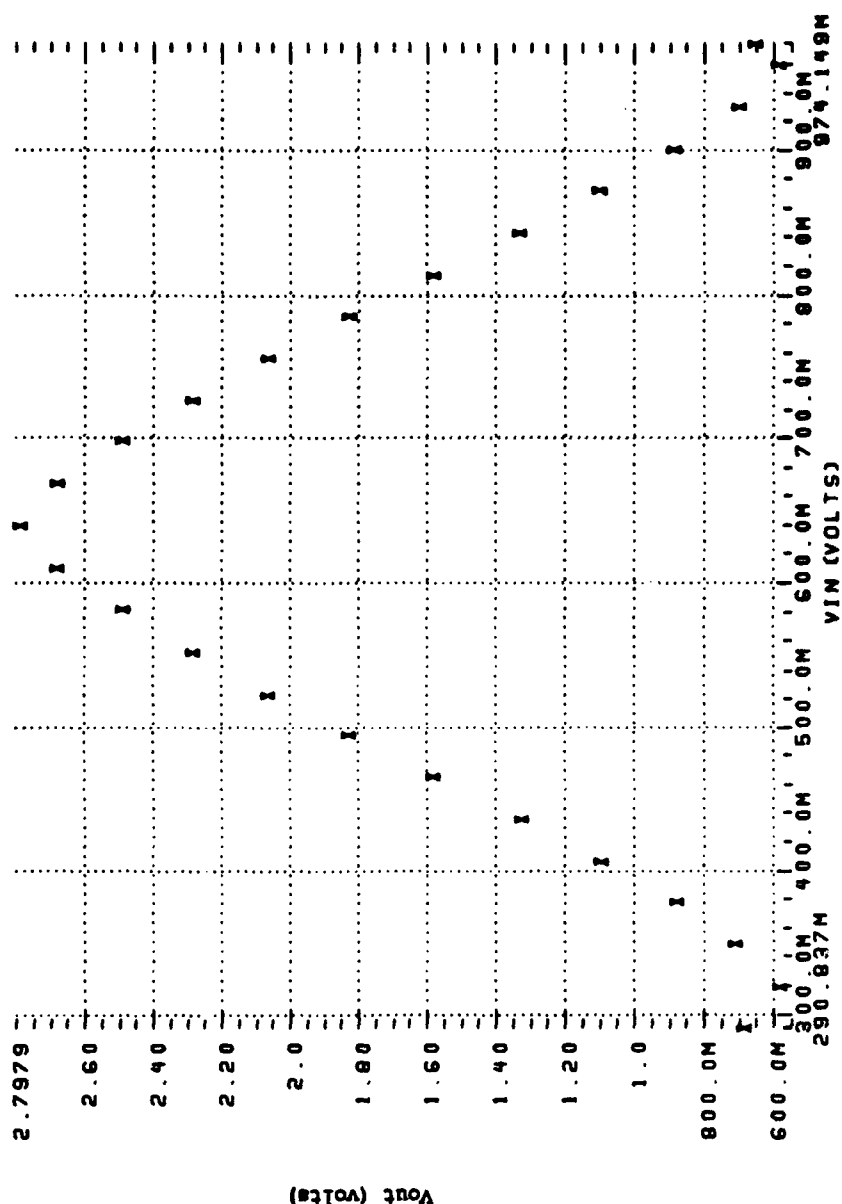


**Figure 4.29:** Modulus 11 comparator levels.

**TABLE 4.4 MOD 7 COMPARATOR LEVELS**

Voltage Threshold Level	Value (Volts)
1	2.58
2	2.27
3	1.92
4	1.54
5	1.16
6	0.858

**TABLE 4.5 MOD 8 COMPARATOR LEVELS**

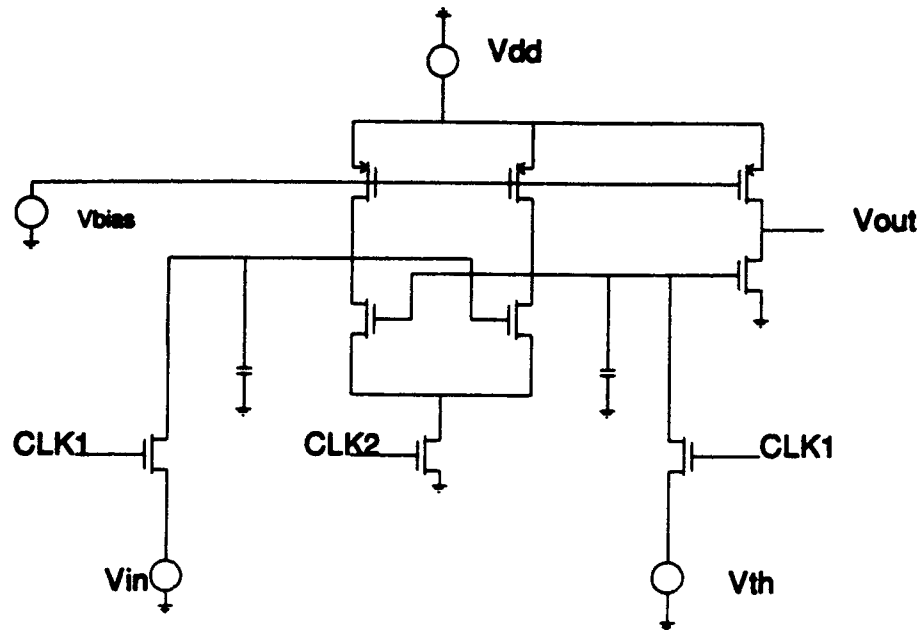
Voltage Threshold Level	Value (Volts)
1	2.61
2	2.33
3	2.02
4	1.69
5	1.34
6	1.02
7	0.762

TABLE 4.6 MOD 11 COMPARATOR LEVELS

Voltage Threshold Level	Value (Volts)
1	2.68
2	2.49
3	2.28
4	1.07
5	1.83
6	1.58
7	1.33
8	1.09
9	0.882
10	0.714

## 2. Comparator Design and Simulation

After the design of the folding circuits were finalized, the next step was to design and simulate a comparator circuit which would not only effectively quantize the folded output but be able to effectively sample it. The sample-and-hold feature is important in order for the comparators to be able resolve a quickly changing circuit. The first attempted design was a clocked comparator shown in Figure 4.30. In this design, two non-overlapping clocks are applied to the gates of a pair of mosfets. One of these mosfets' drain is connected to output of the modulus folding circuit, while the other mosfets' drain is connected to a predetermined threshold voltage. The operation of this comparator is divided into two phases, charge and evaluate. During the charge phase, the CLK1 signal is high, and the CLK2 signal is low. At this point, both the input voltage from the output of the modulus folding circuit and the threshold voltage are sampled. During the evaluate phase, the CLK1 signal is low and the CLK2 signal is high. The diffamp comprised of mosfets M4 and M7 will recursively evaluate the values of the input and the threshold voltages. If the threshold voltage is larger than the input voltage, then the comparator output will be high, or true as shown in Figure 4.31. If the input voltage is higher than the threshold



**Figure 4.30:** Clocked comparator circuit diagram.

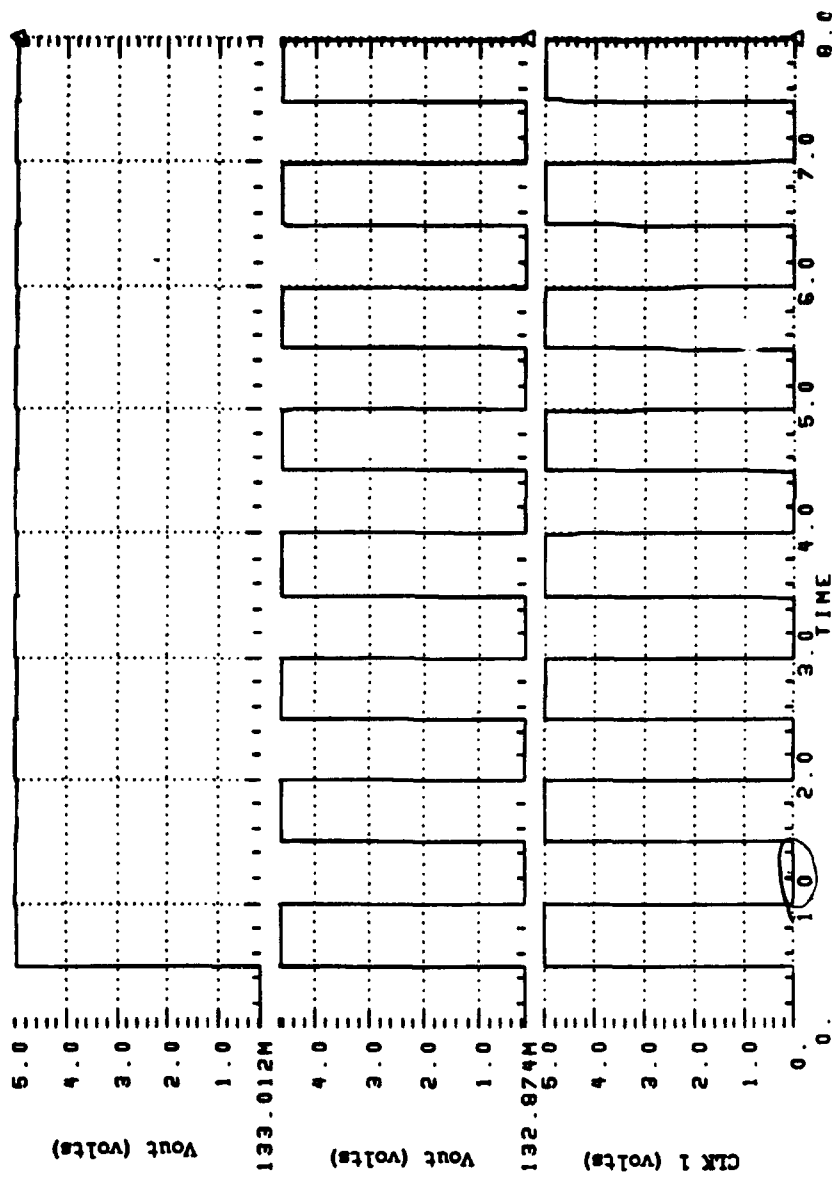


**Figure 4.31:** Clocked comparator's output when threshold voltage is greater than the input voltage.

voltage, then the comparator output will be low, or false as shown in Figure 4.32.

Once this comparator was simulated and found to operate correctly, the appropriate number of these comparators was connected to the modulus folding circuits and simulated. The initial spice simulation that was conducted was a transient analysis of a small segment of the dynamic range. The clocks were operating at a slow rate of 100Hz. As can be seen from the results in Figure 4.33, there where considerable oscillations, not only in the output of the comparator but also in the input which is the output of the modulus folding circuit. It appeared that the clock signals were being fed back into the modulus folding circuit. Even after some adjustments to the biasing of the comparator, the same phenomena continued.

Since this clocked comparator did not operate effectively, a new comparator was designed. Figure 4.34 is a schematic of this new design. Basically, this design consisted of a comparator, composed of a differential amplifier and an inverting output buffer, and a sample-and-hold circuit, comprised of a transmission gate and a capacitor. This comparator operated similarly to the clocked comparator. When the threshold voltage was larger than the input voltage, the output of the comparator would be high. However, when the threshold voltage was less than the voltage, the output of the comparator would be low. The

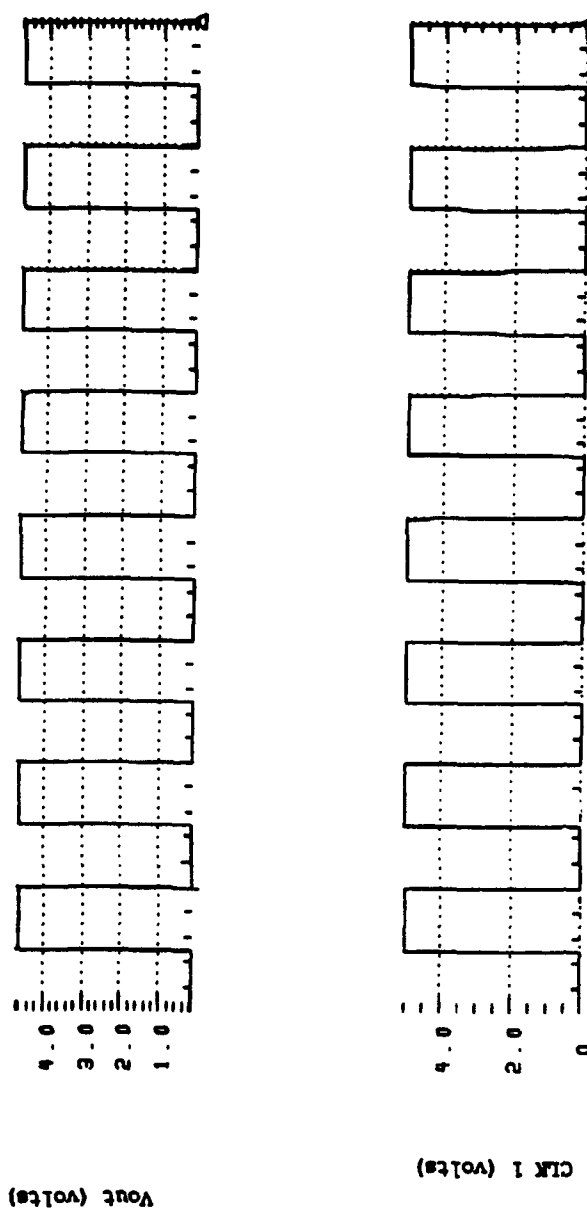


**Figure 4.32:** Clocked comparator's output when the threshold voltage is less than the input voltage.

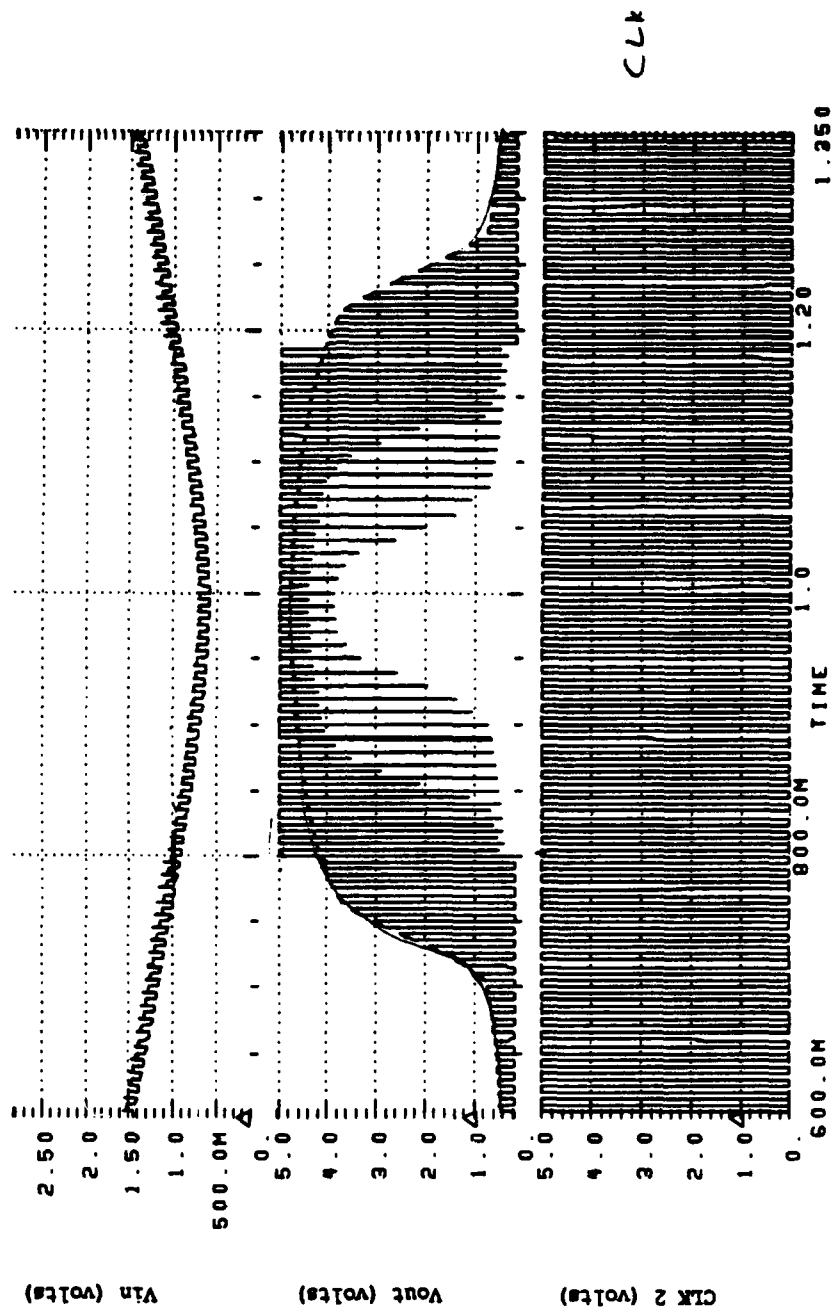


**Figure 4.33:** Clocked comparator output with oscillations.

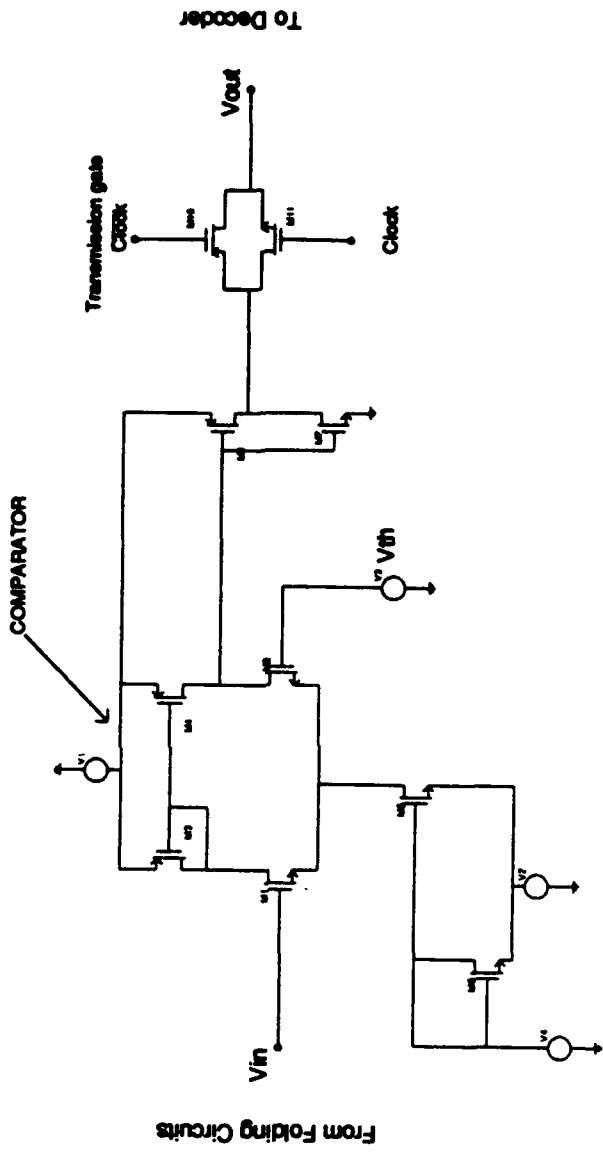


**Figure 4.34:** Static comparator with transmission gate.

sample-and-hold section of the comparator is controlled by two non-overlapping clocks, CLK1 and CLK2. When the CLK1 signal is high and the CLK2 signal is low, the transmission gate lets the signal pass through to charge the capacitor. When the CLK1 signal is low and the CLK2 signal is high, the transmission gate blocks the signal from passing through the gate, which allows the capacitor to retain its charge until CLK1 is high again (see Figure 4.35).

These comparators were connected to the modulus folding circuits, and spice transient analysis simulations were conducted. Figures 4.36-4.47 show the results of these simulations. It can be seen that the comparators were operating appropriately, going high when the output of the modulus folding circuit reaches the value of the predetermined threshold voltage. Appendix A is one of the spice input file which was used to conduct this simulation.

#### B. DIGITAL CIRCUIT DESIGN

After the modulus folding circuits and comparators were designed and simulated successfully, the design and simulation effort was turned to the digital subsystem. The digital subsystem consists of a decoder and a programmed logic array (PLA), as shown in Figure 1.8 and 3.3. The decoder is divided into two functions. The first of which is to transform the comparator output values of each modulus into a binary thermometer format. Table 4.7 depicts the truth table, which

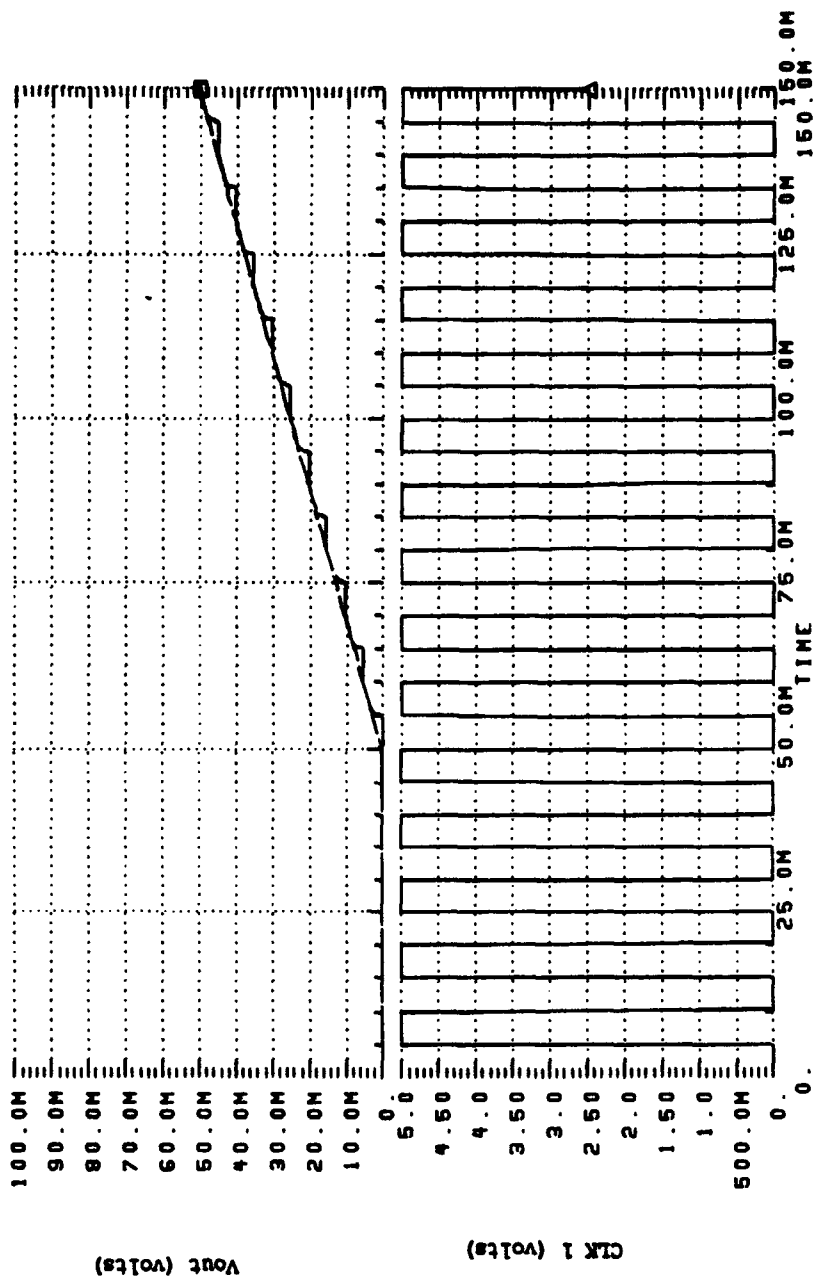


**Figure 4.35:** Operation of a transmission gate.

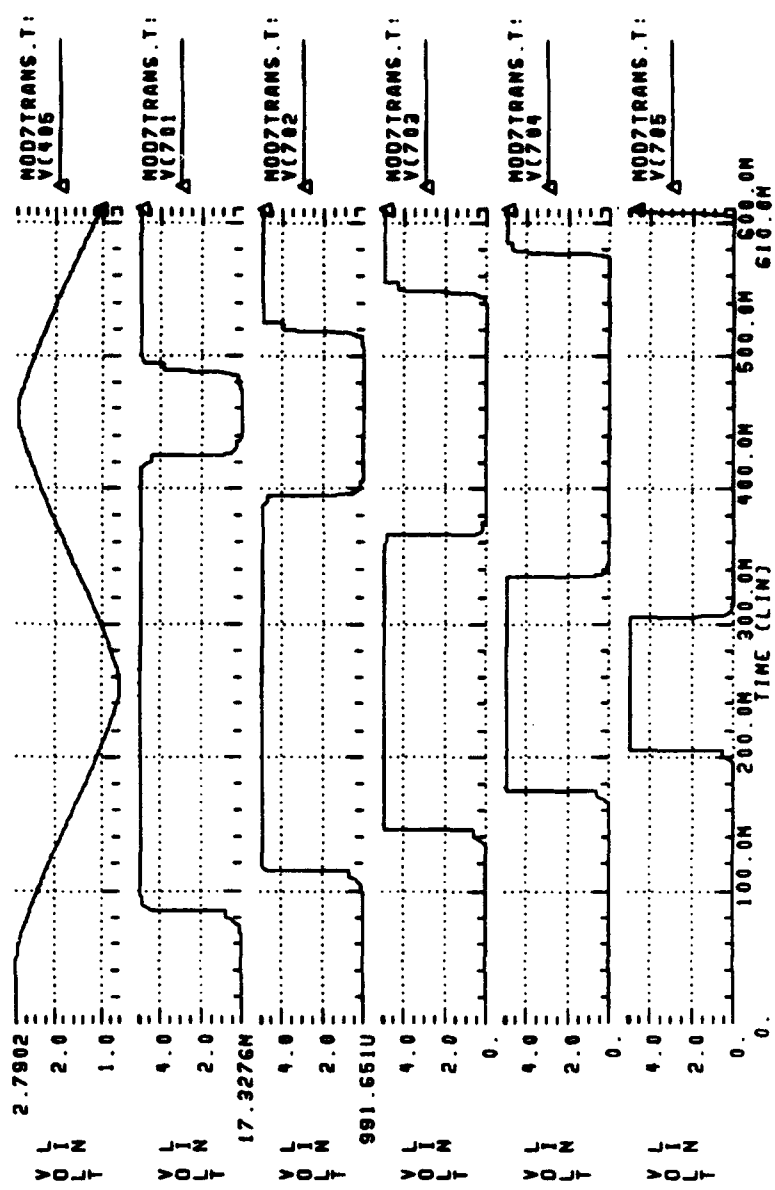


**Figure 4.36:** Mod 7 comparator outputs.

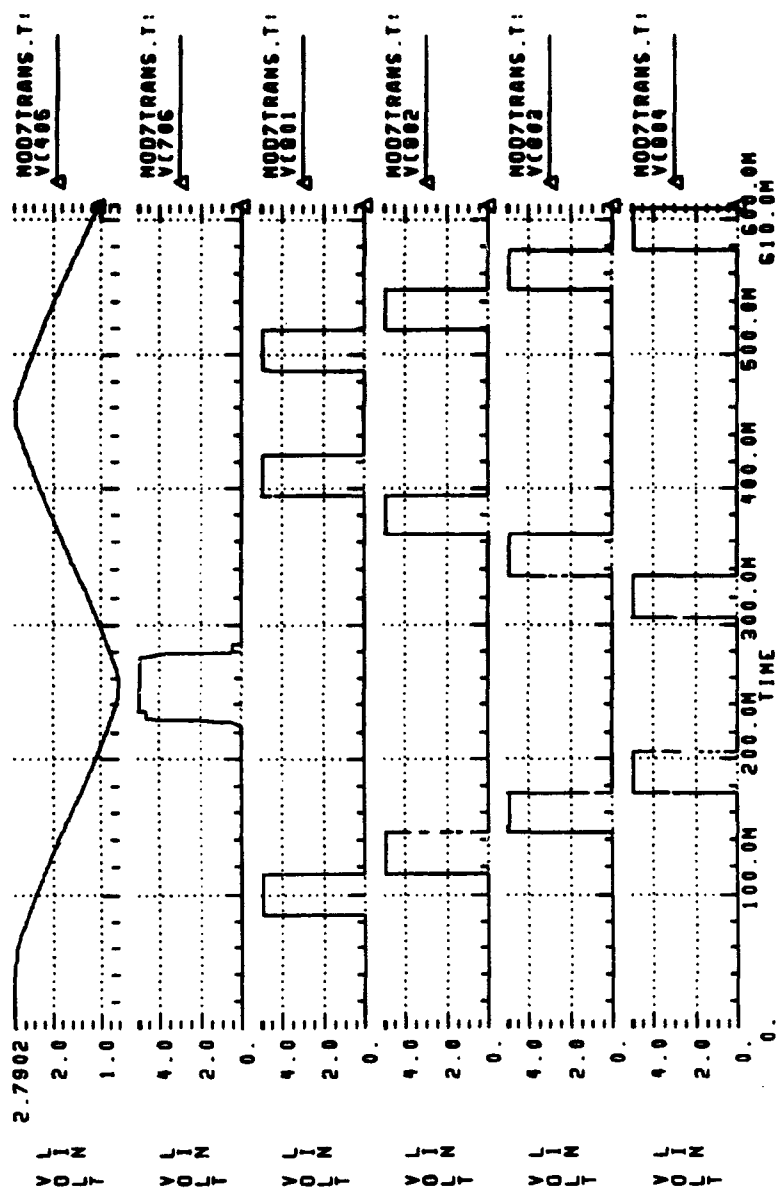


**Figure 4.37:** Mod 7 comparator and 1st decoder outputs.

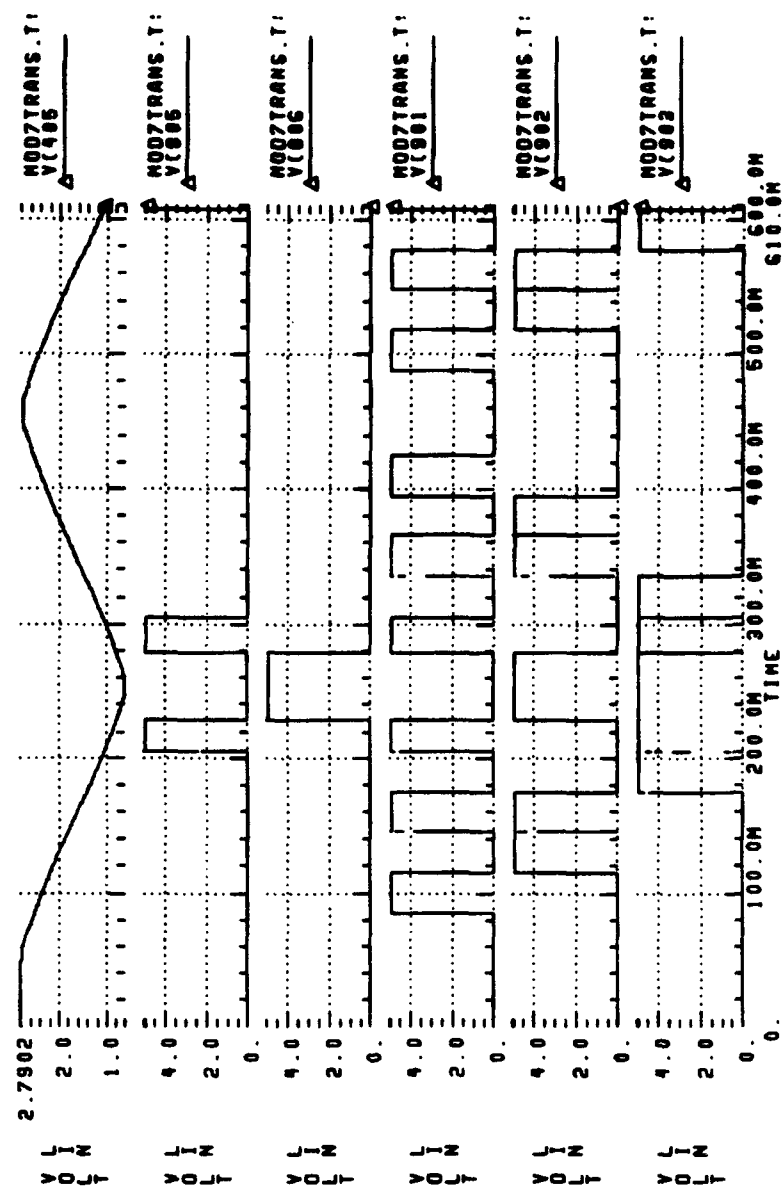


**Figure 4.38:** Mod 7 1st and 2nd decoder outputs.

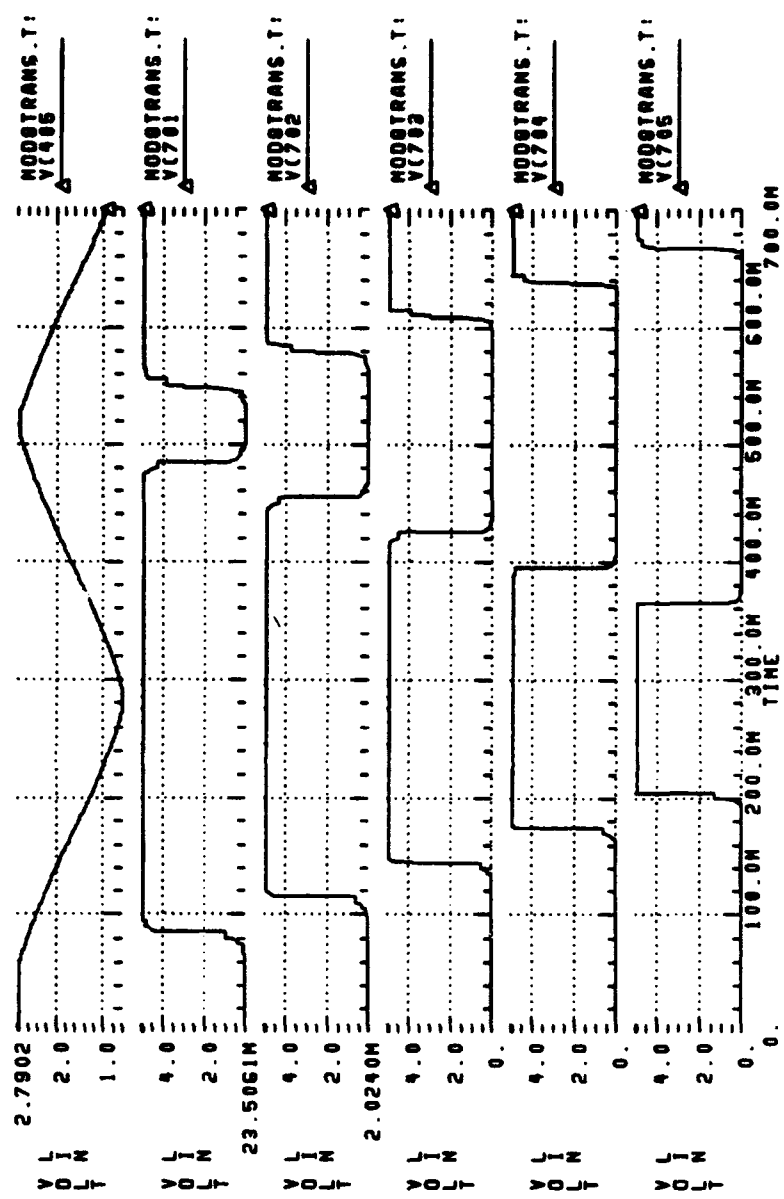


**Figure 4.39:** Mod 8 comparator outputs.

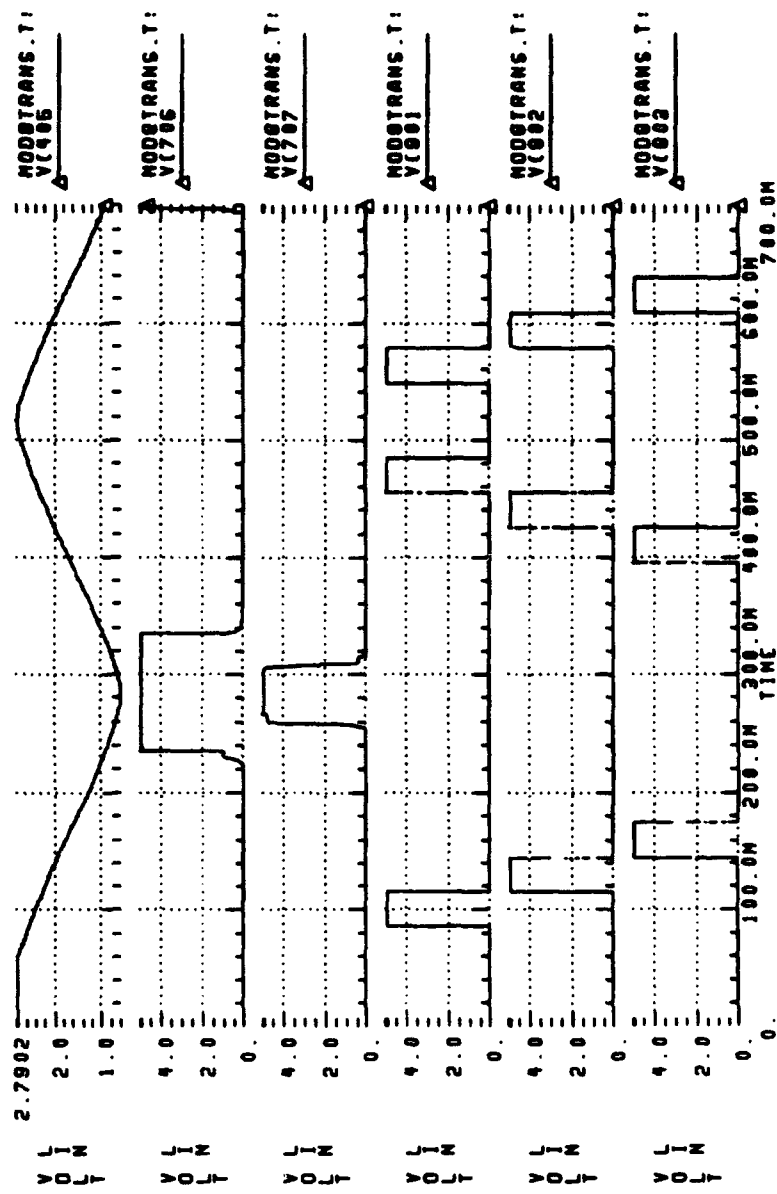


**Figure 4.40:** Mod 8 comparator and 1st decoder outputs.

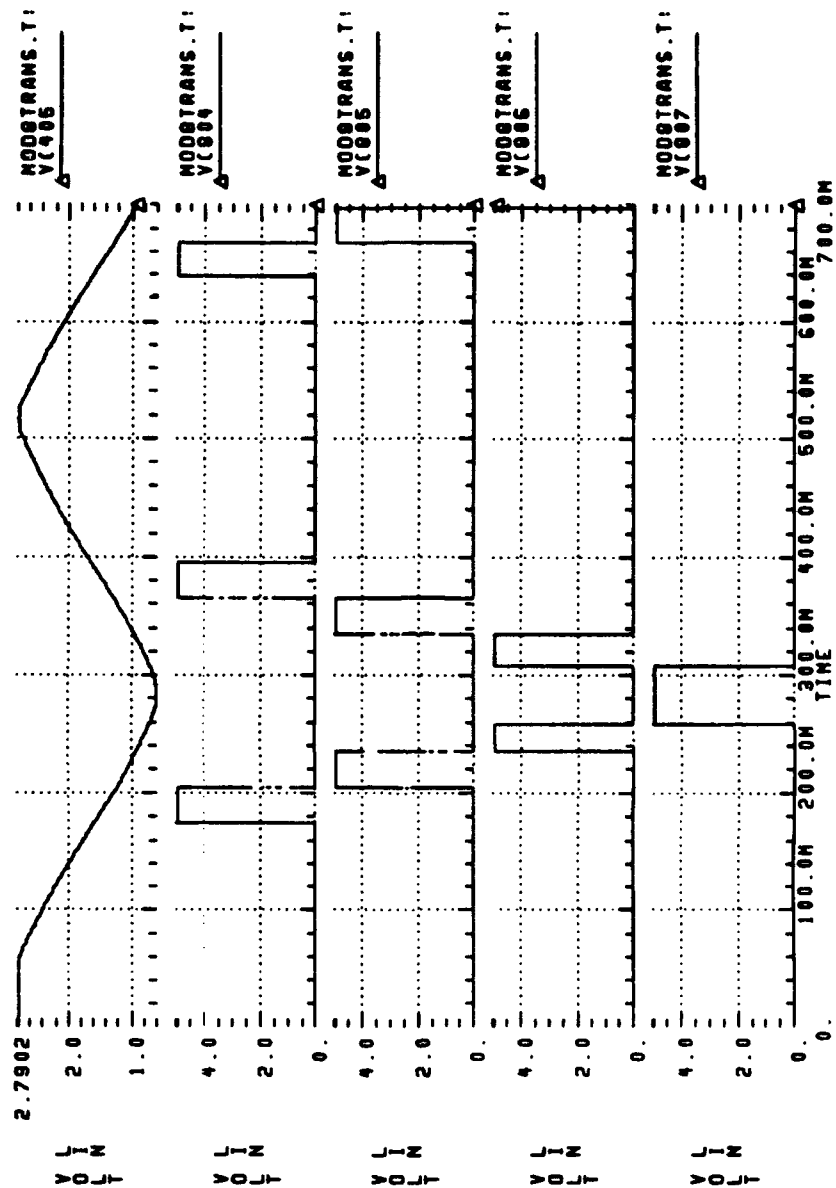


**Figure 4.41:** Mod 8 1st decoder outputs.

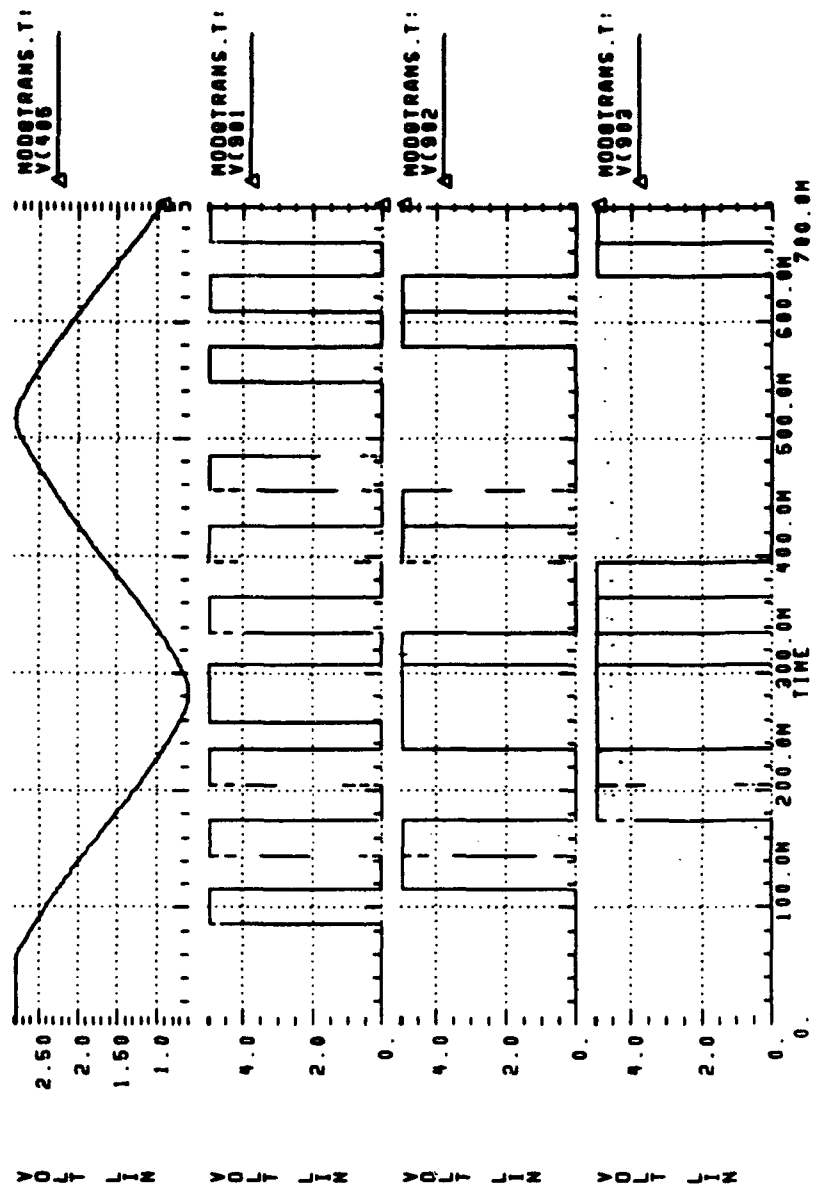


**Figure 4.42:** Mod 8 2nd decoder output.

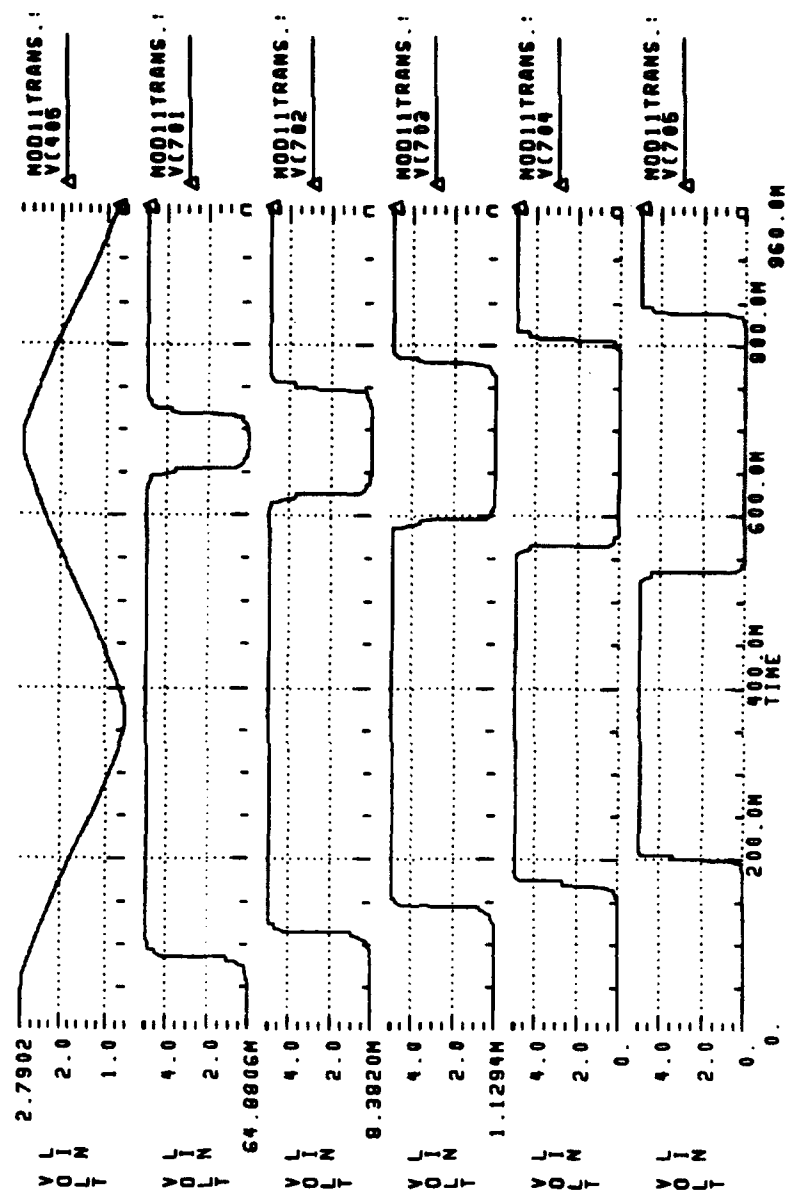


**Figure 4.43:** Mod 11 comparator outputs.

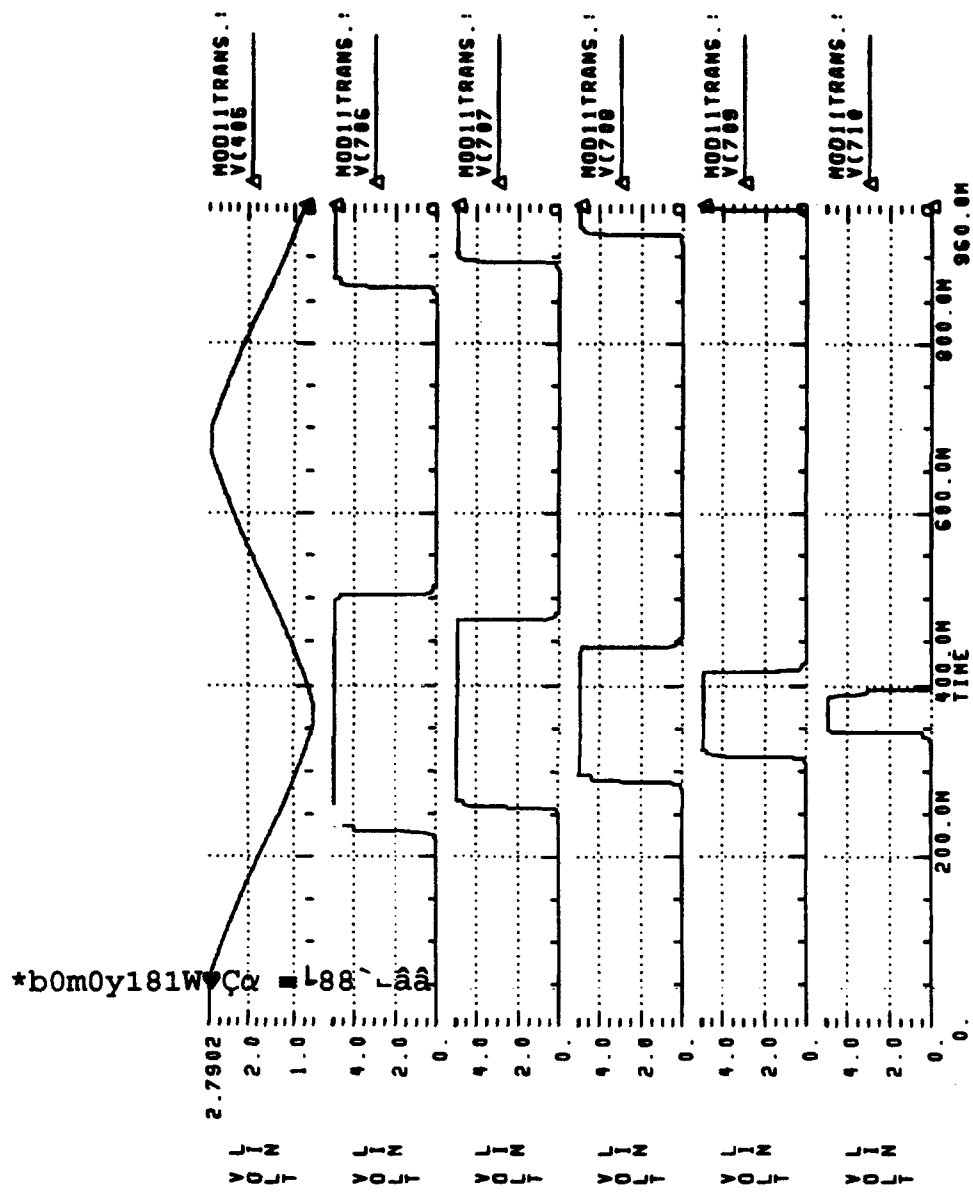
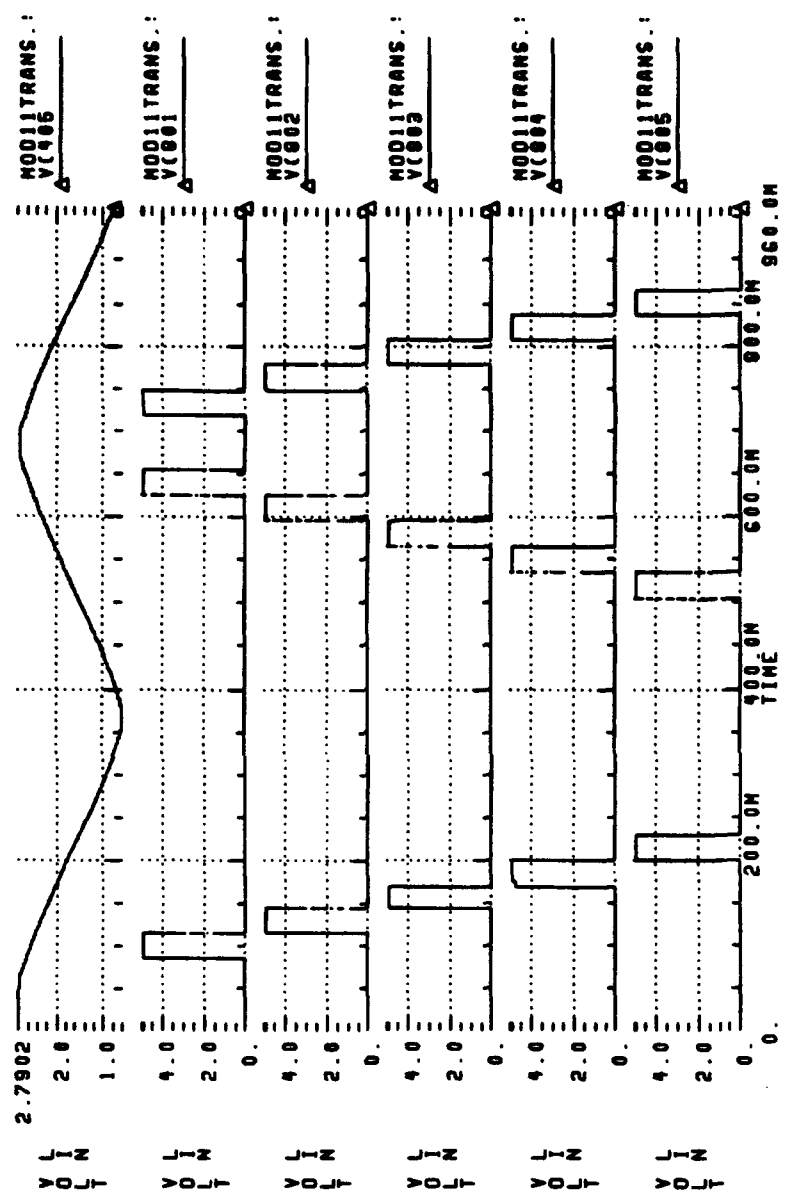
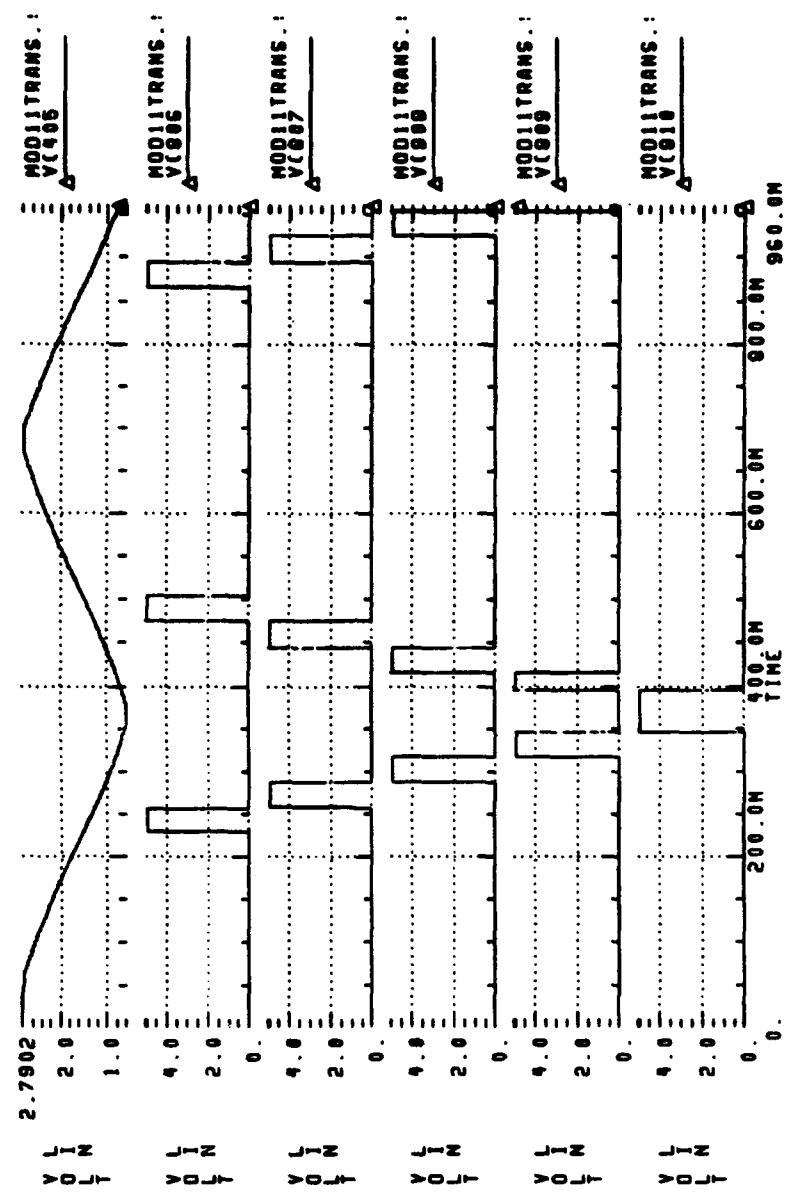


Figure 4.44: Mod 11 comparator outputs continued.



**Figure 4.45:** Mod 11 1st decoder output.



**Figure 4.46:** Mod 11 1st decoder output continued.

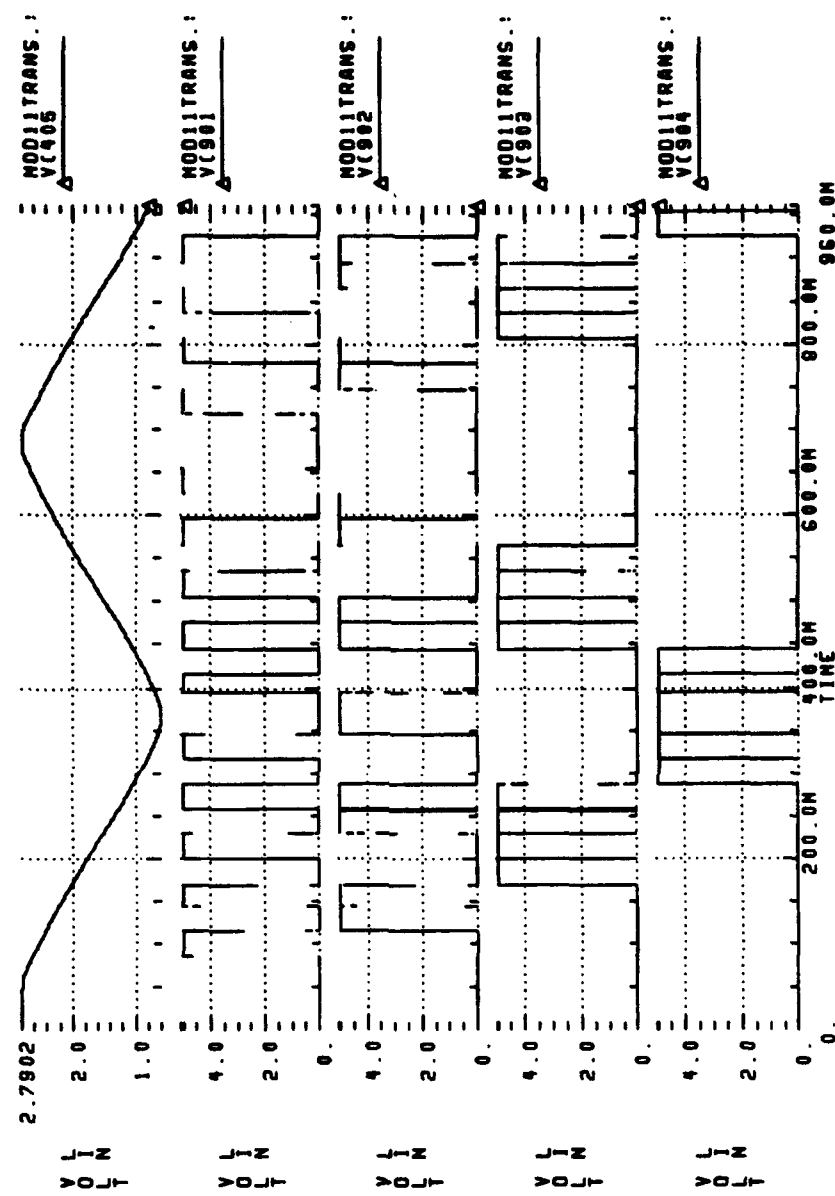
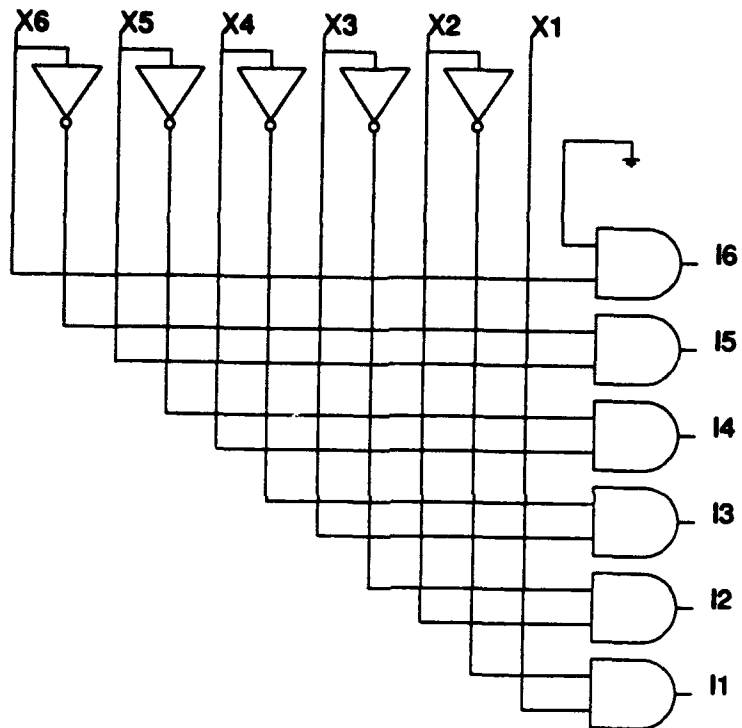


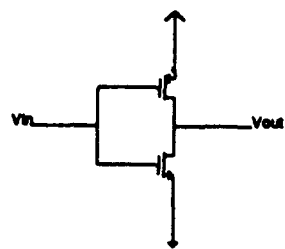
Figure 4.47: Mod 11 2nd decoder output.

illustrates this function for a modulus 7 folding circuit comparator output. For an input from the comparators of 111111, the decoder would translate it as an output of 100000. This functionality would be applied to the other moduli, specifically modulus 8 and modulus 11. Figure 4.48 is the schematics of the digital circuit which implement the logic presented in Table 4.7. The logic gates are implemented using CMOS technology and are shown in Figure 4.49. This part of the decoder was simulated and the results are shown in Figures 4.50 and 4.51, validating this circuit design.

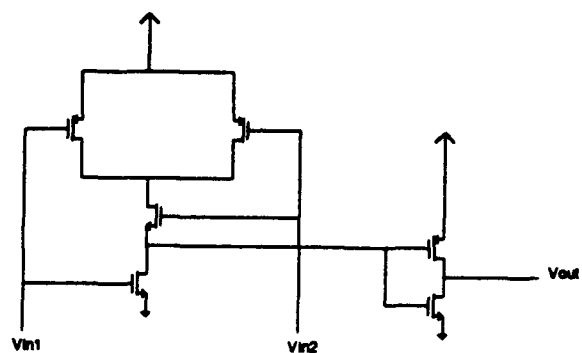
The second function of the decoder, as depicted in Figure 4.52 for mod 7, is to take the thermometer coded output of the first part of the decoder and translate it to a straight binary number. This number is the binary value of the number of comparators that are on, or high at a given moment. As an example, Table 4.8 illustrates the functionality of this part of the decoder in a truth table format for the modulus 7 subcircuit. If the input is 100000, then the output should be 110. Figure 4.53 shows the simulation of the circuit of Figure 4.52. The digital circuits for the other moduli can be readily extracted from the mod 7 design. When the output of each of the modulus decoders are integrated, this represents the analog input voltage of the Analog-to-Digital Converter in the SNS format. As can be seen in the simulations in Figures 4.36-4.47, this decoder worked very well for each of the modulus subcircuits. As the input voltage is swept through



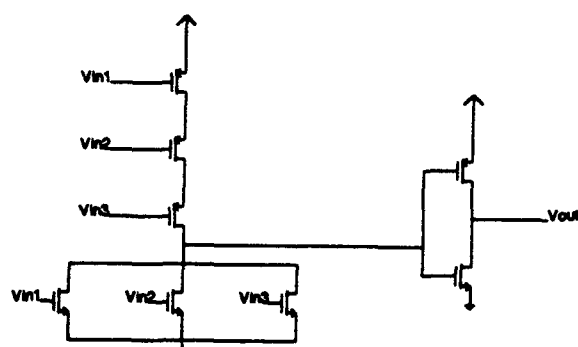
**Figure 4.48:** First half of the mod 7 decoder.



(a) Inverter

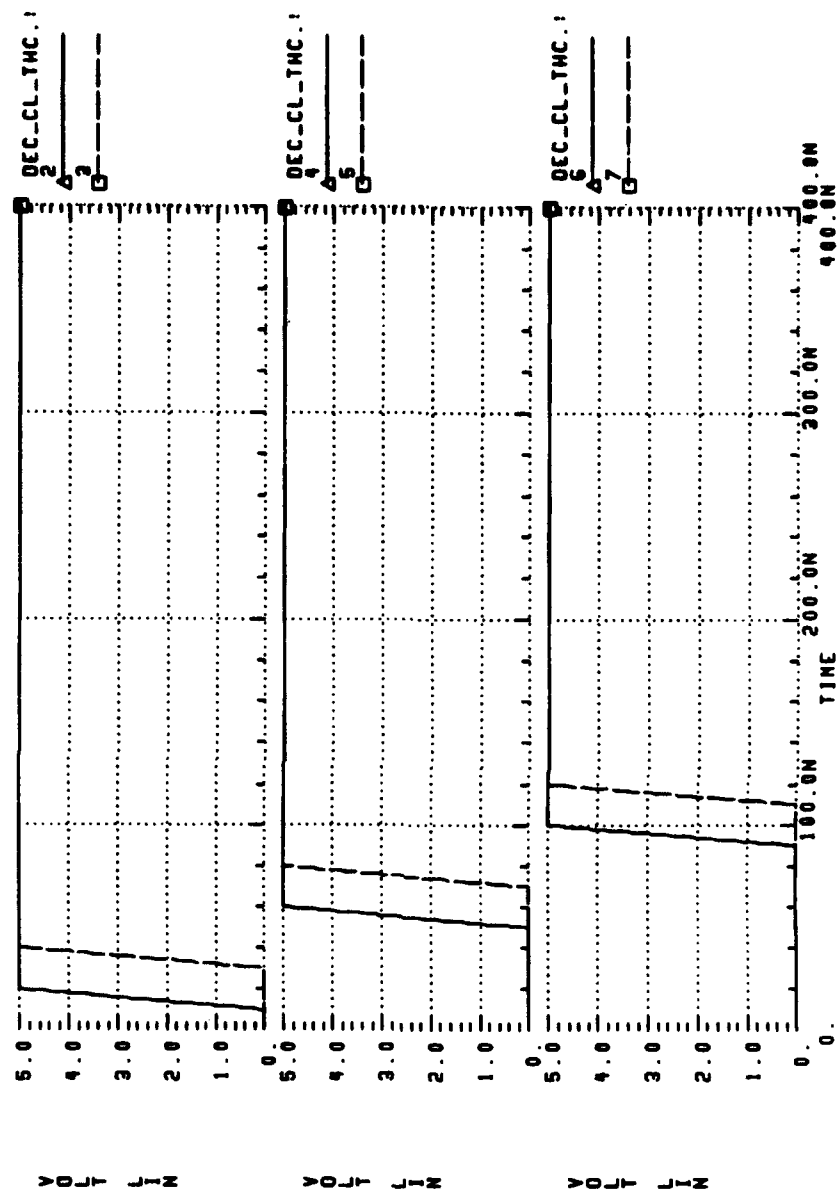


(b) 2-input AND gate

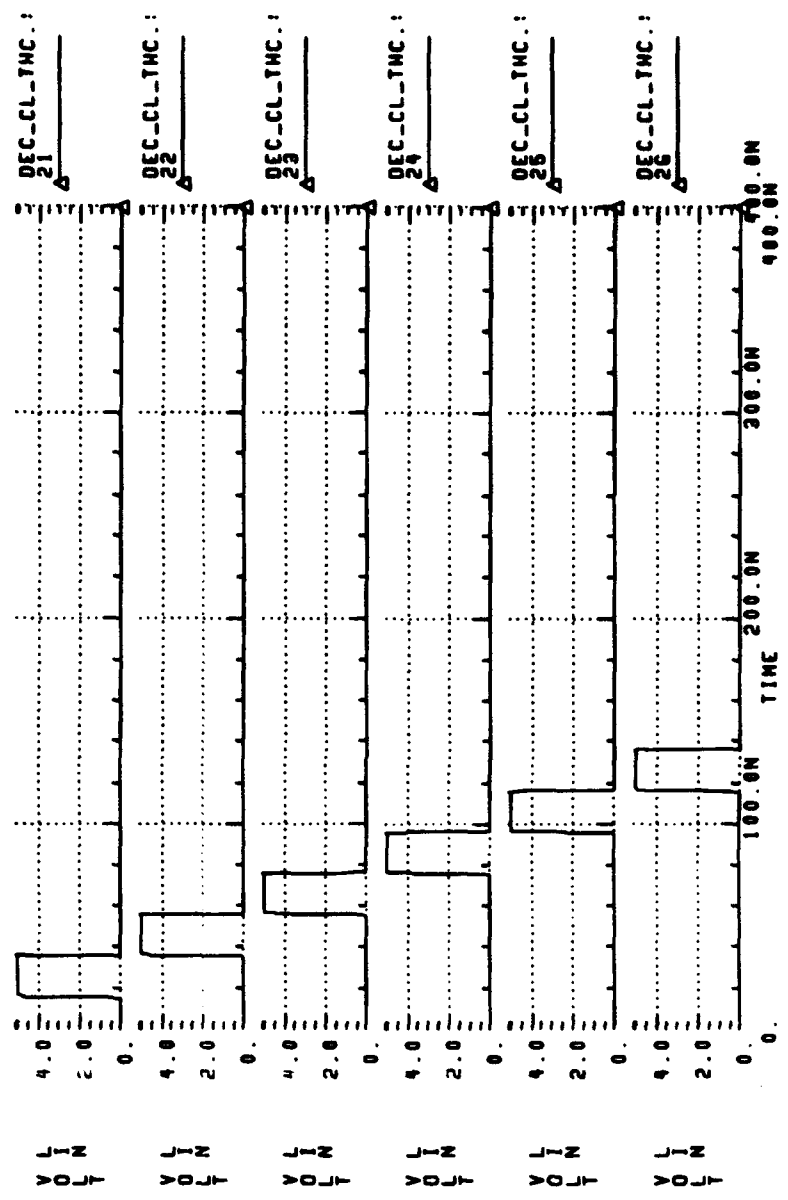


(c) 3-input OR gate

**Figure 4.49:** CMOS gates used in decoder design.



**Figure 4.50:** 1st decoder simulation showing the input comparator levels.



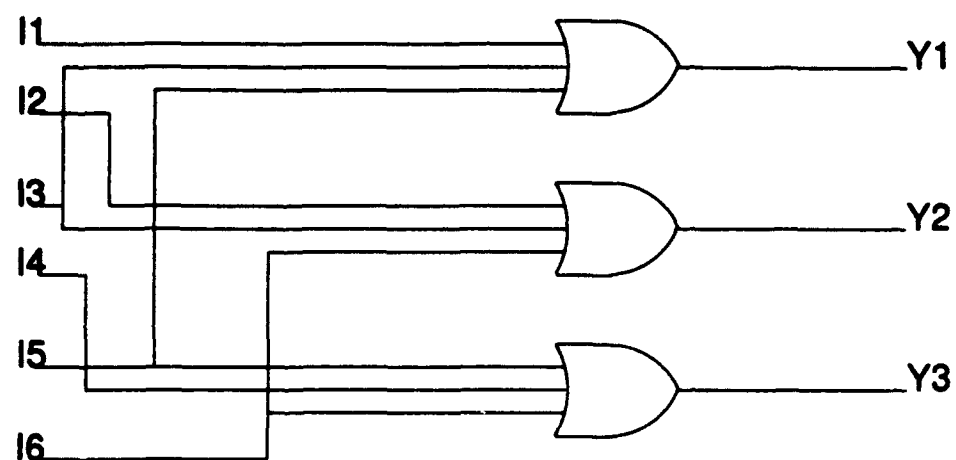
**Figure 4.51:** 1st decoder simulation showing decoder output.

TABLE 4.7 1ST DECODER TRUTH TABLE

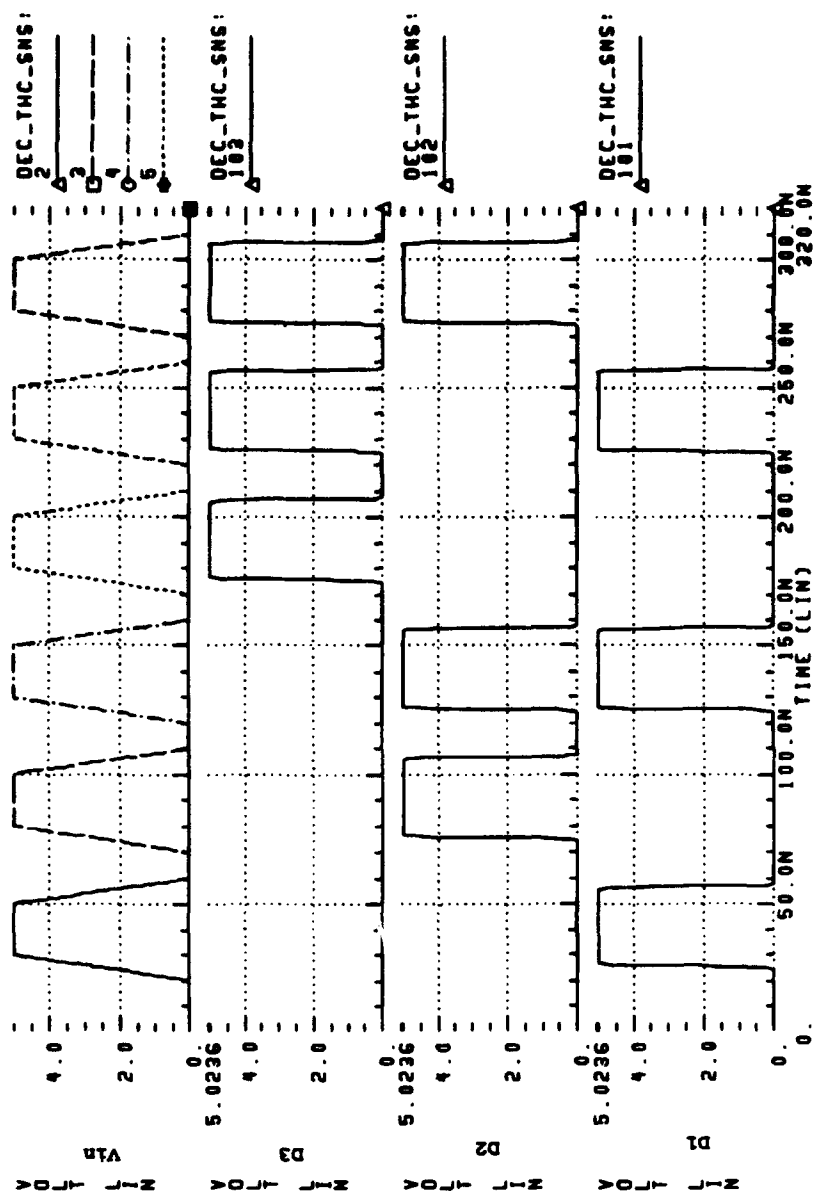
I <sub>6</sub>	I <sub>5</sub>	I <sub>4</sub>	I <sub>3</sub>	I <sub>2</sub>	I <sub>1</sub>		Y <sub>6</sub>	Y <sub>5</sub>	Y <sub>4</sub>	Y <sub>3</sub>	Y <sub>2</sub>	Y <sub>1</sub>
0	0	0	0	0	0		0	0	0	0	0	0
0	0	0	0	0	1		0	0	0	0	0	1
0	0	0	0	1	1		0	0	0	0	1	0
0	0	0	1	1	1		0	0	0	1	0	0
0	0	1	1	1	1		0	0	1	0	0	0
0	1	1	1	1	1		0	1	0	0	0	0
1	1	1	1	1	1		1	0	0	0	0	0

TABLE 4.8 2ND DECODER TRUTH TABLE

I <sub>6</sub>	I <sub>5</sub>	I <sub>4</sub>	I <sub>3</sub>	I <sub>2</sub>	I <sub>1</sub>		Y <sub>3</sub>	Y <sub>2</sub>	Y <sub>1</sub>
0	0	0	0	0	0		0	0	0
0	0	0	0	0	1		0	0	1
0	0	0	0	1	0		0	1	0
0	0	0	1	0	0		0	1	1
0	0	1	0	0	0		1	1	0
0	1	0	0	0	0		1	1	1
1	0	0	0	0	0		1	1	0



**Figure 4.52:** Second half of the mod 7 decoder.



**Figure 4.53:** 2nd decoder simulation showing the decoder output.

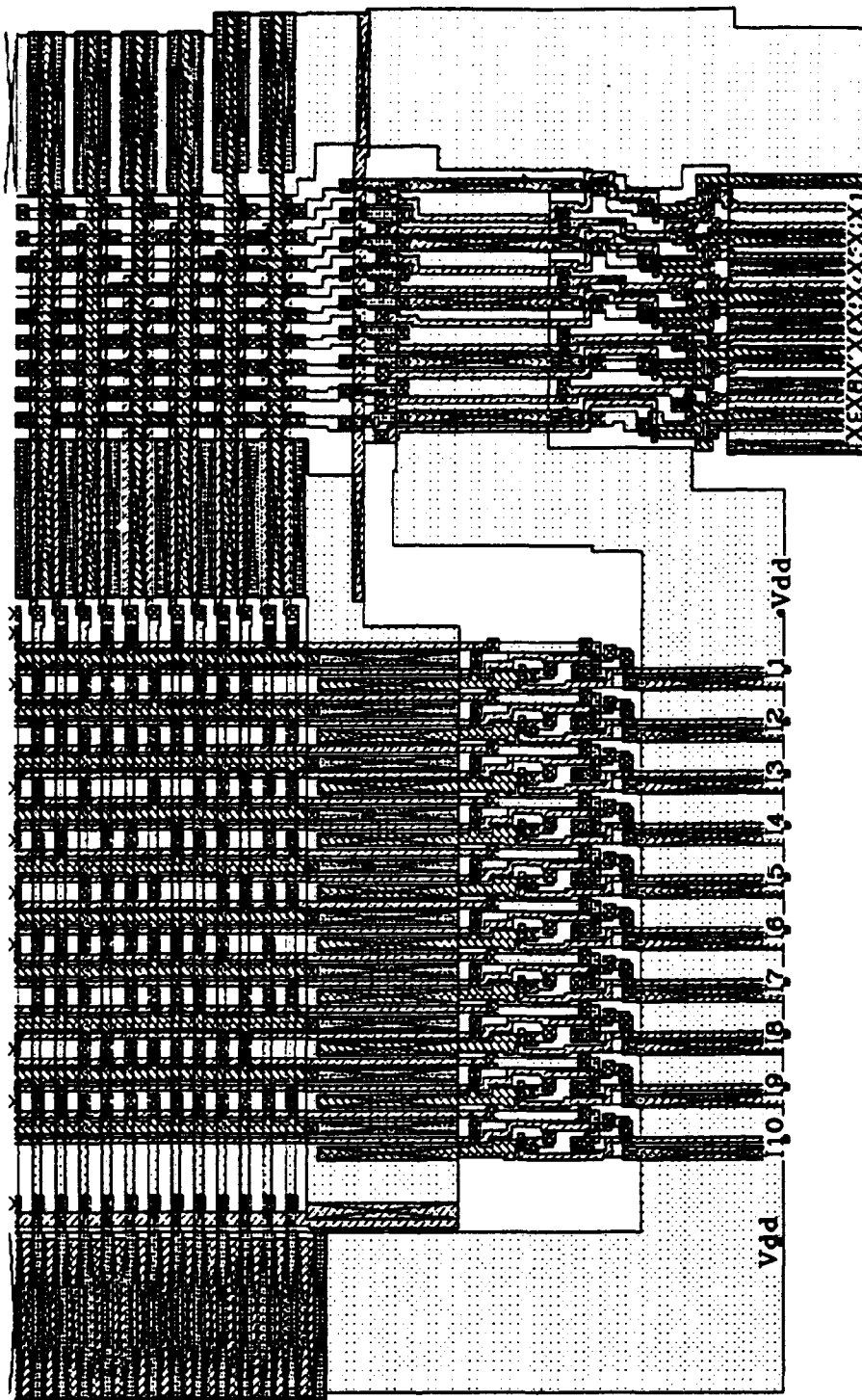


**Figure 4.54:** Partial layout of a PLA.

its dynamic range, each individual modulus subcircuit can be seen stepping through its modulus sequence. For instance, in the modulus 7 subcircuit, the output can be seen to go through the sequence: 000, 001, 010, 011, 100, 101, 110.

The output of the decoder represents the SNS value of the input signal applied to the overall analog-to-digital converter. This output is then fed to a PLA which converts it to a standard binary format. The number of inputs into the PLA would be ten, and for a 9-bit analog-to-digital converter the number of outputs for the PLA would be 9. The design of the PLA is virtually an automatic process. Using U.C. Berkeley CAD tools, all that is needed is to specify the PLA inputs and outputs in a file and then run a PLA generation program to produce a CMOS layout partially shown in Figure 4.54. The input file can be found in Appendix B, but the actual PLA truth table was generated by a MATLAB program which is presented in Appendix C. Information from the PLA layout was extracted to perform digital simulation to investigate the validity of the design (see Appendix D). Once this validation is complete, the PLA would then connect to the rest of the analog-to-digital converter so that a SPICE simulation can be conducted of the entire analog-to-digital converter.

## **V. STRENGTHS, LIMITATIONS, AND FUTURE DEVELOPMENTS**

The greatest contribution or strength of the 9-bit analog-to-digital design presented in this thesis, is the reduction of the number of comparators. In a standard flash ADC, the number of comparators required would be  $2^9 - 1 = 511$ . In the design presented in this thesis, the number of comparators that were used is 23. This is a dramatic reduction which translates to a decrease in power consumption and to smaller chip size. The reduction in the number of comparators should theoretically improve the speed of the ADC. However, it was found that the design could only achieve a maximum frequency in the range of 100kHz instead of the expected Mhz range which have been achieved in other research. This thesis presented data which indicated that increases in the bias current of the folding circuits did improve the frequency response. However, the drawback was the widening of the width of the folded output of the modulus folding circuits. This resulted in destroying the functionality and periodicity of the folded output to implement the preprocessing architecture.

Another area of limitation is the resolution. This thesis initially envisioned a 10-bit ADC but had to be reduced to a 9-bit resolution because of the gain limitation of the CMOS process that was used. In order to achieve a 10-bit resolution, the width of the MOS transistors were

impractically large to achieve the proper width in the folded output of the folding circuits. It is believed that a new process with favorable gain characteristics could provide a better frequency response and enable higher resolution.

Future research endeavors should use a more suitable CMOS process and the results of this thesis to produce a CMOS layout and a physical application specific integrated chip (ASIC). Perhaps, when these steps are achieved a GaAs ADC can be built utilizing the information presented in this thesis to achieve even better performance.

## APPENDIX A

### SPICE INPUT FILE

#### CMOS MOD 7 FOLDING CIRCUIT FOR 9-BIT ADC

\* SPICE3C PMOS and NMOS model level 2 corner parameters for  
\* the VLSI Technology 2.0U CMOS N-well process. 10/23/92  
\* SPICE3C PMOS and NMOS model level 2 nominal parameters,  
\* derived from corner parameters above.

```
.MODEL npf PMOS (LEVEL=2 VTO=-0.75 TOX=400E-10 NSUB=6.0E+15
+ XJ=0.05U LD=0.20U U0=255 UCRIT=0.86E5 UEXP=0.29
+VMAX=3.0E4 + NEFF=2.65 DELTA=1.0 RSH=101 CGSO=1.9E-10
+CGDO=1.9E-10
+ CJ=250U CJSW=350P MJ=0.535 MJSW=0.34 PB=0.8)
```

```
.MODEL nnf NMOS (LEVEL=2 VTO=+0.775 TOX=400E-10 NSUB=8.0E+15
+ XJ=0.15U LD=0.20U U0=650 UCRIT=0.62E5 UEXP=0.125
+VMAX=5.1E4 + NEFF=4.0 DELTA=1.4 RSH=36 CGSO=1.95E-10
+CGDO=1.95E-10
+ CJ=195U CJSW=500P MJ=0.76 MJSW=0.30 PB=0.8)
```

#### \*Sources

VDD 1 0 18V  
VSS 2 0 -18V  
\*Is 4 0 .5mA  
Vop+ 7 0 15V  
vop- 8 0 -15V  
VC+ 500 0 5.0V  
VC- 501 0 -5.0V

#### \*Input Resistors for Op Amp

R1 211 301 1K  
R2 212 301 1K  
R3 213 301 1K  
R4 214 301 1k  
R5 215 301 1K  
R6 216 301 1K  
R7 217 301 1K  
R8 218 301 1K  
R9 219 301 1K  
R10 220 301 1K  
R11 221 301 1K  
R12 222 301 1K  
R13 223 301 1K

R14 224 301 1k  
R15 225 301 1K  
R16 226 301 1K  
R17 227 301 1K  
R18 228 301 1K  
R19 229 301 1K  
R20 230 301 1K  
R21 231 301 1K  
R22 232 301 1K  
R23 233 301 1K  
R24 234 301 1k  
R25 235 301 1K  
R26 236 301 1K  
R27 237 301 1K  
R28 238 301 1K  
R29 239 301 1K  
R30 240 301 1K  
R31 241 301 1K  
R32 242 301 1K  
R33 243 301 1K  
R34 244 301 1k  
R35 245 301 1K  
R36 246 301 1K  
R37 247 301 1K  
R38 248 301 1K

\*Feedback Resistor for the Op Amp  
RF 306 301 20K

\*Signals

\*Vin 3 0  
\*Vin 3 0 PWL(0,0.0 10us,4.0)  
\*Vin 3 0 PWL(0,0.0 10000ms,4.0)  
\*Vin 3 0 PWL(0,0 4ns,4)  
Vin 3 0 PWL 0 0.0V, 40u 15.1V td=32.67n

\*Clocks for Comparators

\*VCLK2 502 0 pulse( 0v 5v .99s .01s .01s .49s 1s)  
\*VCLK2 502 0 pulse( 0v 5v .099s .001s .001s .049s .1s)  
\*VCLK2 502 0 pulse( 0v 5v .0099s .0001s .0001s .0049s  
.01s) \*VCLK2 502 0 pulse( 0v 5v .00495s .00005s .00005s  
.00245s .005s) VCLK2 502 0 pulse( 0v 5v 0.0s .0001s .0001s  
.0049s .01s) \*VCLK1 503 0 pulse(0v 5V .49s .01s .01s .49s  
1s)  
\*VCLK1 503 0 pulse(0v 5V .049s .001s .001s .049s .1s)  
\*VCLK1 503 0 pulse(0v 5V .0049s .0001s .0001s .0049s  
.01s) \*VCLK1 503 0 pulse(0v 5V .00245s .00005s .00005s  
.00245s .005s) VCLK1 503 0 pulse(0v 5V .005s .0001s .0001s  
.0049s .01s)

\*Reference Voltages

V11	11	0	0.0V
V12	12	0	.41V
V13	13	0	.82V
V14	14	0	1.23V
v15	15	0	1.64V
V16	16	0	2.05V
v17	17	0	2.46V
V18	18	0	2.87V
V19	19	0	3.28V
V20	20	0	3.69V
V21	21	0	4.10V
V22	22	0	4.51V
V23	23	0	4.92V
V24	24	0	5.33V
v25	25	0	5.74V
V26	26	0	6.15V
v27	27	0	6.56V
V28	28	0	6.97V
V29	29	0	7.38V
V30	30	0	7.79V
V31	31	0	8.20V
V32	32	0	8.61V
V33	33	0	9.02V
V34	34	0	9.43V
v35	35	0	9.84V
V36	36	0	10.25V
V37	37	0	10.66V
V38	38	0	11.07V
V39	39	0	11.48V
V40	40	0	11.89V
V41	41	0	12.30V
V42	42	0	12.71V
V43	43	0	13.12V
V44	44	0	13.53V
V45	45	0	13.94V
V46	46	0	14.35V
V47	47	0	14.76V
V48	48	0	15.17V

\*Comparator Reference Voltages

V601	601	0	2.58V
v602	602	0	2.27V
V603	603	0	1.92V
V604	604	0	1.54V
V605	605	0	1.16V
V606	606	0	0.858V

\*Folding Ckts external loads

*M5	5	5	1	1	npf	L=2u	W=250u
*M6	6	6	1	1	npf	L=2u	W=250u

**\*Folding Circuit instances**

X1	1	2	3	111	1	1	11	fold1
X2	1	2	3	112	1	1	12	fold2
X3	1	2	3	113	1	1	13	fold3
X4	1	2	3	114	1	1	14	fold4
X5	1	2	3	115	1	1	15	fold5
X6	1	2	3	116	1	1	16	fold6
X7	1	2	3	117	1	1	17	fold7
X8	1	2	3	118	1	1	18	fold8
X9	1	2	3	119	1	1	19	fold9
x10	1	2	3	120	1	1	20	fold10
X11	1	2	3	121	1	1	21	fold11
X12	1	2	3	122	1	1	22	fold12
X13	1	2	3	123	1	1	23	fold13
X14	1	2	3	124	1	1	24	fold14
X15	1	2	3	125	1	1	25	fold15
X16	1	2	3	126	1	1	26	fold16
X17	1	2	3	127	1	1	27	fold17
X18	1	2	3	128	1	1	28	fold18
X19	1	2	3	129	1	1	29	fold19
x20	1	2	3	130	1	1	30	fold20
X21	1	2	3	131	1	1	31	fold21
X22	1	2	3	132	1	1	32	fold22
X23	1	2	3	133	1	1	33	fold23
X24	1	2	3	134	1	1	34	fold24
X25	1	2	3	135	1	1	35	fold25
X26	1	2	3	136	1	1	36	fold26
X27	1	2	3	137	1	1	37	fold27
X28	1	2	3	138	1	1	38	fold28
X29	1	2	3	139	1	1	39	fold29
x30	1	2	3	140	1	1	40	fold30
X31	1	2	3	141	1	1	41	fold31
X32	1	2	3	142	1	1	42	fold32
X33	1	2	3	143	1	1	43	fold33
X34	1	2	3	144	1	1	44	fold34
X35	1	2	3	145	1	1	45	fold35
X36	1	2	3	146	1	1	46	fold36
X37	1	2	3	147	1	1	47	fold37
X38	1	2	3	148	1	1	48	fold38

**\*Emitter follower Circuit instances**

X101	1	2	111	211	emit
X102	1	2	112	212	emit
X103	1	2	113	213	emit
X104	1	2	114	214	emit
X105	1	2	115	215	emit
X106	1	2	116	216	emit
X107	1	2	117	217	emit
X108	1	2	118	218	emit
X109	1	2	119	219	emit

X110 1 2 120 220 emit  
X111 1 2 121 221 emit  
X112 1 2 122 222 emit  
X113 1 2 123 223 emit  
X114 1 2 124 224 emit  
X115 1 2 125 225 emit  
X116 1 2 126 226 emit  
X117 1 2 127 227 emit  
X118 1 2 128 228 emit  
X119 1 2 129 229 emit  
X120 1 2 130 230 emit  
X121 1 2 131 231 emit  
X122 1 2 132 232 emit  
X123 1 2 133 233 emit  
X124 1 2 134 234 emit  
X125 1 2 135 235 emit  
X126 1 2 136 236 emit  
X127 1 2 137 237 emit  
X128 1 2 138 238 emit  
X129 1 2 139 239 emit  
X130 1 2 140 240 emit  
X131 1 2 141 241 emit  
X132 1 2 142 242 emit  
X133 1 2 143 243 emit  
X134 1 2 144 244 emit  
X135 1 2 145 245 emit  
X136 1 2 146 246 emit  
X137 1 2 147 247 emit  
X138 1 2 148 248 emit

\*Op Amp

x200 7 8 301 0 306 opamp

\*Comparators

X301 500 501 405 511 601 comprtr  
X302 500 501 405 512 602 comprtr  
X303 500 501 405 513 603 comprtr  
X304 500 501 405 514 604 comprtr  
X305 500 501 405 515 605 comprtr  
X306 500 501 405 516 606 comprtr

\*transgate

X401 511 1 2 503 502 701 transgate  
X402 512 1 2 503 502 702 transgate  
X403 513 1 2 503 502 703 transgate  
X404 514 1 2 503 502 704 transgate  
X405 515 1 2 503 502 705 transgate  
X406 516 1 2 503 502 706 transgate

```

*****Decoder (Comparator Level -> Thermometer
Code)***** X501 500 701 702 703 704 705 706
801 802 803 804 805 806 decclthc
*****
*****Decoder (Thermometer
Code)***** X601 500 801
802 803 804 805 806 901 902 903 decthcsnsb
*****
***** *Voltage Shifter
M100 405 306 7 1 npf L=2u W=9u
M101 405 405 8 2 nnf L=2u W=5u

*Folding Subcircuit*****
*          V+  V-  Vin  Vout M5  M6  Vref
.subckt fold1 1 20   4    30  7   9   11

*Current sources
I1    8 20   .2mA
I2    5 20   .2mA

*Branch Ampmeters
VID1 7 40 0V
VID2 9 41 0V
VID3 3 42 0V
VID4 10 43 0V
*VID9 1 55 0V
*VID10 57 20 0V

*MOSFETS***
*Difamps
M1    40 3 8 20 nnf L=2u W=130u
M2    41 10 8 20 nnf L=2u W=130u

M3    42 4 5 20 nnf L=2u W=164u
M4    43 11 5 20 nnf L=2u W=164u

*Active Loads
M7    3 3 1 1 npf L=3u W=5u
M8    10 10 1 1 npf L=3u W=5u

*Source Follower/Voltage Shifter
M9    30 8 1 1 npf L=2u W=140u
M10   30 30 20 20 nnf L=2u W=5u
.ends

*Folding Subcircuit*****
*          V+  V-  Vin  Vout M5  M6  Vref

```

```

.subckt fold2 1 20 4 30 7 9 11

*Current sources
I1 8 20 .2mA
I2 5 20 .2mA

*Branch Ampmeters
VID1 7 40 0V
VID2 9 41 0V
VID3 3 42 0V
VID4 10 43 0V
*VID9 1 55 0V
*VID10 57 20 0V
*MOSFETS***

*Diffamps
M1 40 3 8 20 nnf L=2u W=130u
M2 41 10 8 20 nnf L=2u W=130u

M3 42 4 5 20 nnf L=2u W=168u
M4 43 11 5 20 nnf L=2u W=168u

*Active Loads
M7 3 3 1 1 npf L=3u W=5u
M8 10 10 1 1 npf L=3u W=5u

*Source Follower/Voltage Shifter
M9 30 8 1 1 npf L=2u W=140u
M10 30 30 20 20 nnf L=2u W=5u
.ends

*Folding Subcircuit*****
*
      V+ V- Vin Vout M5 M6 Vref
.subckt fold3 1 20 4 30 7 9 11

*Current sources
I1 8 20 .2mA
I2 5 20 .2mA

*Branch Ampmeters
VID1 7 40 0V
VID2 9 41 0V
VID3 3 42 0V
VID4 10 43 0V
*VID9 1 55 0V
*VID10 57 20 0V
*MOSFETS***

*Diffamps
M1 40 3 8 20 nnf L=2u W=130u
M2 41 10 8 20 nnf L=2u W=130u

```

M3 42 4 5 20 nnf L=2u W=170u  
M4 43 11 5 20 nnf L=2u W=170u

\*Active Loads

M7 3 3 1 1 npf L=3u W=5u  
M8 10 10 1 1 npf L=3u W=5u

\*Source Follower/Voltage Shifter

M9 30 8 1 1 npf L=2u W=140u  
M10 30 30 20 20 nnf L=2u W=5u

.ends

\*Folding Subcircuit\*\*\*\*\*

\* V+ V- Vin Vout M5 M6 Vref  
.subckt fold4 1 20 4 30 7 9 11

\*Current sources

I1 8 20 .2mA  
I2 5 20 .2mA

\*Branch Ampmeters

VID1 7 40 0V

VID2 9 41 0V

VID3 3 42 0V

VID4 10 43 0V

\*VID9 1 55 0V

\*VID10 57 20 0V

\*MOSFETS\*\*\*

\*Diffamps

M1 40 3 8 20 nnf L=2u W=130u  
M2 41 10 8 20 nnf L=2u W=130u

M3 42 4 5 20 nnf L=2u W=172u  
M4 43 11 5 20 nnf L=2u W=172u

\*Active Loads

M7 3 3 1 1 npf L=3u W=5u  
M8 10 10 1 1 npf L=3u W=5u

\*Source Follower/Voltage Shifter

M9 30 8 1 1 npf L=2u W=140u  
M10 30 30 20 20 nnf L=2u W=5u

.ends

\*Folding Subcircuit\*\*\*\*\*

\* V+ V- Vin Vout M5 M6 Vref  
.subckt fold5 1 20 4 30 7 9 11

\*Current sources

I1 8 20 .2mA  
I2 5 20 .2mA

\*Branch Ampmeters

VID1 7 40 0V

VID2 9 41 0V

VID3 3 42 0V

VID4 10 43 0V

\*VID9 1 55 0V

\*VID10 57 20 0V

\*MOSFETS\*\*\*

\*Diffamps

M1 40 3 8 20 nnf L=2u W=130u

M2 41 10 8 20 nnf L=2u W=130u

M3 42 4 5 20 nnf L=2u W=174u

M4 43 11 5 20 nnf L=2u W=174u

\*Active Loads

M7 3 3 1 1 npf L=3u W=5u

M8 10 10 1 1 npf L=3u W=5u

\*Source Follower/Voltage Shifter

M9 30 8 1 1 npf L=2u W=140u

M10 30 30 20 20 nnf L=2u W=5u

.ends

\*Folding Subcircuit\*\*\*\*\*

\* V+ V- Vin Vout M5 M6 Vref  
.subckt fold6 1 20 4 30 7 9 11

\*Current sources

I1 8 20 .2mA

I2 5 20 .2mA

\*Branch Ampmeters

VID1 7 40 0V

VID2 9 41 0V

VID3 3 42 0V

VID4 10 43 0V

\*VID9 1 55 0V

\*VID10 57 20 0V

\*MOSFETS\*\*\*

\*Diffamps

M1 40 3 8 20 nnf L=2u W=130u

M2 41 10 8 20 nnf L=2u W=130u

M3 42 4 5 20 nnf L=2u W=176u

M4 43 11 5 20 nnf L=2u W=176u

**\*Active Loads**

M7 3 3 1 1 npf L=3u W=5u  
M8 10 10 1 1 npf L=3u W=5u

**\*Source Follower/Voltage Shifter**

M9 30 8 1 1 npf L=2u W=140u  
M10 30 30 20 20 nnf L=2u W=5u  
.ends

**\*Folding Subcircuit\*\*\*\*\***

\* V+ V- Vin Vout M5 M6 Vref  
.subckt fold7 1 20 4 30 7 9 11

**\*Current sources**

I1 8 20 .2mA  
I2 5 20 .2mA

**\*Branch Ampmeters**

VID1 7 40 0V

VID2 9 41 0V

VID3 3 42 0V

VID4 10 43 0V

\*VID9 1 55 0V

\*VID10 57 20 0V

**\*MOSFETS\*\*\***

**\*Diffamps**

M1 40 3 8 20 nnf L=2u W=130u  
M2 41 10 8 20 nnf L=2u W=130u

M3 42 4 5 20 nnf L=2u W=178u

M4 43 11 5 20 nnf L=2u W=178u

**\*Active Loads**

M7 3 3 1 1 npf L=3u W=5u  
M8 10 10 1 1 npf L=3u W=5u

**\*Source Follower/Voltage Shifter**

M9 30 8 1 1 npf L=2u W=140u  
M10 30 30 20 20 nnf L=2u W=5u  
.ends

**\*Folding Subcircuit\*\*\*\*\***

\* V+ V- Vin Vout M5 M6 Vref  
.subckt fold8 1 20 4 30 7 9 11

**\*Current sources**

I1 8 20 .2mA  
I2 5 20 .2mA

**\*Branch Ampmeters**

VID1 7 40 0V

VID2 9 41 0V

VID3 3 42 0V

VID4 10 43 0V

\*VID9 1 55 0V

\*VID10 57 20 0V

**\*MOSFETS\*\*\***

**\*Diffamps**

M1 40 3 8 20 nnf L=2u W=130u

M2 41 10 8 20 nnf L=2u W=130u

M3 42 4 5 20 nnf L=2u W=180u

M4 43 11 5 20 nnf L=2u W=180u

**\*Active Loads**

M7 3 3 1 1 npf L=3u W=5u

M8 10 10 1 1 npf L=3u W=5u

**\*Source Follower/Voltage Shifter**

M9 30 8 1 1 npf L=2u W=140u

M10 30 30 20 20 nnf L=2u W=5u

.ends

**\*Folding Subcircuit\*\*\*\*\***

\* V+ V- Vin Vout M5 M6 Vref  
.subckt fold9 1 20 4 30 7 9 11

**\*Current sources**

I1 8 20 .2mA

I2 5 20 .2mA

**\*Branch Ampmeters**

VID1 7 40 0V

VID2 9 41 0V

VID3 3 42 0V

VID4 10 43 0V

\*VID9 1 55 0V

\*VID10 57 20 0V

**\*MOSFETS\*\*\***

**\*Diffamps**

M1 40 3 8 20 nnf L=2u W=130u

M2 41 10 8 20 nnf L=2u W=130u

M3 42 4 5 20 nnf L=2u W=180u

M4 43 11 5 20 nnf L=2u W=180u

**\*Active Loads**

```

M7 3 3 1 1 npf L=3u W=5u
M8 10 10 1 1 npf L=3u W=5u

*Source Follower/Voltage Shifter
M9 30 8 1 1 npf L=2u W=140u
M10 30 30 20 20 nnf L=2u W=5u
.ends

*Folding Subcircuit*****
*
      V+ V- Vin Vout M5 M6 Vref
.subckt fold10 1 20 4 30 7 9 11

*Current sources
I1 8 20 .2mA
I2 5 20 .2mA

*Branch Ampmeters
VID1 7 40 0V
VID2 9 41 0V
VID3 3 42 0V
VID4 10 43 0V
*VID9 1 55 0V
*VID10 57 20 0V
*MOSFETS***
*Diffamps
M1 40 3 8 20 nnf L=2u W=130u
M2 41 10 8 20 nnf L=2u W=130u

M3 42 4 5 20 nnf L=2u W=186u
M4 43 11 5 20 nnf L=2u W=186u

*Active Loads
M7 3 3 1 1 npf L=3u W=5u
M8 10 10 1 1 npf L=3u W=5u

*Source Follower/Voltage Shifter
M9 30 8 1 1 npf L=2u W=140u
M10 30 30 20 20 nnf L=2u W=5u
.ends

*Folding Subcircuit*****
*
      V+ V- Vin Vout M5 M6 Vref
.subckt fold11 1 20 4 30 7 9 11

*Current sources
I1 8 20 .2mA
I2 5 20 .2mA

```

**\*Branch Ampmeters**

VID1 7 40 0V

VID2 9 41 0V

VID3 3 42 0V

VID4 10 43 0V

\*VID9 1 55 0V

\*VID10 57 20 0V

**\*MOSFETS\*\*\***

**\*Diffamps**

M1 40 3 8 20 nnf L=2u W=130u

M2 41 10 8 20 nnf L=2u W=130u

M3 42 4 5 20 nnf L=2u W=188u

M4 43 11 5 20 nnf L=2u W=188u

**\*Active Loads**

M7 3 3 1 1 npf L=3u W=5u

M8 10 10 1 1 npf L=3u W=5u

**\*Source Follower/Voltage Shifter**

M9 30 8 1 1 npf L=2u W=140u

M10 30 30 20 20 nnf L=2u W=5u

.ends

**\*Folding Subcircuit\*\*\*\*\***

\* V+ V- Vin Vout M5 M6 Vref  
.subckt fold12 1 20 4 30 7 9 11

**\*Current sources**

I1 8 20 .2mA

I2 5 20 .2mA

**\*Branch Ampmeters**

VID1 7 40 0V

VID2 9 41 0V

VID3 3 42 0V

VID4 10 43 0V

\*VID9 1 55 0V

\*VID10 57 20 0V

**\*MOSFETS\*\*\***

**\*Diffamps**

M1 40 3 8 20 nnf L=2u W=130u

M2 41 10 8 20 nnf L=2u W=130u

M3 42 4 5 20 nnf L=2u W=192u

M4 43 11 5 20 nnf L=2u W=192u

**\*Active Loads**

M7 3 3 1 1 npf L=3u W=5u

```

M8    10 10 1 1 npf L=3u W=5u

*Source Follower/Voltage Shifter
M9    30 8 1 1 npf L=2u W=140u
M10   30 30 20 20 nnf L=2u W=5u
.ends

*Folding Subcircuit*****
*          V+ V- Vin Vout M5 M6 Vref
.subckt fold13 1 20 4 30 7 9 11

*Current sources
I1    8 20 .2mA
I2    5 20 .2mA

*Branch Ampmeters
VID1 7 40 0V
VID2 9 41 0V
VID3 3 42 0V
VID4 10 43 0V
*VID9 1 55 0V
*VID10 57 20 0V
*MOSFETS***
*Diffamps
M1    40 3 8 20 nnf L=2u W=130u
M2    41 10 8 20 nnf L=2u W=130u

M3    42 4 5 20 nnf L=2u W=196u
M4    43 11 5 20 nnf L=2u W=196u

*Active Loads
M7    3 3 1 1 npf L=3u W=5u
M8    10 10 1 1 npf L=3u W=5u

*Source Follower/Voltage Shifter
M9    30 8 1 1 npf L=2u W=140u
M10   30 30 20 20 nnf L=2u W=5u
.ends

*Folding Subcircuit*****
*          V+ V- Vin Vout M5 M6 Vref
.subckt fold14 1 20 4 30 7 9 11

*Current sources
I1    8 20 .2mA
I2    5 20 .2mA

```

**\*Branch Ampmeters**

VID1 7 40 0V

VID2 9 41 0V

VID3 3 42 0V

VID4 10 43 0V

\*VID9 1 55 0V

\*VID10 57 20 0V

**\*MOSFETS\*\*\***

**\*Diffamps**

M1 40 3 8 20 nnf L=2u W=130u

M2 41 10 8 20 nnf L=2u W=130u

M3 42 4 5 20 nnf L=2u W=200u

M4 43 11 5 20 nnf L=2u W=200u

**\*Active Loads**

M7 3 3 1 1 npf L=3u W=5u

M8 10 10 1 1 npf L=3u W=5u

**\*Source Follower/Voltage Shifter**

M9 30 8 1 1 npf L=2u W=140u

M10 30 30 20 20 nnf L=2u W=5u

.ends

**\*Folding Subcircuit\*\*\*\*\***

\* V+ V- Vin Vout M5 M6 Vref

.subckt fold15 1 20 4 30 7 9 11

**\*Current sources**

I1 8 20 .2mA

I2 5 20 .2mA

**\*Branch Ampmeters**

VID1 7 40 0V

VID2 9 41 0V

VID3 3 42 0V

VID4 10 43 0V

\*VID9 1 55 0V

\*VID10 57 20 0V

**\*MOSFETS\*\*\***

**\*Diffamps**

M1 40 3 8 20 nnf L=2u W=130u

M2 41 10 8 20 nnf L=2u W=130u

M3 42 4 5 20 nnf L=2u W=204u

M4 43 11 5 20 nnf L=2u W=204u

**\*Active Loads**

M7 3 3 1 1 npf L=3u W=5u

```

M8 10 10 1 1 npf L=3u W=5u
*Source Follower/Voltage Shifter
M9 30 8 1 1 npf L=2u W=140u
M10 30 30 20 20 nnf L=2u W=5u
.ends

*Folding Subcircuit*****
*
V+ V- Vin Vout M5 M6 Vref
.subckt fold16 1 20 4 30 7 9 11

*Current sources
I1 8 20 .2mA
I2 5 20 .2mA

*Branch Ampmeters
VID1 7 40 0V
VID2 9 41 0V
VID3 3 42 0V
VID4 10 43 0V
*VID9 1 55 0V
*VID10 57 20 0V
*MOSFETS***
*Diffamps
M1 40 3 8 20 nnf L=2u W=130u
M2 41 10 8 20 nnf L=2u W=130u

M3 42 4 5 20 nnf L=2u W=208u
M4 43 11 5 20 nnf L=2u W=208u

*Active Loads
M7 3 3 1 1 npf L=3u W=5u
M8 10 10 1 1 npf L=3u W=5u

*Source Follower/Voltage Shifter
M9 30 8 1 1 npf L=2u W=140u
M10 30 30 20 20 nnf L=2u W=5u
.ends

*Folding Subcircuit*****
*
V+ V- Vin Vout M5 M6 Vref
.subckt fold17 1 20 4 30 7 9 11

*Current sources
I1 8 20 .2mA
I2 5 20 .2mA

```

**\*Branch Ampmeters**

VID1 7 40 0V

VID2 9 41 0V

VID3 3 42 0V

VID4 10 43 0V

\*VID9 1 55 0V

\*VID10 57 20 0V

**\*MOSFETS\*\*\***

**\*Diffamps**

M1 40 3 8 20 nnf L=2u W=130u

M2 41 10 8 20 nnf L=2u W=130u

M3 42 4 5 20 nnf L=2u W=212u

M4 43 11 5 20 nnf L=2u W=212u

**\*Active Loads**

M7 3 3 1 1 npf L=3u W=5u

M8 10 10 1 1 npf L=3u W=5u

**\*Source Follower/Voltage Shifter**

M9 30 8 1 1 npf L=2u W=140u

M10 30 30 20 20 nnf L=2u W=5u

.ends

**\*Folding Subcircuit\*\*\*\*\***

\* V+ V- Vin Vout M5 M6 Vref  
.subckt fold18 1 20 4 30 7 9 11

**\*Current sources**

I1 8 20 .2mA

I2 5 20 .2mA

**\*Branch Ampmeters**

VID1 7 40 0V

VID2 9 41 0V

VID3 3 42 0V

VID4 10 43 0V

\*VID9 1 55 0V

\*VID10 57 20 0V

**\*MOSFETS\*\*\***

**\*Diffamps**

M1 40 3 8 20 nnf L=2u W=130u

M2 41 10 8 20 nnf L=2u W=130u

M3 42 4 5 20 nnf L=2u W=216u

M4 43 11 5 20 nnf L=2u W=216u

**\*Active Loads**

M7 3 3 1 1 npf L=3u W=5u

M8 10 10 1 1 npf L=3u W=5u

\*Source Follower/Voltage Shifter

M9 30 8 1 1 npf L=2u W=140u

M10 30 30 20 20 nnf L=2u W=5u

.ends

\*Folding Subcircuit\*\*\*\*\*

\* V+ V- Vin Vout M5 M6 Vref

.subckt fold19 1 20 4 30 7 9 11

\*Current sources

I1 8 20 .2mA

I2 5 20 .2mA

\*Branch Ampmeters

VID1 7 40 0V

VID2 9 41 0V

VID3 3 42 0V

VID4 10 43 0V

\*VID9 1 55 0V

\*VID10 57 20 0V

\*MOSFETS\*\*\*

\*Diffamps

M1 40 3 8 20 nnf L=2u W=130u

M2 41 10 8 20 nnf L=2u W=130u

M3 42 4 5 20 nnf L=2u W=220u

M4 43 11 5 20 nnf L=2u W=220u

\*Active Loads

M7 3 3 1 1 npf L=3u W=5u

M8 10 10 1 1 npf L=3u W=5u

\*Source Follower/Voltage Shifter

M9 30 8 1 1 npf L=2u W=140u

M10 30 30 20 20 nnf L=2u W=5u

.ends

\*Folding Subcircuit\*\*\*\*\*

\* V+ V- Vin Vout M5 M6 Vref

.subckt fold20 1 20 4 30 7 9 11

\*Current sources

I1 8 20 .2mA

I2 5 20 .2mA

**\*Branch Ampmeters**

VID1 7 40 0V

VID2 9 41 0V

VID3 3 42 0V

VID4 10 43 0V

\*VID9 1 55 0V

\*VID10 57 20 0V

**\*MOSFETS\*\*\***

**\*Diffamps**

M1 40 3 8 20 nnf L=2u W=130u

M2 41 10 8 20 nnf L=2u W=130u

M3 42 4 5 20 nnf L=2u W=224u

M4 43 11 5 20 nnf L=2u W=224u

**\*Active Loads**

M7 3 3 1 1 npf L=3u W=5u

M8 10 10 1 1 npf L=3u W=5u

**\*Source Follower/Voltage Shifter**

M9 30 8 1 1 npf L=2u W=140u

M10 30 30 20 20 nnf L=2u W=5u

.ends

**\*Folding Subcircuit\*\*\*\*\***

\* V+ V- Vin Vout M5 M6 Vref

.subckt fold21 1 20 4 30 7 9 11

**\*Current sources**

I1 8 20 .2mA

I2 5 20 .2mA

**\*Branch Ampmeters**

VID1 7 40 0V

VID2 9 41 0V

VID3 3 42 0V

VID4 10 43 0V

\*VID9 1 55 0V

\*VID10 57 20 0V

**\*MOSFETS\*\*\***

**\*Diffamps**

M1 40 3 8 20 nnf L=2u W=130u

M2 41 10 8 20 nnf L=2u W=130u

M3 42 4 5 20 nnf L=2u W=228u

M4 43 11 5 20 nnf L=2u W=228u

**\*Active Loads**

M7 3 3 1 1 npf L=3u W=5u

M8 10 10 1 1 npf L=3u W=5u

```

*Source Follower/Voltage Shifter
M9 30 8 1 1 npf L=2u W=140u
M10 30 30 20 20 nnf L=2u W=5u
.ends

*Folding Subcircuit*****
*
*          V+ V- Vin Vout M5 M6 Vref
.subckt fold22 1 20 4 30 7 9 11

*Current sources
I1 8 20 .2mA
I2 5 20 .2mA

*Branch Ampmeters
VID1 7 40 0V
VID2 9 41 0V
VID3 3 42 0V
VID4 10 43 0V
*VID9 1 55 0V
*VID10 57 20 0V
*MOSFETS***
*Diffamps
M1 40 3 8 20 nnf L=2u W=130u
M2 41 10 8 20 nnf L=2u W=130u

M3 42 4 5 20 nnf L=2u W=232u
M4 43 11 5 20 nnf L=2u W=232u

*Active Loads
M7 3 3 1 1 npf L=3u W=5u
M8 10 10 1 1 npf L=3u W=5u

*Source Follower/Voltage Shifter
M9 30 8 1 1 npf L=2u W=140u
M10 30 30 20 20 nnf L=2u W=5u
.ends

*Folding Subcircuit*****
*
*          V+ V- Vin Vout M5 M6 Vref
.subckt fold23 1 20 4 30 7 9 11

*Current sources
I1 8 20 .2mA
I2 5 20 .2mA

*Branch Ampmeters
VID1 7 40 0V
VID2 9 41 0V
VID3 3 42 0V

```

VID4 10 43 0V  
\*VID9 1 55 0V  
\*VID10 57 20 0V  
\*MOSFETS\*\*\*  
\*Diffamps  
M1 40 3 8 20 nnf L=2u W=130u  
M2 41 10 8 20 nnf L=2u W=130u

M3 42 4 5 20 nnf L=2u W=236u  
M4 43 11 5 20 nnf L=2u W=236u

\*Active Loads

M7 3 3 1 1 npf L=3u W=5u  
M8 10 10 1 1 npf L=3u W=5u

\*Source Follower/Voltage Shifter

M9 30 8 1 1 npf L=2u W=140u

M10 30 30 20 20 nnf L=2u W=5u

.ends

\*Folding Subcircuit\*\*\*\*\*

\* V+ V- Vin Vout M5 M6 Vref  
.subckt fold24 1 20 4 30 7 9 11

\*Current sources

I1 8 20 .2mA

I2 5 20 .2mA

\*Branch Ammeters

VID1 7 40 0V

VID2 9 41 0V

VID3 3 42 0V

VID4 10 43 0V

\*VID9 1 55 0V

\*VID10 57 20 0V

\*MOSFETS\*\*\*

\*Diffamps

M1 40 3 8 20 nnf L=2u W=130u

M2 41 10 8 20 nnf L=2u W=130u

M3 42 4 5 20 nnf L=2u W=240u

M4 43 11 5 20 nnf L=2u W=240u

\*Active Loads

M7 3 3 1 1 npf L=3u W=5u

M8 10 10 1 1 npf L=3u W=5u

\*Source Follower/Voltage Shifter

M9 30 8 1 1 npf L=2u W=140u

M10 30 30 20 20 nnf L=2u W=5u

```

.ends

*Folding Subcircuit*****
*          V+ V- Vin Vout M5 M6 Vref
.subckt fold25 1 20 4 30 7 9 11

*Current sources
I1 8 20 .2mA
I2 5 20 .2mA

*Branch Ampmeters
VID1 7 40 0V
VID2 9 41 0V
VID3 3 42 0V
VID4 10 43 0V
*VID9 1 55 0V
*VID10 57 20 0V
*MOSFETS***
*Diffamps
M1 40 3 8 20 nnf L=2u W=130u
M2 41 10 8 20 nnf L=2u W=130u

M3 42 4 5 20 nnf L=2u W=244u
M4 43 11 5 20 nnf L=2u W=244u

*Active Loads
M7 3 3 1 1 npf L=3u W=5u
M8 10 10 1 1 npf L=3u W=5u

*Source Follower/Voltage Shifter
M9 30 8 1 1 npf L=2u W=140u
M10 30 30 20 20 nnf L=2u W=5u
.ends

*Folding Subcircuit*****
*          V+ V- Vin Vout M5 M6 Vref
.subckt fold26 1 20 4 30 7 9 11

*Current sources
I1 8 20 .2mA
I2 5 20 .2mA

*Branch Ampmeters
VID1 7 40 0V
VID2 9 41 0V
VID3 3 42 0V
VID4 10 43 0V
*VID9 1 55 0V
*VID10 57 20 0V

```

**\*MOSFETS\*\*\***

**\*Diffamps**

M1 40 3 8 20 nnf L=2u W=130u  
M2 41 10 8 20 nnf L=2u W=130u

M3 42 4 5 20 nnf L=2u W=248u  
M4 43 11 5 20 nnf L=2u W=248u

**\*Active Loads**

M7 3 3 1 1 npf L=3u W=5u  
M8 10 10 1 1 npf L=3u W=5u

**\*Source Follower/Voltage Shifter**

M9 30 8 1 1 npf L=2u W=140u

M10 30 30 20 20 nnf L=2u W=5u

.ends

**\*Folding Subcircuit\*\*\*\*\***

\* V+ V- Vin Vout M5 M6 Vref  
.subckt fold27 1 20 4 30 7 9 11

**\*Current sources**

I1 8 20 .2mA

I2 5 20 .2mA

**\*Branch Ampmeters**

VID1 7 40 0V

VID2 9 41 0V

VID3 3 42 0V

VID4 10 43 0V

\*VID9 1 55 0V

\*VID10 57 20 0V

**\*MOSFETS\*\*\***

**\*Diffamps**

M1 40 3 8 20 nnf L=2u W=130u  
M2 41 10 8 20 nnf L=2u W=130u

M3 42 4 5 20 nnf L=2u W=252u

M4 43 11 5 20 nnf L=2u W=252u

**\*Active Loads**

M7 3 3 1 1 npf L=3u W=5u

M8 10 10 1 1 npf L=3u W=5u

**\*Source Follower/Voltage Shifter**

M9 30 8 1 1 npf L=2u W=140u

M10 30 30 20 20 nnf L=2u W=5u

.ends

**\*Folding Subcircuit\*\*\*\*\***

```

*          V+ V- Vin Vout M5 M6 Vref
.subckt fold28 1 20 4    30 7 9 11

*Current sources
I1 8 20 .2mA
I2 5 20 .2mA

*Branch Ampmeters
VID1 7 40 0V
VID2 9 41 0V
VID3 3 42 0V
VID4 10 43 0V
*VID9 1 55 0V
*VID10 57 20 0V
*MOSFETS***

*Diffamps
M1 40 3 8 20 nnf L=2u W=130u
M2 41 10 8 20 nnf L=2u W=130u

M3 42 4 5 20 nnf L=2u W=258u
M4 43 11 5 20 nnf L=2u W=258u

*Active Loads
M7 3 3 1 1 npf L=3u W=5u
M8 10 10 1 1 npf L=3u W=5u

*Source Follower/Voltage Shifter
M9 30 8 1 1 npf L=2u W=140u
M10 30 30 20 20 nnf L=2u W=5u
.ends

*Folding Subcircuit*****
*          V+ V- Vin Vout M5 M6 Vref
.subckt fold29 1 20 4    30 7 9 11

*Current sources
I1 8 20 .2mA
I2 5 20 .2mA

*Branch Ampmeters
VID1 7 40 0V
VID2 9 41 0V
VID3 3 42 0V
VID4 10 43 0V
*VID9 1 55 0V
*VID10 57 20 0V
*MOSFETS***

*Diffamps
M1 40 3 8 20 nnf L=2u W=130u

```

M2 41 10 8 20 nnf L=2u W=130u

M3 42 4 5 20 nnf L=2u W=264u

M4 43 11 5 20 nnf L=2u W=264u

\*Active Loads

M7 3 3 1 1 npf L=3u W=5u

M8 10 10 1 1 npf L=3u W=5u

\*Source Follower/Voltage Shifter

M9 30 8 1 1 npf L=2u W=140u

M10 30 30 20 20 nnf L=2u W=5u

.ends

\*Folding Subcircuit\*\*\*\*\*

\* V+ V- Vin Vout M5 M6 Vref  
.subckt fold30 1 20 4 30 7 9 11

\*Current sources

I1 8 20 .2mA

I2 5 20 .2mA

\*Branch Ampmeters

VID1 7 40 0V

VID2 9 41 0V

VID3 3 42 0V

VID4 10 43 0V

\*VID9 1 55 0V

\*VID10 57 20 0V

\*MOSFETS\*\*\*

\*Diffamps

M1 40 3 8 20 nnf L=2u W=130u

M2 41 10 8 20 nnf L=2u W=130u

M3 42 4 5 20 nnf L=2u W=270u

M4 43 11 5 20 nnf L=2u W=270u

\*Active Loads

M7 3 3 1 1 npf L=3u W=5u

M8 10 10 1 1 npf L=3u W=5u

\*Source Follower/Voltage Shifter

M9 30 8 1 1 npf L=2u W=140u

M10 30 30 20 20 nnf L=2u W=5u

.ends

\*Folding Subcircuit\*\*\*\*\*

\* V+ V- Vin Vout M5 M6 Vref  
.subckt fold31 1 20 4 30 7 9 11

**\*Current sources**

I1 8 20 .2mA  
I2 5 20 .2mA

**\*Branch Ampmeters**

VID1 7 40 0V  
VID2 9 41 0V  
VID3 3 42 0V  
VID4 10 43 0V  
\*VID9 1 55 0V  
\*VID10 57 20 0V

**\*MOSFETS\*\*\***

**\*Diffamps**

M1 40 3 8 20 nnf L=2u W=130u  
M2 41 10 8 20 nnf L=2u W=130u  
  
M3 42 4 5 20 nnf L=2u W=282u  
M4 43 11 5 20 nnf L=2u W=282u

**\*Active Loads**

M7 3 3 1 1 npf L=3u W=5u  
M8 10 10 1 1 npf L=3u W=5u

**\*Source Follower/Voltage Shifter**

M9 30 8 1 1 npf L=2u W=140u  
M10 30 30 20 20 nnf L=2u W=5u

.ends

**\*Folding Subcircuit\*\*\*\*\***

\* V+ V- Vin Vout M5 M6 Vref  
.subckt fold32 1 20 4 30 7 9 11

**\*Current sources**

I1 8 20 .2mA  
I2 5 20 .2mA

**\*Branch Ampmeters**

VID1 7 40 0V  
VID2 9 41 0V  
VID3 3 42 0V  
VID4 10 43 0V  
\*VID9 1 55 0V  
\*VID10 57 20 0V

**\*MOSFETS\*\*\***

**\*Diffamps**

M1 40 3 8 20 nnf L=2u W=130u  
M2 41 10 8 20 nnf L=2u W=130u

M3 42 4 5 20 nnf L=2u W=294u  
M4 43 11 5 20 nnf L=2u W=294u

\*Active Loads

M7 3 3 1 1 npf L=3u W=5u  
M8 10 10 1 1 npf L=3u W=5u

\*Source Follower/Voltage Shifter

M9 30 8 1 1 npf L=2u W=140u  
M10 30 30 20 20 nnf L=2u W=5u  
.ends

\*Folding Subcircuit\*\*\*\*\*

\* V+ V- Vin Vout M5 M6 Vref  
.subckt fold33 1 20 4 30 7 9 11

\*Current sources

I1 8 20 .2mA  
I2 5 20 .2mA

\*Branch Ampmeters

VID1 7 40 0V  
VID2 9 41 0V  
VID3 3 42 0V  
VID4 10 43 0V  
\*VID9 1 55 0V  
\*VID10 57 20 0V

\*MOSFETS\*\*\*

\*Diffamps

M1 40 3 8 20 nnf L=2u W=130u  
M2 41 10 8 20 nnf L=2u W=130u  
  
M3 42 4 5 20 nnf L=2u W=296u  
M4 43 11 5 20 nnf L=2u W=296u

\*Active Loads

M7 3 3 1 1 npf L=3u W=5u  
M8 10 10 1 1 npf L=3u W=5u

\*Source Follower/Voltage Shifter

M9 30 8 1 1 npf L=2u W=140u  
M10 30 30 20 20 nnf L=2u W=5u  
.ends

\*Folding Subcircuit\*\*\*\*\*

\* V+ V- Vin Vout M5 M6 Vref  
.subckt fold34 1 20 4 30 7 9 11

\*Current sources

I1 8 20 .2mA  
I2 5 20 .2mA

\*Branch Ampmeters

VID1 7 40 0V

VID2 9 41 0V

VID3 3 42 0V

VID4 10 43 0V

\*VID9 1 55 0V

\*VID10 57 20 0V

\*MOSFETS\*\*\*

\*Diffamps

M1 40 3 8 20 nnf L=2u W=130u

M2 41 10 8 20 nnf L=2u W=130u

M3 42 4 5 20 nnf L=2u W=300u

M4 43 11 5 20 nnf L=2u W=300u

\*Active Loads

M7 3 3 1 1 npf L=3u W=5u

M8 10 10 1 1 npf L=3u W=5u

\*Source Follower/Voltage Shifter

M9 30 8 1 1 npf L=2u W=140u

M10 30 30 20 20 nnf L=2u W=5u

.ends

\*Folding Subcircuit\*\*\*\*\*

\* V+ V- Vin Vout M5 M6 Vref

.subckt fold35 1 20 4 30 7 9 11

\*Current sources

I1 8 20 .2mA

I2 5 20 .2mA

\*Branch Ampmeters

VID1 7 40 0V

VID2 9 41 0V

VID3 3 42 0V

VID4 10 43 0V

\*VID9 1 55 0V

\*VID10 57 20 0V

\*MOSFETS\*\*\*

\*Diffamps

M1 40 3 8 20 nnf L=2u W=130u

M2 41 10 8 20 nnf L=2u W=130u

M3 42 4 5 20 nnf L=2u W=310u  
M4 43 11 5 20 nnf L=2u W=310u

\*Active Loads

M7 3 3 1 1 npf L=3u W=5u  
M8 10 10 1 1 npf L=3u W=5u

\*Source Follower/Voltage Shifter

M9 30 8 1 1 npf L=2u W=140u  
M10 30 30 20 20 nnf L=2u W=5u

.ends

\*Folding Subcircuit\*\*\*\*\*

\* V+ V- Vin Vout M5 M6 Vref  
.subckt fold36 1 20 4 30 7 9 11

\*Current sources

I1 8 20 .2mA  
I2 5 20 .2mA

\*Branch Ampmeters

VID1 7 40 0V

VID2 9 41 0V

VID3 3 42 0V

VID4 10 43 0V

\*VID9 1 55 0V

\*VID10 57 20 0V

\*MOSFETS\*\*\*

\*Diffamps

M1 40 3 8 20 nnf L=2u W=130u  
M2 41 10 8 20 nnf L=2u W=130u

M3 42 4 5 20 nnf L=2u W=320u

M4 43 11 5 20 nnf L=2u W=320u

\*Active Loads

M7 3 3 1 1 npf L=3u W=5u

M8 10 10 1 1 npf L=3u W=5u

\*Source Follower/Voltage Shifter

M9 30 8 1 1 npf L=2u W=140u

M10 30 30 20 20 nnf L=2u W=5u

.ends

\*Folding Subcircuit\*\*\*\*\*

\* V+ V- Vin Vout M5 M6 Vref  
.subckt fold37 1 20 4 30 7 9 11

\*Current sources

I1 8 20 .2mA  
I2 5 20 .2mA

\*Branch Ampmeters

VID1 7 40 0V

VID2 9 41 0V

VID3 3 42 0V

VID4 10 43 0V

\*VID9 1 55 0V

\*VID10 57 20 0V

\*MOSFETS\*\*\*

\*Diffamps

M1 40 3 8 20 nnf L=2u W=130u

M2 41 10 8 20 nnf L=2u W=130u

M3 42 4 5 20 nnf L=2u W=326u

M4 43 11 5 20 nnf L=2u W=326u

\*Active Loads

M7 3 3 1 1 npf L=3u W=5u

M8 10 10 1 1 npf L=3u W=5u

\*Source Follower/Voltage Shifter

M9 30 8 1 1 npf L=2u W=140u

M10 30 30 20 20 nnf L=2u W=5u

.ends

\*Folding Subcircuit\*\*\*\*\*

\* V+ V- Vin Vout M5 M6 Vref  
.subckt fold38 1 20 4 30 7 9 11

\*Current sources

I1 8 20 .2mA

I2 5 20 .2mA

\*Branch Ampmeters

VID1 7 40 0V

VID2 9 41 0V

VID3 3 42 0V

VID4 10 43 0V

\*VID9 1 55 0V

\*VID10 57 20 0V

\*MOSFETS\*\*\*

\*Diffamps

M1 40 3 8 20 nnf L=2u W=130u

M2 41 10 8 20 nnf L=2u W=130u

```
M3 42 4 5 20 nnf L=2u W=330u  
M4 43 11 5 20 nnf L=2u W=330u
```

\*Active Loads

```
M7 3 3 1 1 npf L=3u W=5u  
M8 10 10 1 1 npf L=3u W=5u
```

\*Source Follower/Voltage Shifter

```
M9 30 8 1 1 npf L=2u W=140u  
M10 30 30 20 20 nnf L=2u W=5u  
.ends
```

\*\*\*\*\*Emitter Follower\*\*\*\*\*

```
* V+ V- Vin Vout  
.subckt emit 1 4 2 6  
M2 1 2 6 4 nnf L=10u W=3u  
.ends
```

```
*opamp subcircuit Vdd Vss V- V+ Vout  
.subckt opamp 1 2 7 9 6
```

\*Passive Elements

```
Rbias 1 3 2K  
Rz 5 10 13K  
CC 10 6 5pF
```

\*Fets

```
M1 4 7 8 2 nnf L=10u W=40u  
M2 5 9 8 2 nnf L=10u W=40u  
M3 4 4 1 1 npf L=22u W=10u  
M4 5 4 1 1 npf L=22u W=10u  
M5 6 5 1 1 npf L=10u W=45u  
M6 6 3 2 2 nnf L=10u W=10u  
M7 8 3 2 2 nnf L=50u W=10u  
M8 3 3 2 2 nnf L=10u W=10u
```

```
.ends
```

\*\*\*\*\*Comparator Subcircuits\*\*\*\*\*

```
* Vdd Vss Vn Vout Vp  
.subckt comprtr 1 2 6 9 8  
VB 10 0 dc .8v  
M1 4 6 7 0 nnf W=10u L=10u  
M2 5 8 7 0 nnf W=10u L=10u  
M3 4 4 1 1 npf W=12u L=3u  
M4 5 4 1 1 npf W=12u L=3u
```

```

M5 7 10 2 0 nnf W=10u L=10u
M6 9 5 1 1 npf W=4u L=2u
M7 9 5 0 0 nnf W=4u L=2u

.ends

*****Transmission Gate *****
*
      Vin VDD VSS  VC1 VC2 Vout
.subckt transgate 1 10 20 4 2 3

*Vdd 10 0 5
*VCC 20 0 0.0

M1 3 2 1 10 npf W=3u L=2u
M2 1 4 3 20 nnf w=6u L=2u

C1 3 0 inf ic=0
.ends

*****Decoder (Comparator Level to Thermometer Code) *****
*
      Vdd v1 v2 v3 v4 v5 v6 vo1 vo2 vo3 vo4 vo5
vo6 .subckt decclthc 1 2 3 4 5 6 7 21 22 23 24
25 26
*Inverter Instantiations
X1 1 3 11 inv
X2 1 4 12 inv
X3 1 5 13 inv
X4 1 6 14 inv
X5 1 7 15 inv
X6 1 0 16 inv

```

```

*AND 2-input Instantiations
X101 1 2 11 21 and2
X102 1 3 12 22 and2
X103 1 4 13 23 and2
X104 1 5 14 24 and2
X105 1 6 15 25 and2
X106 1 7 16 26 and2

```

\*\*\*\*\*Subcircuit Definitions\*\*\*\*\*

\*\*\*\*\*Inverter Subcircuit\*\*\*\*\*

```

*          Vdd  Vin  Vout
.subckt inv  1     2     3

*Fet's
M1  3 2 1 1  npf  W=7u L=2u
M2  3 2 0 0  nnf  W=3u L=2u

.ends

*****AND 2-Input Subcircuit*****
*          Vdd  VA   VB   Vout
.subckt and2  1    2    3    6

*FET's
M1  4 2 1 1  npf  W=7u L=2u
M2  4 3 1 1  npf  W=7u L=2u
M3  6 4 1 1  npf  W=7u L=2u
M4  4 3 5 0  nnf  W=3u L=2u
M5  5 2 0 0  nnf  W=3u L=2u
M6  6 4 0 0  nnf  W=3u L=2u

.ends

.ends

*****Decoder (Thermometer Code to SNS Binary)
***** *
.subckt decthcsnsb  1 2 3 4 5 6 7  101 102 103

*OR Gate Instantiations
X1  1 2 4 6 101  or3
X2  1 3 4 7 102  or3
X3  1 5 6 7 103  or3

*****OR Gate Subcircuit*****
*          Vdd  VA   VB   VC       Vout
.subckt or3   1    3    5    7      11

*FET's
M1  4 3 1 1  npf  W=7u L=2u
M2  6 5 4 1  npf  W=7u L=2u
M3  10 7 6 1  npf  W=7u L=2u
M5  11 10 1 1  npf  W=7u L=2u
M6  10 3 0 0  nnf  W=3u L=2u
M7  10 5 0 0  nnf  W=3u L=2u
M8  10 7 0 0  nnf  W=3u L=2u
M10 11 10 0 0  nnf  W=3u L=2u

```

.ends

.ends

\*\*\*\*\*Simulation Parameters\*\*\*\*\*

.option dcon=1 post probe  
\*.dc vin 0.0V .82V .029286

\*.probe tran v(3) v(405) V(701) V(702) V(703) V(704) V(705)  
V(706) V(801) V(802) \*V(803) V(804) V(805) V(806) V(901)  
V(902) V(903) .probe v(405)

.tran 65.6ns 1.63us

.end

APPENDIX B  
INPUT FILE FOR PLA GENERATION

```
#Thesis PLA
a pla
b I10 I9 I8 I7 I6 I5 I4 I3 I2 I1
    X9 X8 X7 X6 X5 X4 X3 X2 X1
#.type fr
#####PLA Truth Table#####
10
9
512
0000000000 0000000000
0001001001 0000000001
0010010010 0000000010
0011011011 0000000011
0100100100 0000000100
0101101101 0000000101
0110110110 0000000110
0111111110 0000000111
1000111101 000001000
1001110100 000001001
1010101011 000001010
1010100010 000001011
1001011001 000001100
1000010000 000001101
0111001000 000001110
0110000001 000001111
0101000010 000010000
0100001011 000010001
0011010100 000010010
0010011101 000010011
0001100110 000010100
0000101110 000010101
0000110101 000010110
0001111100 000010111
0010111011 000011000
0011110010 000011001
0100101001 000011010
0101100000 000011011
0110011000 000011100
0111010001 000011101
1000001010 000011110
1001000011 000011111
1010000100 000100000
1010001101 000100001
1001010110 000100010
1000011110 000100011
```

0111100101 000100100  
0110101100 000100101  
0101110011 000100110  
0100111010 000100111  
0011111001 000101000  
0010110000 000101001  
0001101000 000101010  
0000100001 000101011  
0000011010 000101100  
0001010011 000101101  
0010001100 000101110  
0011000101 000101111  
0100000110 000110000  
0101001110 000110001  
0110010101 000110010  
0111011100 000110011  
1000100011 000110100  
1001101010 000110101  
1010110001 000110110  
1010111000 000110111  
1001111000 000111000  
1000110001 000111001  
0111101010 000111010  
0110100011 000111011  
0101011100 000111100  
0100010101 000111101  
0011001110 000111110  
0010000110 000111111  
0001000101 001000000  
0000001100 001000001  
0000010011 001000010  
0001011010 001000011  
0010100001 001000100  
0011101000 001000101  
0100110000 001000110  
0101111001 001000111  
0110111010 001001000  
0111110011 001001001  
1000101100 001001010  
1001100101 001001011  
1010011110 001001100  
1010010110 001001101  
1001001101 001001110  
1000000100 001001111  
0111000011 001010000  
0110001010 001010001  
0101010001 001010010  
0100011000 001010011  
0011100000 001010100  
0010101001 001010101  
0001110010 001010110

0000111011 001010111  
0000111100 001011000  
0001110101 001011001  
0010101110 001011010  
0011100110 001011011  
0100011101 001011100  
0101010100 001011101  
0110001011 001011110  
0111000010 001011111  
1000000001 001100000  
1001001000 001100001  
1010010000 001100010  
1010011001 001100011  
1001100010 001100100  
1000101011 001100101  
011110100 001100110  
0110111101 001100111  
0101111110 001101000  
0100110110 001101001  
0011101101 001101010  
0010100100 001101011  
0001011011 001101100  
0000010010 001101101  
0000001001 001101110  
0001000000 001101111  
0010000000 001110000  
0011001001 001110001  
0100010010 001110010  
0101011011 001110011  
0110100100 001110100  
0111101101 001110101  
1000110110 001110110  
1001111110 001110111  
1010111101 001111000  
1010110100 001111001  
1001101011 001111010  
1000100010 001111011  
0111011001 001111100  
0110010000 001111101  
0101001000 001111110  
0100000001 001111111  
0011000010 010000000  
0010001011 010000001  
0001010100 010000010  
0000011101 010000011  
0000100110 010000100  
0001101110 010000101  
0010110101 010000110  
0011111100 010000111  
0100111011 010001000  
0101110010 010001001

0110101001 010001010  
0111100000 010001011  
1000011000 010001100  
1001010001 010001101  
1010001010 010001110  
1010000011 010001111  
1001000100 010010000  
1000001101 010010001  
0111010110 010010010  
0110011110 010010011  
0101100101 010010100  
0100101100 010010101  
0011110011 010010110  
0010111010 010010111  
0001111001 010011000  
0000110000 010011001  
0000101000 010011010  
0001100001 010011011  
0010011010 010011100  
0011010011 010011101  
0100001100 010011110  
0101000101 010011111  
0110000110 010100000  
0111001110 010100001  
1000010101 010100010  
1001011100 010100011  
1010100011 010100100  
1010101010 010100101  
1001110001 010100110  
1000111000 010100111  
0111111000 010101000  
0110110001 010101001  
0101101010 010101010  
0100100011 010101011  
0011011100 010101100  
0010010101 010101101  
0001001110 010101110  
0000000110 010101111  
0000000101 010110000  
0001001100 010110001  
0010010011 010110010  
0011011010 010110011  
0100100001 010110100  
0101101000 010110101  
0110110000 010110110  
0111111001 010110111  
1000111010 010111000  
1001110011 010111001  
1010101100 010111010  
1010100101 010111011  
1001011110 010111100

1000010110 010111101  
0111001101 010111110  
0110000100 010111111  
0101000011 011000000  
0100001010 011000001  
0011010001 011000010  
0010011000 011000011  
0001100000 011000100  
0000101001 011000101  
0000110010 011000110  
0001111011 011000111  
0010111100 011001000  
0011110101 011001001  
0100101110 011001010  
0101100110 011001011  
0110011101 011001100  
0111010100 011001101  
1000001011 011001110  
1001000010 011001111  
1010000001 011010000  
1010001000 011010001  
1001010000 011010010  
1000011001 011010011  
0111100010 011010100  
0110101011 011010101  
0101110100 011010110  
0100111101 011010111  
0011111110 011011000  
0010110110 011011001  
0001101101 011011010  
0000100100 011011011  
0000011011 011011100  
0001010010 011011101  
0010001001 011011110  
0011000000 011011111  
0100000000 011100000  
0101001001 011100001  
0110010010 011100010  
0111011011 011100011  
1000100100 011100100  
1001101101 011100101  
1010110110 011100110  
1010111110 011100111  
1001111101 011101000  
1000110100 011101001  
0111101011 011101010  
0110100010 011101011  
0101011001 011101100  
0100010000 011101101  
0011001000 011101110  
0010000001 011101111

0001000010 011110000  
0000001011 011110001  
0000010100 011110010  
0001011101 011110011  
0010100110 011110100  
0011101110 011110101  
0100110101 011110110  
0101111100 011110111  
0110111011 011111000  
0111110010 011111001  
1000101001 011111010  
1001100000 011111011  
1010011000 011111100  
1010010001 011111101  
1001001010 011111110  
1000000011 011111111  
0111000100 1000000000  
0110001101 1000000001  
0101010110 1000000010  
0100011110 1000000011  
0011100101 1000000100  
0010101100 1000000101  
0001110011 1000000110  
0000111010 1000000111  
0000111001 100001000  
0001110000 100001001  
0010101000 100001010  
0011100001 100001011  
0100011010 100001100  
0101010011 100001101  
0110001100 100001110  
0111000101 100001111  
1000000110 100010000  
1001001110 100010001  
1010010101 100010010  
1010011100 100010011  
1001100011 100010100  
1000101010 100010101  
0111110001 100010110  
0110111000 100010111  
0101111000 100011000  
0100110001 100011001  
0011101010 100011010  
0010100011 100011011  
0001011100 100011100  
0000010101 100011101  
0000001110 100011110  
0001000110 100011111  
0010000101 100100000  
0011001100 100100001  
0100010011 100100010

0101011010 100100011  
0110100001 100100100  
0111101000 100100101  
1000110000 100100110  
1001111001 100100111  
1010111010 100101000  
1010110011 100101001  
1001101100 100101010  
1000100101 100101011  
0111011110 100101100  
0110010110 100101101  
0101001101 100101110  
0100000100 100101111  
0011000011 100110000  
0010001010 100110001  
0001010001 100110010  
0000011000 100110011  
0000100000 100110100  
0001101001 100110101  
0010110010 100110110  
0011111011 100110111  
0100111100 100111000  
0101110101 100111001  
0110101110 100111010  
0111100110 100111011  
1000011101 100111100  
1001010100 100111101  
1010001011 100111110  
10100000010 100111111  
1001000001 101000000  
1000001000 101000001  
0111010000 101000010  
0110011001 101000011  
0101100010 101000100  
0100101011 101000101  
0011110100 101000110  
0010111101 101000111  
0001111110 101001000  
0000110110 101001001  
0000101101 101001010  
0001100100 101001011  
0010011011 101001100  
0011010010 101001101  
0100001001 101001110  
0101000000 101001111  
0110000000 101010000  
0111001001 101010001  
1000010010 101010010  
1001011011 101010011  
1010100100 101010100  
1010101101 101010101

1001110110 101010110  
1000111110 101010111  
0111111101 101011000  
0110110100 101011001  
0101101011 101011010  
0100100010 101011011  
0011011001 101011100  
0010010000 101011101  
0001001000 101011110  
0000000001 101011111  
0000000010 101100000  
0001001011 101100001  
0010010100 101100010  
0011011101 101100011  
0100100110 101100100  
0101101110 101100101  
0110110101 101100110  
0111111100 101100111  
1000111011 101101000  
1001110010 101101001  
1010101001 101101010  
1010100000 101101011  
1001011000 101101100  
1000010001 101101101  
0111001010 101101110  
0110000011 101101111  
0101000100 101110000  
0100001101 101110001  
0011010110 101110010  
0010011110 101110011  
0001100101 101110100  
0000101100 101110101  
0000110011 101110110  
0001111010 101110111  
0010111001 101111000  
0011110000 101111001  
0100101000 101111010  
0101100001 101111011  
0110011010 101111100  
0111010011 101111101  
1000001100 101111110  
1001000101 101111111  
1010000110 110000000  
1010001110 110000001  
1001010101 110000010  
1000011100 110000011  
0111100011 110000100  
0110101010 110000101  
0101110001 110000110  
0100111000 110000111  
0011111000 110001000

0010110001 110001001  
0001101010 110001010  
0000100011 110001011  
0000011100 110001100  
0001010101 110001101  
0010001110 110001110  
0011000110 110001111  
0100000101 110010000  
0101001100 110010001  
0110010011 110010010  
0111011010 110010011  
1000100001 110010100  
1001101000 110010101  
1010110000 110010110  
1010111001 110010111  
1001111010 110011000  
1000110011 110011001  
0111101100 110011010  
0110100101 110011011  
0101011110 110011100  
0100010110 110011101  
0011001101 110011110  
0010000100 110011111  
0001000011 110100000  
00000001010 110100001  
00000010001 110100010  
0001011000 110100011  
0010100000 110100100  
0011101001 110100101  
0100110010 110100110  
0101111011 110100111  
0110111100 110101000  
0111110101 110101001  
1000101110 110101010  
1001100110 110101011  
1010011101 110101100  
1010010100 110101101  
1001001011 110101110  
1000000010 110101111  
0111000001 110110000  
0110001000 110110001  
0101010000 110110010  
0100011001 110110011  
0011100010 110110100  
0010101011 110110101  
0001110100 110110110  
0000111101 110110111  
0000111110 110111000  
0001110110 110111001  
0010101101 110111010  
0011100100 110111011

0100011011 110111100  
0101010010 110111101  
0110001001 110111110  
0111000000 110111111  
1000000000 111000000  
1001001001 111000001  
1010010010 111000010  
1010011011 111000011  
1001100100 111000100  
1000101101 111000101  
0111110110 111000110  
0110111110 111000111  
0101111101 111001000  
0100110100 111001001  
0011101011 111001010  
0010100010 111001011  
0001011001 111001100  
0000010000 111001101  
0000001000 111001110  
0001000001 111001111  
0010000010 111010000  
0011001011 111010001  
0100010100 111010010  
0101011101 111010011  
0110100110 111010100  
0111101110 111010101  
1000110101 111010110  
1001111100 111010111  
1010111101 111011000  
1010110010 111011001  
1001101001 111011010  
1000100000 111011011  
0111011100 111011100  
0110010001 111011101  
0101001010 111011110  
0100000011 111011111  
0011000100 111100000  
0010001101 111100001  
0001010110 111100010  
0000011110 111100011  
0000100101 111100100  
0001101100 111100101  
0010110011 111100110  
0011111101 111100111  
0100111100 111101000  
0101110000 111101001  
110101000 111101010  
0111100001 111101011  
1000011101 111101100  
1001010011 111101101  
1010001100 111101110

1010000101	111101111
1001000110	111110000
10000001110	111110001
0111010101	111110010
0110011100	111110011
0101100011	111110100
0100101010	111110101
0011110001	111110110
0010111000	111110111
0001111000	111111000
0000110001	111111001
0000101010	111111010
0001100011	111111011
0010011100	111111100
0011010101	111111101
0100001110	111111110
0101000110	111111111

## APPENDIX C

### MATLAB PROGRAM TO GENERATE PLA TRUTH TABLE

```
*This M-file generates a truth table for a pla used in  
thesis
```

```
clear
```

```
* input Vectors
```

```
seed7=[0 0 0  
0 0 1  
0 1 0  
0 1 1  
1 0 0  
1 0 1  
1 1 0  
1 1 0  
1 0 1  
1 0 0  
0 1 1  
0 1 0  
0 0 1  
0 0 0];
```

```
seed8=[0 0 0  
0 0 1  
0 1 0  
0 1 1  
1 0 0  
1 0 1  
1 1 0  
1 1 1  
1 1 1  
1 1 0  
1 0 1  
1 0 0  
0 1 1  
0 1 0  
0 0 1  
0 0 0];
```

```

seed11=[0 0 0 0
        0 0 0 1
        0 0 1 0
        0 0 1 1
        0 1 0 0
        0 1 0 1
        0 1 1 0
        0 1 1 1
        1 0 0 0
        1 0 0 1
        1 0 1 0
        1 0 1 0
        1 0 0 1
        1 0 0 0
        0 1 1 1
        0 1 1 0
        0 1 0 1
        0 1 0 0
        0 0 1 1
        0 0 1 0
        0 0 0 1
        0 0 0 0];

sz7=max(size(seed7));
sz8=max(size(seed8));
sz11=max(size(seed11));

n7=ceil(512/sz7);
n8=ceil(512/sz8);
n11=ceil(512/sz11);

for j=1:n7
    input7=[input7;seed7];
end

for j=1:n8
    input8=[input8;seed8];
end

for j=1:n11
    input11=[input11;seed11];
end

input7=input7(1:512,:);
input8=input8(1:512,:);

```

```

input11=input11(1:512,:);

snsv=[input11 input8 input7];

%This produces a 9-bit binary table

seedb1=[zeros(1,1);ones(1,1)];
seedb2=[zeros(2,1);ones(2,1)];
seedb3=[zeros(4,1);ones(4,1)];
seedb4=[zeros(8,1);ones(8,1)];
seedb5=[zeros(16,1);ones(16,1)];
seedb6=[zeros(32,1);ones(32,1)];
seedb7=[zeros(64,1);ones(64,1)];
seedb8=[zeros(128,1);ones(128,1)];
seedb9=[zeros(256,1);ones(256,1)];

szb1=max(size(seedb1));
szb2=max(size(seedb2));
szb3=max(size(seedb3));
szb4=max(size(seedb4));
szb5=max(size(seedb5));
szb6=max(size(seedb6));
szb7=max(size(seedb7));
szb8=max(size(seedb8));

nb1=ceil(512/szb1);
nb2=ceil(512/szb2);
nb3=ceil(512/szb3);
nb4=ceil(512/szb4);
nb5=ceil(512/szb5);
nb6=ceil(512/szb6);
nb7=ceil(512/szb7);
nb8=ceil(512/szb8);

for j=1:nb1
    outputb1=[outputb1;seedb1];
end

for j=1:nb2
    outputb2=[outputb2;seedb2];
end

for j=1:nb3

```

```

        outputb3=[outputb3;seedb3];
end

for j=1:nb4
    outputb4=[outputb4;seedb4];
end

for j=1:nb5
    outputb5=[outputb5;seedb5];
end

for j=1:nb6
    outputb6=[outputb6;seedb6];
end

for j=1:nb7
    outputb7=[outputb7;seedb7];
end

for j=1:nb8
    outputb8=[outputb8;seedb8];
end

output=[seedb9 outputb8 outputb7 outputb6 outputb5 outputb4
outputb3 ...
    outputb2 outputb1];

s=3;
for j=1:512
    sbg(j)=s;
end
sbg=sbg';

platt=[snsv sbg output]

```

APPENDIX D  
DIGITAL SIMULATION OF PLA

```
sun2:/home5/esparza/thesis/magic
* esim thespla3.sim
ESIM (V3.5 03/27/91)
7482 transistors, 562 nodes (521 pulled up)
sim> I
initialization took 1539 steps
sim> I
initialization took 0 steps
sim> w I10 I9 I8 I7 I6 I5 I4 I3 I2 I1 X9 X8 X7 X6 X5 X4 X3
X2 X1
sim> V I10 00000
sim> V I9 00001
sim> V I8 00110
sim> V I7 01010
sim> V I6 00001
sim> V I5 00110
sim> V I4 01010
sim> V I3 00001
sim> V I2 00110
sim> V I1 01010
sim> I
initialization took 0 steps
sim> G
>00000:I10
>00001:I9
>00110:I8
>01010:I7
>00001:I6
>00110:I5
>01010:I4
>00001:I3
>00110:I2
>01010:I1
>00000:X9
>00000:X8
>00000:X7
>00000:X6
>00000:X5
>00000:X4
>00001:X3
>00110:X2
>01010:X1
sim> Q
```

#### LIST OF REFERENCES

1. Coughlin, R.F., and Driscoll, F.F., Operational Amplifiers & Linear Integrated Circuits, pp. 401-418, 4th ed., Prentice-Hall, Inc., 1991.
2. Analog Devices, Inc., Analog-Digital Conversion Handbook, pp. 211-220., Prentice-Hall, Inc., 1986.
3. Hnatek, E.R., A User's Handbook of D/A and A/D Converters, pp. 14-21., John Wiley & Sons, Inc., 1976.
4. Jaeger, R.C., "Tutorial: Analog Data Acquisition Technology, Part II-Analog-to-Digital Conversion," *IEEE Micro*, Vol. 2, No. 3, pp. 50-54, 1982.
5. Van Valburg, J., and Van de Plassche, J., "An 8-b 650MHz Folding ADC," *IEEE Journal of Solid-State Circuits*, Vol. 27, No. 12, 1992.
6. Van Der Plassche, R. J., and Van Der Grift, R. E. J., "A High Speed 7-bit A/D Converter," *IEEE Journal of Solid State Circuits*, Vol 14, pp. 938-943, 1979.
7. Arbel, A. and Kurz, R., "Fast ADC," *IEEE Transactions on Nuclear Science*, Vol. 22, pp. 446-451, 1975.
8. Fiedler, U. and Seitzer, D., "A High-Speed 8-bit A/D Converter Based on a Gray-Code Multiple Folding Circuit," *IEEE Journal of Solid State Circuits*, Vol. 14, pp. 547-551, 1979.
9. Van Der Grift, R. E. J., and Van Der Plassche, R. J., "A Monolithic 8-bit Video A/D Converter," *IEEE Journal of Solid State Circuits*, Vol. 19, pp. 374-378, 1984.
10. Van Der Grift, R. E. J., Rutten, I. W. J. M., and Van Der Veen, M., "An 8-bit Video ADC Incorporating Folding and Interpolation techniques," *IEEE Journal of Solid State Circuits*, Vol. 22, pp. 944-953, 1987.
11. Van Der Plassche, R. J., and Baltus, P., "An 8-bit 100 Mhz Full-Nyquist Analog-to-Digital Converter," *IEEE Journal of Solid State Circuits*, Vol 23, pp. 1334-1344, 1988.

12. Esparza, J. A., and Pace, P. E., "A Preprocessing Architecture for Resolution Enhancement in High Speed Analog-to-Digital Converters," 1993 IEEE International Symposium on Circuits and Systems, Vol. 2, pp 1140-1143, 1993.
13. Pace, P. E., and Styer, D., "High Resolution Encoding Process for an Integrated Optical Analog-to-Digital Converter," accepted for publication by Optical Engineering, November , 1993.

## BIBLIOGRAPHY

Allen, P. E., and Holdberg, D. R., CMOS Analog Circuit Design, Holt, Rinehart, and Winston, Inc., 1987.

Geiger, R. L., Allen, P. E., and Strader, N. R., VLSI Design Techniques for Analog and Digital Circuits, McGraw-Hill, Inc., 1990.

Sedra, A. S., and Smith, K. C., Microelectronic Circuits, Holt, Rinehart, and Winston, Inc., 1991.

Weste, N., and Eshraghian, K., Principles of CMOS VLSI Design: A Systems Perspective, Addison-Wesley, Inc., 1985.

**INITIAL DISTRIBUTION LIST**

	<b>No. Copies</b>
1. Defense Technical Information Center Cameron Station Alexandria VA 22304-6145	2
2. Library, Code 052 Naval Postgraduate School Monterey CA 93943-5002	2
3. Chairman, Code EC Department of Electrical and Computer Engineering Naval Postgraduate School Monterey, CA 93943-5121	1
4. Professor Phillip E. Pace, Code EC/Pc Department of Electrical and Computer Engineering Naval Postgraduate School Monterey, CA 93943	3
5. Professor Douglas J. Fouts, Code EC/Fs Department of Electrical and Computer Engineering Code EC/FS Naval Postgraduate School Monterey, CA 93943	1
6. Director, Training and Education MCCDC, Code C46 1019 Elliot Road Quantico, VA 22134-5027	1
7. Department Chairman Department of Electrical Engineering U.S. Naval Academy Annapolis, MD 21412	1
8. Capt. Jorge A. Esparza, USMC 6 Sellers Road, Apartment D Annapolis, MD 21402	3
9. Ms. Socorro Esparza 902 E. Brown Street Santa Ana, CA 92701	1